May 2021

Determination of the Metabolism, Distribution, and Concentration of Calcitroic Acid

Elliot Di Milo
University of Wisconsin-Milwaukee

DETERMINATION OF THE METABOLISM, DISTRIBUTION, AND CONCENTRATION OF CALCITROIC ACID

by

Elliot Di Milo

A Dissertation Submitted in

Partial Fulfillment of the

Requirements for the Degree of

Doctor of Philosophy

in Chemistry

At

The University of Wisconsin-Milwaukee

May 2021

ABSTRACT

DETERMINATION OF THE METABOLISM, DISTRIBUTION, AND CONCENTRATION OF CALCITROIC ACID

by

Elliot S. Di Milo

The University of Wisconsin-Milwaukee, 2021

Under the Supervision of Professor Alexander (Leggy) Arnold

Near the turn of the 20th century scientist were beginning to discover compounds that were essential for humans beyond the previous establish, protein, grains, and fat[1]. This ushered in a new field of studying a class of molecules that were considered "vital amines" later shortened to vitamins[2]. Vitamin D was the fourth of this new class of compound that was identified and over the next decades was shown to play a vital role in the homeostasis of calcium and phosphorous[3, 4]. The dominant active form of vitamin D is formed within the body through a series of oxidation reactions acting upon its dietary source vitamin D_2 or UV light activated precursor 7-dehydrocloesteroil leading to the main active form 1,25$(OH)_2$ D_3, calcitriol[5-7]. In the 1980s exploration into the activity of other vitamin D metabolites was conducted by Esvelt and it was found that the final metabolic product of the activated pathway for vitamin D, calcitroic acid, had activity in complex formation with the vitamin D receptor (VDR)[8]. Our work focuses on the implementation of new methods of separation and measurement that were not available at the time of that study to explore the endogenous localization and concentration of calcitroic acid.

This work utilizes the methods of liquid chromatographic separation with tandem mass spectrometric detection[9]. An analytical method was optimized based on the ionization and fragmentation of calcitroic acid for the detection in *in vitro* and *in vivo* studies. This method was pair with a reverse phase ultra-high performance liquid chromatographic separation (UHPLC–MS/MS).

The metabolic stability of calcitroic acid was explored to determine whether it was a true end product of the metabolism of vitamin D[10]. It was found that calcitroic acid was stabile under enzymatic oxidative conditions. The conjugation of calcitroic acid for excretion and circulation was explored using *in vitro* assays.

Separation methods were optimized for sample extraction of calcitroic acid from mouse tissues. A strong anion exchange (SPE) method was developed for the analysis to allow for removal of interfering species during *in vivo* studies. The concentration of native calcitroic acid was then measured in several different mouse tissues and determined to be below the limit of detection for the developed method. Alternative forms of selectively during these studies were explored based on the derivatization of calcitroic acid using dienophile dyes.

To understand the role that the VDR in inflammatory bowel disease (IBD), A outbred mouse model was optimized for the screening efficacy of compounds, including calcitroic acid[11]. Optimization to the measurements conducted within the study, vehicle and delivering of the drugs as well as the chemical irritant and sample preparation were optimized for low variance measurement to be conducted on the reduction of colitis in mice.

1. Deluca, H. F., History of the discovery of vitamin D and its active metabolites. *BoneKEy Reports* **2014,** *3*.
2. Funk, C., On the chemical nature of the substance which cures polyneuritis in birds induced by a diet of polished rice. *J Physiol* **1911,** *43* (5), 395-400.
3. McCollum, E. V.; Davis, M., The Necessity of Certain Lipins in the Diet during Growth. *J. Biol. Chem* **1913,** *15*, 167-175.
4. Hart, E. B.; McCollum, E. V.; Steenbock, H.; Humphrey, G. C., Physiological Effect on Growth and Reproduction of Rations Balanced from Restricted Sources. *Proceedings of the National Academy of Sciences* **1917,** *3* (5), 374-382.
5. Velluz, L.; Amiard, G., Pre-calciferol. *C R Hebd Seances Acad Sci* **1949,** *228* (8), 692-4.
6. Bikle, D. D., Vitamin D metabolism, mechanism of action, and clinical applications. *Chemistry & biology* **2014,** *21* (3), 319-329.
7. Blunt, J. W.; DeLuca, H. F.; Schnoes, H. K., 25-Hydroxycholecalciferol. A biologically active metabolite of vitamin D3. *Biochemistry* **1968,** *7* (10), 3317-3322.
8. Esvelt, R. P.; De Luca, H. F., Calcitroic acid: Biological activity and tissue distribution studies. *Archives of Biochemistry and Biophysics* **1981,** *206* (2), 403-413.
9. Onisko, B. L.; Esvelt, R. P.; Schnoes, H. K.; DeLuca, H. F., Metabolites of 1 alpha, 25-dihydroxyvitamin D3 in rat bile. *Biochemistry* **1980,** *19* (17), 4124-30.
10. Reddy, G. S.; Tserng, K. Y., Calcitroic acid, end product of renal metabolism of 1,25-dihydroxyvitamin D3 through the C-24 oxidation pathway. *Biochemistry* **1989,** *28* (4), 1763-1769.
11. Froicu, M.; Cantorna, M. T., Vitamin D and the vitamin D receptor are critical for control of the innate immune response to colonic injury. *BMC Immunol* **2007,** *8*, 5.

DEDICATION

I would like to dedicate my thesis to my Grandmother Carol Williams.

TABLE OF CONTENTS

1 Introduction to Vitamin D 1

1.1 History of Vitamin D 1

1.2 Vitamin D Metabolic Pathways 2

1.3 Vitamin D Metabolic Activity 5

1.4 Significance of Vitamin D Metabolites 6

1.5 Conclusion 7

2 Liquid Chromatographic Mass Spectrometric Measurement of Calcitroic Acid 11

2.1 Instrumental Techniques 11

2.2.1 Introduction to Mass Analyzer 11

2.2.2 Introduction to Ionization Source 13

2.2.3 Mass Spectrometric Optimizations for Calcitroic Acid Analysis 15

2.3.1 Introduction to Liquid Chromatography 22

2.3.2 Liquid Chromatographic Optimization for Calcitroic Acid Analysis 25

2.4 Conclusion 32

3 Metabolic Stability of Calcitroic Acid 34

3.1 Phase I Metabolism of Calcitroic Acid 34

3.2 Phase II Metabolism of Calcitroic Acid 37

3.2.1 Glucuronic Acid Conjugation of Calcitroic Acid 38

3.2.1 Sulfate Conjugation of Calcitroic Acid 41

3.2.2 Amino Acid Conjugation of Calcitroic Acid 43

3.3 Conclusion 44

4 Identification and Quantification of Calcitroic acid in Biological Settings 47

4.1 Introduction 47

4.2 The need for Separation Methods Beyond Liquid Chromatography 47

4.3 Liquid–Liquid Extraction 49

4.4 Solid Phase Extraction 50

4.4.1 Reverse Phase Solid Phase Extraction 51

4.4.2 Weak anion exchange Solid Phase Extraction 55

4.4.3 Strong Anion Exchange Solid Phase Extraction 56

4.6 Molecular Filtration 65

4.7 Stability of Calcitroic Acid Under Extraction Procedure Conditions 68
4.8 Quantification of Calcitroic Acid Concentration is Tissue Samples..... 69
4.9 Conclusion 77
5 Derivatization Reactions of Calcitroic Acid 80
5.1 Introduction to Vitamin D metabolite derivatization 80
5.2 Instrumental Considerations Metabolite Analysis..... 81
5.3 Applications of Derivatization Reactions on Calcitroic Acid 82
5.4 Isotope Labeling of Calcitroic Acid 86
5.5 Conclusion 88
6 Modeling Inflammatory Bowel Disease 91
6.1 Introduction to Inflammatory Bowel Disease..... 91
6.2 Experimental Design 92
6.3 Quantification of Colitis..... 93
6.4 Experimental Design Optimization in Studies..... 97
6.4.1 Optimization Irritant Concentration..... 97
6.4.2 Removing Nonchemical Inflammation 105
6.4.3 Colon Homogenate Preparation..... 108
6.4.4 Corticosteroid Administration..... 110
6.4.5 Corticosteroids as Positive Controls..... 113
6.4.6 Other Measurements of Colitis Intensity 121
6.5 Future Studies on Inflammation 123
6.6 Conclusion 123
REFERENCES..... 125
CURRICULUM VITAE..... 131

LIST OF FIGURES

Figure 1 – Mass Spectrum of a 50 µM standard solution of calcitroic acid. The peaks that are labeled are attributed to the analyte of the study. Ions below 200 m/z remain within this spectrum but were also present within blanks on the sample instrument and were considered background signal. 17
Figure 2 – Overlay of two calibration curves of calcitroic acid based on the precursor ion for the method. The circles represent the dehydrated form and the triangles the protonated form. The sensitivity as well as the lower limit of detection was greatly improved working with the dehydrated form. 20
Figure 3 – Chromatograms of 50 µM standard solutions of calcitroic acid. Sample A was a working stock solution of calcitroic acid that was used for the initial development of the dehydrated CTA method. Sample B was a crude solid stock that was prepared to confirm no degradation was behind the ratio of ions observed in the original sample. The chromatogram of the working sample contains few impurities will maintaining the same retention time of the solid samples predominant peak. 22
Figure 4 – TLC plate of standard solutions of calcitroic acid. The left lane was the working stock solution of calcitroic acid used for the dehydrated calcitroic acid method. The right lane was the crude solid stock calcitroic acid. 22
Figure 5 – Chromatogram of calcitroic acid separated from two internal standards Verapamil and INT–777. This method demonstrating proper separation. Note the concentration of CTA is quite high in this sample allowing this method only to be used in samples with high concentrations. 27
Figure 6 – Comparison of diluent composition on the chromatography of calcitroic acid samples. Chromatogram A, B, C, and D are diluted in 0.1% acetic acid, 5% acetic acid, 0.5 % acetic acid, and 5 % formic acid, respectively. We observed that as the concentration and strength of the acid was decreased, the number of peaks that attributed to degradation products decrease. . 28
Figure 7 – Initial chromatographic overlay of the instrumental internal standards screened with strong enough ionization for mass spectrometric optimization. All three of the internal standards had poor retention on the column under the initial conditions and further optimization was required to improve retention. 30
Figure 8 – Chromatograms of 1 µM 4,5–DPI standard solutions prepared with different diluent compositions. The diluent composition has consequences for the extraction procedure that is described in chapter 4. 30
Figure 9– A chromatograph of a standard solution of calcitroic acid and 4,5–DPI using the developed separation. The gradient is overlayed in light blue in concentration of organic mobile phase as a percentage. 32
Figure 10 – Oxidative microsomal stability assay of calcitroic acid conducted with both human (triangles) and mouse (squares). The slope of the natural log of each assay was determined to not significantly deviate from zero suggesting no activity. 36

Figure 11 – Glucuronidation metabolic stability assay using human liver microsomes n = 6 for MIDD 0301. The monitoring of the loss of MIDD 0301 is reflected on the left while the right shows the normalized signal of its glucuronide increasing during the assay. The half-life was determined to be 110.7 min. 41
Figure 12 – The metabolic stability assay of calcitroic acid normalized against an instrumental internal standard. The linear regression of the natural log of the signal did not significantly deviate from zero suggesting no activity. For this reason, no metabolic values were assigned for this assay. 41
Figure 13 – Initial method to explore the simplest form of sample preparation for chromatographic separation. It was found that the background signal was too high, and the chromatographic separation did not allow for the quantification of calcitroic acid. 48
Figure 14 – An absorbance spectrum of calcitroic acid and two separate solvents of the determination of the optimal intensity of the detection during the extraction optimization. This was paired with a PDA contour and it was determined that accounting for impurities, 264 nm would be used as the wavelength for detection. 53
Figure 15 – The calculated extraction efficiency through the reverse phase extraction and the expected losses at each step of the procedure. This method had the highest recovery rate of calcitroic acid standards out of any of the explored solid phase extractions. 54
Figure 16 – A comparison of the recovery during a spiked sample of calcitroic acid that had undergone the reverse solid phase extraction procedure to a sample that underwent the extraction and then was spiked with calcitroic acid at the same concentration. The observed loss of calcitroic acid was too large to move forward with this method. 55
Figure 17 – A comparison of calcitroic acid present in solvents of the weak anion exchange procedure. It was observed that a majority of the calcitroic acid remained within the initial load solution not properly interacting with the stationary phase. 56
Figure 18 – A comparison of the three different types of solid phase extraction explored within this study. It was found that the greatest recovery was observed in standard solutions with the C18 stationary phase, but the strong anion exchange method provided greater amounts of selectivity than the other stationary phases. 59
Figure 19 – A chromatogram of a standard sample of calcitroic acid that underwent the strong anion exchange method. It was found that there was unexpected signal from the standard sample that was attributed to the degradation of the sample under acidic conditions. 60
Figure 20 – A comparison of the ratio of the peaks observed in chromatograms of standard solutions of calcitroic acid dependent upon the concentration and type of acid during the final elution step. It was found that the type of acid as well as its concentration significantly contributed to the ratio of the observed peaks in the chromatograms. 61
Figure 21 – A representative chromatogram of the separation that was achieved with an online solid phase extraction of calcitroic acid. No peaks observed in the chromatogram corresponded with the expected retention time of calcitroic acid standard solutions suggesting the reported signal was background. 64

Figure 22 – A chromatogram of a spiked mouse plasma extract through the SAX-SPE method. The sample had a negligible peak that came from the spiked standard. It was speculated that the signal was lower than expected due to unspecific protein binding preventing the analyte from reaching the solid phase extraction method. 66
Figure 23 – A comparison of A calcitroic acid sample with a standard solution that did not undergo membrane filtration. It was found that there were significant losses during the process but due to the low standard deviation between the samples these could be accounted for in the calculation of the initial concentrations of calcitroic acid in samples. 67
Figure 24 – A chromatogram of a native mouse plasma sample worked up through the SAX-SPE extraction procedure. Several peaks of a single product ion at retention times not matching standard solutions of calcitroic acid were observed. It was concluded that calcitroic acid was not present in theses samples at a concentration above the limit of detection. 70
Figure 25 – A chromatogram of a calcitroic acid spiked solution mouse plasma to measure the extraction efficiency through the procedure. It was found that when a sample was spiked to a concentration of 10 µM the measured concentration after the extraction was 8.86 µM giving an 88.6 % recovery through the procedure. 71
Figure 26 – A collection of chromatograms of tissue samples that underwent the described strong anion exchange extraction procedure. Several peaks were observed in the chromatograms that contained fragmentation seen in calcitroic acid. The retention time as well as the product ion ratios did not match what had previously been seen in chromatograms of calcitroic acid standards. A standard sample of calcitroic acid is shown at the bottom for comparison of the retention times a sense of scale of the signal intensity. 73
Figure 27 – A chromatogram of a liver extract sample that was spiked with calcitroic acid after the extraction procedure to compare the retention time of the native signal with the standard under these matrix conditions. It was observed that the retention time of calcitroic acid was not affected by the biological matrix in an of the samples measured. 74
Figure 28 – A set of two chromatograms showing both the $[M+H]^+$ (bottom) and the dehydrate product ions (top). Several peaks were observed in both chromatographic methods thought the ratio of intensity seems to change between the two methods of detection. 75
Figure 29 – A set of two chromatograms of the same fecal sample from a mouse given an oral dose of vitamin D3. The sample follows a similar pattern to what was seen in the mouse given vitamin D2. The sample's chromatogram contained similar peaks as the large intestinal sample collected in non-treated mice. 76
Figure 30 – Thin layer chromatogramphy in 1:9 MeOH:EtOAc comparing the starting materials to the shwon on the right and left under 365 nm, and 254 nm light respectivily. The loss of the starting material and the formation of a central peak between the retention of the starting materials suggested the reaction had occurred. 84
Figure 31 – A set of spectra reflecting Calcitroic Acid, Reaction after 2 h, and the Cookson reagent, DMEQ-TAD, top, middle, and bottom, respectively. 85

Figure 32 – An overlay of the starting materials of the reactions with the reaction mixture sample run for 2h. No peaks that were seen the reaction mixture were unaccounted for in the starting material chromatograms. 86
Figure 33 – Weight loss of the mice of the mice as a percentage of the initial body weight at the beginning of the study. The two graphs on the left represent the indiviual mice within the study and the graph on the left shows the groups combined for statistical analysis. 99
Figure 34 – Images of the colons in the positive control group of the intial IBD study. The explected length of an untreated colon would be near 9.5 cm while all members of this group fell below that meaure. 99
Figure 35 – Collection of MPO assays conducted on the three different groups of the intial study. The left side of the graph contains both the mice given vehicle and the chemical irritant, DNBS while the figure below it shows mice with no chemical irratant. The graph on the right is the MPO assay conducted upon mice that were given 1.0 mg/kg dexamethasone after installation of DNBS. 101
Figure 36 – A comparsion of the treated and vehicle groups of mice in the replicate of the intial study. No statistical signifcance was seen between the two groups. 102
Figure 37 – Colon images of the replicate of the initial sample conditions. The severity of the inflamation seen in these groups was greater than what was measured in the first study. 102
Figure 38 – Overlay of the MPO assay indiviual colon homogenates for the vehicle group (black) and the positive control group (red). 103
Figure 39 – Comparison of the vehicle (blue) and positive control group (red) now provided a higher concentration of 5 mg/kg dexamethasone. 104
Figure 40 – Collected colon images of mice during the study (V for vehicle and PC for the postive control). The postive control received the higher concentration of 5 mg/kg dexamethasone. 104
Figure 41 – MPO assay overlay of the higher dose 5 mg/kg dexamethasone group (red) compared to the vehicle (black). 105
Figure 42 – A comparision of mice weights indivual (left) and grouped (right) for mice treated with a new vehicle. 106
Figure 43 – Colons collected from the two groups of mice vehicle (top) and dexamethsone (bottom). The varience in length as well as localized inflamation was observed in this study similar to previous studies. 107
Figure 44 – The MPO Assay overlay of the postive control (red) and vehicle (black) groups. Several colon homogenates had higher than expected activity based on the visual and weight loss observed during the study. 107
Figure 45 – Weight lose of inividual mice (left) and grouped (right) as a percentage of the initial weight at the beginning of the study. No statistical difference was observed between the two groups. 109
Figure 46 – Colon images of mice in the vehicle group (top) and the positive control (bottom). High levels of inflamation were present in both groups. 109

Figure 47 – MPO assay overlay of indiviual mice from the vehicle and positive control groups. The colons underwent manual fecal remove to try and preserve oxidative activity. 110
Figure 48 – Comparison weights of individual mice (left) and grouped (right) given vehicle and 5.0 mg/kg dexamethasone through oral gavage. 111
Figure 49 – Images of colons of mice give vehicle (top) and the mice provided with 5.0 mg/kg dexamethasone (bottom) through oral gavage. 112
Figure 50 – Overlay of the MPO assay of the positive control (red) and negative control (black). The “soft” sample preparation method was used for this study. 113
Figure 51 – Weight comparison of indidual mice (right) and the grouped weight change (left). Positive control mice were given a 5 mg/kg prednisone through oral gavage. 115
Figure 52 – Colons of vehicle mice (left) compared to mice treated with 5.0 mg/kg prednisone (right). 115
Figure 53 – MPO Assay overlay of the mice treated with prednisone (red) and vehicle (black). Multiple colon homogenatates did not show any absorbance and were excluded from the measurement. 116
Figure 54 – Comparision of the wieghts of inidivual mice by weight lose (left) and weight over the study (left). 118
Figure 55 – MPO assay of the two mice treated with dextran sodium sulfate. 118
Figure 56 – Replicate of the DSS model10-day study n=4. 119
Figure 57 – Weight lose of individual mice shown as a percentage of total starting mass (right) and indiviual mass (left). 121
Figure 58 – A compareson to the expected length of a mouse colon to the measure length of the mice within the study (left). The MPO assay of the mice treated with 3.0% DSS and provided vehicle (right). 121

LIST OF TABLES

Table 1 – A summary of the reagents and their respective concentrations for the phase II microsomal stability assay of hepatic glucuronidation. 39

LIST OF SCHEMATICS

Schematic 1 – Metabolic pathways for the cholecalciferol with a representation of conversion into calcidiol for circulation. 3
Schematic 2 – Representation of the oxidative pathway that vitamin D undergoes through the active form calcitriol. 4
Schematic 3 – Metabolic pathway of vitamin D bypassing the active form for clearance. 5
Schematic 4 – Schematic representation of a triple quadrupole mass spectrometer. Often an exterior vacuum is present to reduce the strain on the interior vacuums shown[35]. 13
Schematic 5 – The proposed structures of the transitions of calcitroic acid generated within the collision cell. The ions 339.23 and 121.10 were used as the quantification ion and finger printing ion, respectively. 18
Schematic 6 – Proposed product ion transitions of the dehydrated form of calcitroic acid. Two of the structures are based on the speculations made on the $\{M+H]^+$ product ions. 21
Schematic 7 – Overlay of the three terms of the van Deemter model. Each curve can be summed to find the optimal conditions for a chromatographic separation[38]. 24
Schematic 8 – Structures of the screened molecules for instrumental internal standards for the UHPLC–MS/MS method. 29
Schematic 9 – A proposed reaction for the formation of a glucuronic acid conjugate. Other possible sites for this conjugation could occur on the 3-hydroxyl position as well as the carboxyl. 38
Schematic 10 – A representation of the conversion of calcitroic acids conjugation with a sulfate. Both hydroxyl groups could potentially undergo this conjugation as well as the carboxyl moiety. 42
Schematic 11 – The representation of the proposed reaction of the calcitroic acid conjugate formation with amino acids and taurine. Unlike the previous conjugation reactions this reaction would be localized to the carboxyl functional group. 43
Schematic 12 – A representation of the basic procedure of a solid phase extraction. Solvents would be matched with the type of analyte and stationary phase for the best performance[59]. 51
Schematic 13 – A representation of the reverse phase extraction procedure of calcitroic acid tissue extraction. The solvent composition of the load solution was adjusted by the evaporation of the samples and reconstitution in the appropriate solvent. 53
Schematic 14 – A summary highlighting the selectivity gained through a strong anion stationary phase. 58
Schematic 15 – The workflow of the sample extraction procedure incorporating the strong anion exchange solid phase extraction. The concentration of the acid used in the final elution was lowered from the initial 5% to make the method compatible with calcitroic acid. 62
Schematic 16 –A final summary of the extraction procedure with the membrane filtration step. Samples were evaporated between the membrane filtration and the SAX-SPE to allow for matching of the loading step solvent. 68

Schematic 17 – A representation of the dieneophile reagent acting upon the analyte through a Diels-Alder reaction. 81
Schematic 18 – A representation of speculated reaction between calcitroic acid and the DMEQ-TAD forming the fluorescent derivative used for UHPLC measurement. 83
Schematic 19 – Representation of the reduction of coppric to copprous by amino acids. The reduced form is then chelated to form a redshifted complex. 95
Schematic 20 – The chemical reaction that occurs in the designed myeloperoxidase assay. Hydrogen peroxide is oxidized enzymatically into hypochlorite which then acts upon the o-dianisidine. 97
Schematic 21 – Structure of the corticosteroids used within the studies..... 114
Schematic 22 – Structure of the polymer of DSS size can range from 5 kDa to 60 kDa..... 117

LIST OF ABBREVIATIONS

^{1}H-NMR	Proton Nuclear Magnetic Resonance Spectroscopy
4,5-DPI	4,5-Diphenyleneiodonium Chloride
8040	Shimadzu Triple Quadrupole Mass Spectrometer Series 8040
AAT	Acyl-coA: Amino Acid N-Acyltransferase
APCI	Atmospheric Pressure Chemical Ionization
ATP	Adenosine Triphosphate
BACS	Acyl-coA Synthetase
BCA	Bicinchoninic Acid
BEH	Bridged Ethylene Hybrid
BSA	Bovine Serum Albumin
C18	Octadecyl Silica
CFW	Swiss Webster
CTA	Calcitroic Acid
CYP24A1	Cytochrome P450 Family 24 Subfamily A Member 1
CYP27A1	Cytochrome P450 Family 27 Subfamily A Member 1
CYP27B1	Cytochrome P450 Family 27 Subfamily B Member 1
CYP2R1	Cytochrome P450 Family 2 Subfamily R Member 1
DMEQ-TAD	Ethyl]-3h-1,2,4-Triazole-3,5(4h)-Dione
DMSO	Dimethyl Sulfoxide
DNBS	2,4-Dinitrobenzene Sulfonic Acid
DSS	Dextrin Sodium Sulfate
DUSI	Dual Source Ionization
EI	Electron Impact
ESI	Electrospray Ionization
EtOH	Ethanol
GC-MS	Gas Chromatography Mass Spectrometry
Glu-PO_4	Glucose 6-Phosphate
HPLC	High Performance Liquid Chromatography
HPMC	Hydroxypropyl Methylcellulose
IBD	Inflammatory Bowel Disease
IL	Interleukin
IP	Intraperitoneal Injection
MeOH	Methanol
MIDD 0301	Milwaukee Institute for Drug Discovery Compound 0301
MP	Mobile Phase
MPO	Myeloperoxidase Assay
MRM	Multiple Reaction Monitoring
MS/MS	Tandem Mass Spectrometry
MS^{n}	Multistage Mass Spectrometry

NADPH	Reduced Form of Nicotinamide Adenine Dinucleotide Phosphate
NADP+	Nicotinamide Adenine Dinucleotide Phosphate
P450	Superfamily of Oxidative Enzymes
PAPS	3'-Phosphoadenosine-5’-Phosphosulfate
PBS	Phosphate-Buffered Saline
PC	Positive Control
PDA	Photodiode Array
PG	Propylene Glycol
RXR	Retinoid X Receptor
SAX-SPE	Strong Anion Exchange Solid Phase Extraction
SPE	Solid Phase Extraction
SULTS	Sulfotransferase
TLC	Thin Layer Chromatography
UDPGA	Uridine Diphosphate Glucuronic Acid
UHPLC	Ultra-High Performance Liquid Chromatography
UV	Ultraviolet
UV-VIS	Ultraviolet Visible
VDR	Vitamin D Receptor
Vitamin D2	ergocalciferol
Vitamin D3	cholecalciferol
WAX-SPE	Weak Anion Solid Phase Extraction

ACKNOWLEDGMENTS

The experience of higher education is a privilege that many never get to experience in their life. While this has been the most challenging time of my life, I feel the sense of gaining so much from the opportunity to be a doctoral student at the University of Wisconsin-Milwaukee. I could never overstate that amount of gratitude that I feel towards my research advisor Prof. Leggy Arnold. I would like to thank your patience and constant interest in our research together.

What has made my time at our university, so enriching is all the members of the Arnold research group who I truly know I would not be who I am today without meeting and working with. Working in a multidisciplinary lab you have all shared your favorite parts chemistry with our group and I am truly grateful to been able to spend 5 years with such intelligent and interesting people.

I would like to also acknowledge my Mom, Pop, and brother Soren. They have been a constant source of support, and motivation. My family gave me the opportunity to receive higher education and I could not be more thankful for the experience. I would like to thank all my distant family, Aunts, Uncles, and Cousins. You have all been role models for me throughout my life.

I would be remiss not to thank my undergraduate research advisor, Professor Aldstadt. You sparked an interest in analytical chemistry that inspired me to seek a graduate degree. The thought of roasted coffee or fresh bread still makes me think back to working on the Maillard reaction kinetic in your group.

1 Introduction to Vitamin D

1.1 History of Vitamin D

During the turn of the twentieth century nutritional requirements were still in the very early stages of development. Von Liebig was the first to suggest that a balance of different proteins, grains, minerals, and fats were required for physiological homeostasis. Near the turn of the 20th century, scientists were starting to question the ability to sustain life on the three macronutrients. Funk first postulated the need of essential dietary requirements called vital amines with the discovery of vitamin A[2]. This nomenclature was carried forward for the future classifications of compounds shortened to vitamins. A sample of cod liver oil that was separated into a non-aqueous and aqueous portion and were given the names vitamin A and B, respectively. It was speculated that the disease rickets was caused by a deficiency in vitamin A at the time. Mellanby was a English chemist who was interested in the treatment of rickets and demonstrated in a canine model that there was a dietary link to the disease, suggesting vitamin A deficiency [12]. McCollum was skeptical of the finding of Mellanby and looked to find if a different vitamin was behind the treatment of the disease. McCollum hypothesized that vitamin A was not taking place in the efficacy of the treatment[3]. He took a sample of the cod liver oil and bubbled oxygen through the mixture to deactivate the present Vitamin A. After the oxidation, the effect of the mixture on the treatment of rickets remained[3, 4].

While the field of dietary vitamin D was the first place that it was discovered, the history behind biologically synthesized vitamin D had a large impact on the treatment of rickets as well all over the world at the beginning of the 20th century. Huldschinsky and Chick both found a

correlation with the exposure to ultraviolet light in subject with sufficient fat present in their diets seemed to treat rickets as well[13, 14]. Steenbock added to this work exploring rickets within rats that were exposed to UV light as well as animals that were given food that was exposed the this light source and found that both proved effective in the prevention of rickets[15]. He concluded that some species was being activated within the food source that was leading to the treatment of the disease. The evidence of 7-dehydrocholesterol as the precursor to vitamin D_3 through UV light activation would not become a validated mechanism until that mid-1970s[16, 17].

Scientist concluded the fat-soluble portion of cod liver extract contained some other essential component and sought to identify the active compound. Askew et al. worked on the identification and were the first to separate vitamin D_2[18]. Because the moniker of vitamin C was already assigned to the water soluble species responsible of the treatment of scurvy, the fourth vitamin was given the title of vitamin D[19]. A misidentification led to the discarding of the original vitamin D_1 making vitamin D_2 the first form to be separated and confirmed.

1.2 Vitamin D Metabolic Pathways

Vitamin D metabolism was overshadowed by other vitamins but over the next decades vitamin D was found to have an interesting metabolic pathway decades after its initial separation. Further separation of the aqueous portion demonstrated that vitamin B was a class of compounds of similar structure with interesting metabolism, which dominated the field vitamin research for decades[1]. Once the function of calcium and phosphate homeostasis was determined

as a function of vitamin D metabolism, the efficacy of the forms of vitamin D were determined[20, 21]. In the process the predominant members of the metabolic pathway were determined.

The metabolic pathways of vitamin D undergo two routes dependent upon the activation of the compound. The distinction between vitamin D_2 and D_3 effects the initial metabolic pathway of the material. As shown in **Schematic 1**, 7-dehydrocholesterol can be converted into cholecalciferol through exposure to UV light[5]. Vitamin D_2 undergoes a different reaction to desaturate the 22,23-sidechain paired with the demethylation at the 24-position, producing Vitamin D_3. This reaction is enzymatically done by CYP24A1 leading again to cholecalciferol, vitamin D_3[6]. The activation to the circulating form of vitamin D is then mitigated by another oxidative P450 enzyme either CYP24A1 or CYP2R1[7]. The product of this metabolism is calcidiol, or 25-(OH) D_3.

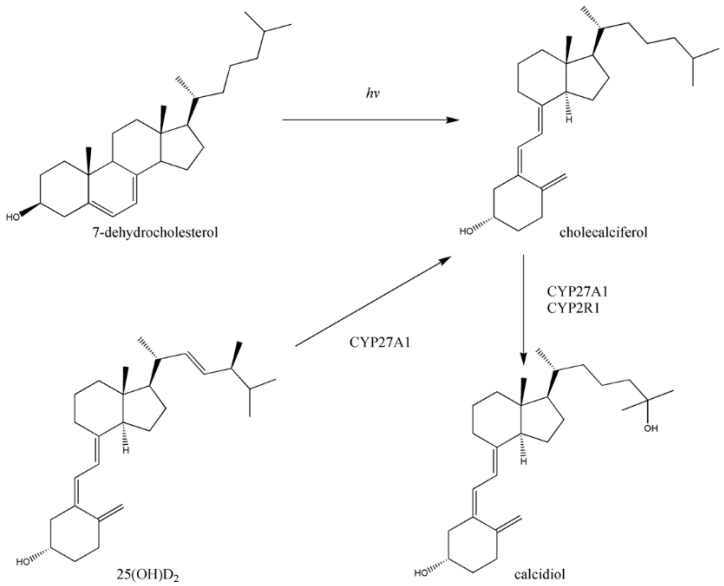

Schematic 1 – Metabolic pathways for the cholecalciferol with a representation of conversion into calcidiol for circulation.

At this point the metabolism branches between an activated form of the vitamin with high efficacy and an inactive clearance pathway. A representation of the pathway is shown in **Schematic 2.** The most biologically active form of vitamin D was found to be calcitriol, which strongly induces the formation of the vitamin D receptor complex[22]. This is formed from the further oxidation of calcidiol by the P450 enzyme CYP27B1 located within renal cells[6]. Due to the high activity of calcitriol, it is well regulated. The conversion to a less active metabolite is necessary to maintain homeostasis within animals. A series of P450 controlled reactions allow for a series of oxidative reactions that lead to the sidechain shortening of calcitriol through, 24-oxo-1,23,25(OH)$_3$D$_3$[23]. This compound is then oxidized to 24,26,26,27-tentranor-1,23(OH)$_2$D$_3$ by the CYP24A1 enzyme. Finally, the last observed oxidation of vitamin D conducted by CYP24A1 converts the species to the speculated exception product. 1α-hydroxy-23-carboxy-24,25,6,27-teranorvitamin D$_3$, referred to as calcitroic acid[24].

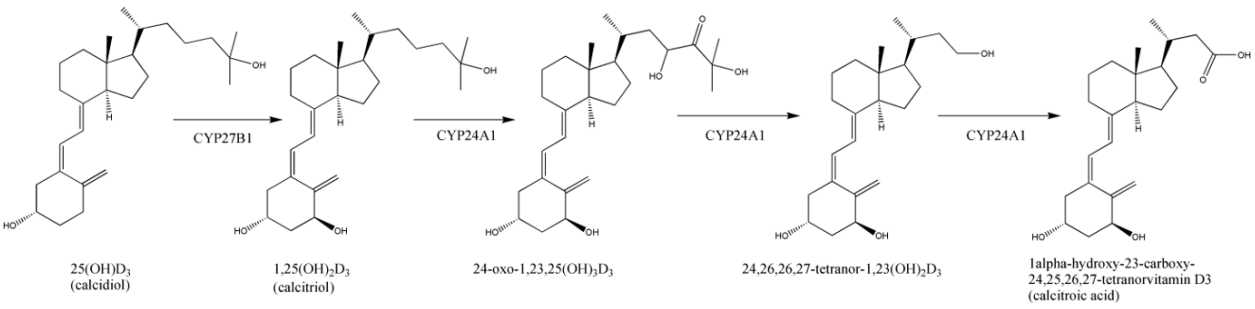

Schematic 2 – Representation of the oxidative pathway that vitamin D undergoes through the active form calcitriol.

While calcitriol is of interest to study the function of vitamin D, the metabolism is equally as important for the clearance of vitamin D and identification of possible pathways in maintaining homeostasis. A representation of the pathway is shown in **Schematic 3**. Calcidiol alternatively to taking on the hydroxyl at the α1 position, can begin the chain shortening reaction that calcitriol

was seen to undergo above. The same enzyme CYP24A1 is responsible for the oxidation reaction that covert calcidiol into 24-oxo-23,25(OH)$_2$D$_3$ and then to 24,26,26,27-tetranor-23(OH)D$_3$[25-27]. Finally, the conversion into the less active clearance product, 23-caroxy-24,25,26,27-tetranorvitamin D$_3$, or calcioic acid is the current established product for excretion through the bile duct and in urine[28].

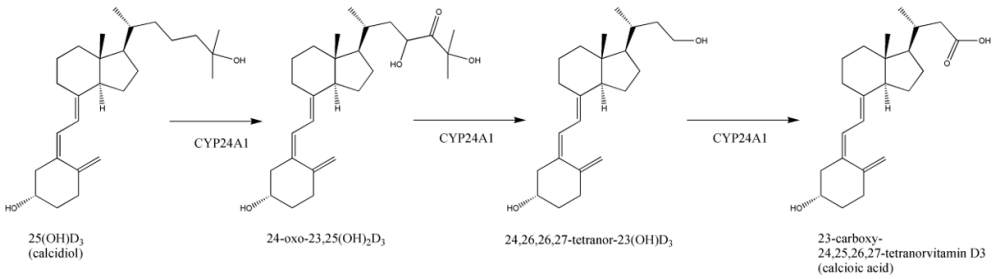

Schematic 3 – Metabolic pathway of vitamin D bypassing the active form for clearance.

1.3 Vitamin D Metabolic Activity

Understanding of the activity of vitamin D came first in function then in form. Early work as described in **Section 1.1** focused on the treatment of the disease rickets. Experiments were performed to understand the nature of the disease with the incubation of bone samples with blood samples of animals that had been treated with vitamin D[29]. It was found that significant decalcification occurred within the samples suggesting a regulation of circulating and stored calcium and phosphate levels.

The first crystallization of the vitamin D receptor (VDR), a member of the nuclear receptor family, allowed for greater understanding of vitamin D activity[30]. The expression of this receptor was found to be mainly present within the endocrine system and well as the

intestinal track further adding to the understanding of the calcium homeostasis being a negative feedback loop where the intestinal absorption of calcium was regulated by this new nuclear receptor. As previously mentioned, calcitriol was identified as the dominant ligand for this receptor showing the greatest complex formation and gene expression[31]. Vitamin D analogs act as a ligand with the VDR and recruit retinoid X receptor (RXR) to form a heterodimer complex[32].

Esvelt sought to build upon the roles of the metabolic activity of vitamin D metabolites and found activity within the final oxidative product, calcitroic acid in the VDR complex formed during *in vitro* studies[8]. Activity of a lower magnitude than calcitriol was observed with calcitroic acid and calcitroic acid methyl ester. Their work also included the dosing of mice with calcitroic acid and exploring the distribution of calcitroic acid. At the time of these measurement, a synthesis route for calcitroic acid had not yet been developed preventing radiolabeled measurement of the dosed samples. Mass spectrometry liquid chromatography was far away from the modern methods developed around these methods of measurement.

1.4 Significance of Vitamin D Metabolites

Vitamin D is an essential compound for regular cellular proliferation and homeostasis[31]. For this reason, vitamin D is a common dietary supplement in both the forms of vitamin D_2 and D_3. Alternatively, to the dietary source's vitamin D is metabolized through a light activated reaction on 7-dehydrocholesterol within the skin. While there are many analogs of vitamin D, the most common circulating form is 25-(OH)D_3, which can be metabolized into the most active form

1,25-$(OH)_2D_3$ binding VDR to form a complex that regulates gene expression. Clearance of 1,25-$(OH)_2D_3$ occurs through a series of oxidative metabolism reactions mitigated by P450 enzymes. The previously determined excretion product of this metabolism is calcitroic acid. For this reason, people are exposed to calcitroic acid daily but the activity, localization, and further metabolism of endogenous calcitroic acid has not previously been explored.

The hope of this project was to increase the understanding of the biological activity of calcitroic acid and determine if it plays a role in inflammatory mitigation observed with vitamin D supplements. In addition, this work was based on the question of whether calcitroic acid is the true end product of the vitamin D metabolic pathway. The role calcitroic acid adds to the body of vitamin D pharmacology and provides possible new options for drug design for the treatment of diseases that are centered around the pathways that it takes place within.

1.5 Conclusion

The study of vitamin D has a long history dating back to the first classification of vital amines. While at first overlooked during the initial separation and through to be a component of vitamin A from cod liver oil, vitamin D was later found to play a significant role in regulating cellular function and calcium and phosphate homeostasis in animal[20, 21]. The initial finding of vitamin D were thought to be complete until it was proven that the multiple forms of vitamin D and the possible metabolic pathway allows for negative feedback regulation of calcium and phosphate homeostasis. A deeper understanding of vitamin D metabolic regulation grew to the position where is sits today where many oxidative P450 enzymes that are responsible for its

activation, and clearance have been identified. Modern methods have been developed for the quantification of vitamin D levels within patients allowing for its concentration to be used as a diagnostic tool in medicine[33, 34].

Activity was observed in the form of calcitroic acid, a compound previously considered to be an end product of the vitamin D metabolic pathway[8]. The work described within this dissertation lays out the exploration of the presence of calcitroic acid at concentrations able to mitigate a biological response. The work set out to build upon the body of vitamin D research in hopes to identify new mechanisms that could be targeted for drug discovery.

References

1. Funk, C., On the chemical nature of the substance which cures polyneuritis in birds induced by a diet of polished rice. *J Physiol* **1911,** *43* (5), 395-400.

2. Mellanby, E., An Experimental Investigation on Rickets. *Nutrition Reviews* **1976,** *34* (11), 338-340.

3. McCollum, E. V.; Davis, M., The Necessity of Certain Lipins in the Diet during Growth. *J. Biol. Chem* **1913,** *15*, 167-175.

4. Hart, E. B.; McCollum, E. V.; Steenbock, H.; Humphrey, G. C., Physiological Effect on Growth and Reproduction of Rations Balanced from Restricted Sources. *Proceedings of the National Academy of Sciences* **1917,** *3* (5), 374-382.

5. Chick, H.; Dalyell, E.; Hume, M.; Smith, H. H.; Mackay, H. M., The Ætiology of Rickets in Infants : Prophylactic and Curative Observations at the Vieanna University Kinderklinik. *The Lancet* **1922,** *200* (5157), 7-11.

6. Huldschinsky, K., Heilung von Rachitis durch künstliche Höhensonne. *DMW - Deutsche Medizinische Wochenschrift* **1919,** *45* (26), 712-713.

7. Steenbock, H., THE INDUCTION OF GROWTH PROMOTING AND CALCIFYING PROPERTIES IN A RATION BY EXPOSURE TO LIGHT. *Science* **1924,** *60* (1549), 224-5.

8. Esvelt, R. P.; Schnoes, H. K.; DeLuca, H. F., Vitamin D3 from rat skins irradiated in vitro with ultraviolet light. *Archives of Biochemistry and Biophysics* **1978,** *188* (2), 282-286.

9. Havinga, E., Vitamin D, example and challenge. *Experientia* **1973,** *29* (10), 1181-93.

10. Askew, F. A.; Bourdillon, R. B.; Bruce, H. M.; Jenkins, R. G. C.; Webster, T. A., The Distillation of Vitamin D. *Proceedings of the Royal Society. Series B.* **1930,** *107*, 76-90.

11. Drummond, J. C., The Nomenclature of the so-called Accessory Food Factors (Vitamins). *Biochemical Journal* **1920,** *14* (5), 660-660.

12. Deluca, H. F., History of the discovery of vitamin D and its active metabolites. *BoneKEy Reports* **2014,** *3*.

13. Bauer, G. C.; Carlsson, A., Metabolism of bone salt investigated by simultaneous administration of 45Ca and 32P to rats. *J Bone Joint Surg Br* **1955,** *37-B* (4), 658-62.

14. Carlsson, A., Tracer experiments on the effect of vitamin D on the skeletal metabolism of calcium and phosphorus. *Acta Physiol Scand* **1952,** *26* (2-3), 212-20.

15. Velluz, L.; Amiard, G., Pre-calciferol. *C R Hebd Seances Acad Sci* **1949,** *228* (8), 692-4.

16. Bikle, D. D., Vitamin D metabolism, mechanism of action, and clinical applications. *Chemistry & biology* **2014,** *21* (3), 319-329.

17. Blunt, J. W.; DeLuca, H. F.; Schnoes, H. K., 25-Hydroxycholecalciferol. A biologically active metabolite of vitamin D3. *Biochemistry* **1968,** *7* (10), 3317-3322.

18. DeLuca, H. F.; Holick, M. F.; Schnoes, H. K.; Suda, T.; Cousins, R. J., Isolation and identification of 1,25-dihydroxycholecalciferol. A metabolite of vitamin D active in intestine. *Biochemistry* **1971,** *10* (14), 2799-2804.

19. Sakaki, T.; Sawada, N.; Komai, K.; Shiozawa, S.; Yamada, S.; Yamamoto, K.; Ohyama, Y.; Inouye, K., Dual metabolic pathway of 25-hydroxyvitamin D3 catalyzed by human CYP24. *European journal of biochemistry* **2000,** *267* (20), 6158-65.

20. Reddy, G. S.; Tserng, K. Y., Calcitroic Acid, End Product of Renal Metabolism of 1,25-Dihydroxyvitamin D3 through C-24 Oxidation Pathway. *Biochem J* **1989,** *28*, 1763-1769.

21. Jones, G.; Prosser, D. E.; Kaufmann, M., 25-Hydroxyvitamin D-24-hydroxylase (CYP24A1): its important role in the degradation of vitamin D. *Arch Biochem Biophys* **2012,** *523* (1), 9-18.

22. Jones, G.; Kung, M.; Kano, K., The isolation and identification of two new metabolites of 25-hydroxyvitamin D3 produced in the kidney. *J Biol Chem* **1983,** *258* (21), 12920-8.

23. Reddy, G. S.; Tserng, K. Y.; Thomas, B. R.; Dayal, R.; Norman, A. W., Isolation and identification of 1,23-dihydroxy-24,25,26,27-tetranorvitamin D3, a new metabolite of 1,25-dihydroxyvitamin D3 produced in rat kidney. *Biochemistry* **1987,** *26* (1), 324-31.

24. Reddy, G. S.; Omdahl, J. L.; Robinson, M.; Wang, G.; Palmore, G. T.; Vicchio, D.; Yergey, A. L.; Tserng, K. Y.; Uskokovic, M. R., 23-carboxy-24,25,26,27-tetranorvitamin D3 (calcioic acid) and 24-carboxy-25,26,27-trinorvitamin D3 (cholacalcioic acid): end products of 25-hydroxyvitamin D3 metabolism in rat kidney through C-24 oxidation pathway. *Arch Biochem Biophys* **2006,** *455* (1), 18-30.

25. Shipley, P. G.; Kramer, B.; Howland, J., Calcification of Rachitic Bone In Vitro. *American Journal of Diseases of Children* **1925,** *30* (1), 37-39.

26. Brumbaugh, P. F.; Haussler, M. R., lα,25-dihydroxyvitamin D3 receptor: competitive binding of vitamin D analogs. *Life Sciences* **1973,** *13* (12), 1737-1746.

27. Pike, W. M., M; Lee, S.M., The Vitamin D Receptor: Biochemical, Molecular, Biological, and Genomic Era Investigations. In *Vitamin D*, Pike, W. S., N. K., Ed. 2011; Vol. 3rd Ed, pp 97-135.

28. Reschly, E. J.; Krasowski, M. D., Evolution and function of the NR1I nuclear hormone receptor subfamily (VDR, PXR, and CAR) with respect to metabolism of xenobiotics and endogenous compounds. *Curr Drug Metab* **2006,** *7* (4), 349-65.

29. Esvelt, R. P.; De Luca, H. F., Calcitroic acid: Biological activity and tissue distribution studies. *Archives of Biochemistry and Biophysics* **1981,** *206* (2), 403-413.

30. Brumbaugh, P. F.; Haussler, D. H.; Bursac, K. M.; Haussler, M. R., Filter assay for 1alpha, 25-dihydroxyvitamin D3. Utilization of the hormone's target tissue chromatin receptor. *Biochemistry* **1974,** *13* (20), 4091-7.

31. Galior, K.; Ketha, H.; Grebe, S.; Singh, R. J., 10 years of 25-hydroxyvitamin-D testing by LC-MS/MS-trends in vitamin-D deficiency and sufficiency. *Bone Rep* **2018,** *8*, 268-273.

2 Liquid Chromatographic Mass Spectrometric Measurement of Calcitroic Acid

2.1 Instrumental Techniques

The analysis of calcitroic acid has previously been conducted through radiolabeling. This included the administration of radioactively labeled vitamin D_3 to rats[9]. The advantage to a method such as this includes great sensitivity that is available with the detection of radioactive species and no background interference from native biological samples. The tradeoff with this method is its inability to determine the structure of radioactive species. In addition, to this hindrance, the cost of radiolabeling comes with either labor intensive reactions or the purchasing of derivatized materials. Due to these limitations the measurement of calcitroic acid through liquid chromatographic tandem mass spectrometric detection was explored.

2.2.1 Introduction to Mass Analyzer

An Alternative to radiolabeled methods, calcitroic acid can be detected using mass spectrometric detection. Mass spectrometry is a sensitive analytical method that operates on the principle of ionization of analytes and then subjecting them to an electromagnetic field. The field then can separate out these species based on the ratio of their charge to mass. This allows only specific species to reach an ion detector[35]. By cycling through different electromagnetic fields in a series called a scan, the instrument can measure the quantity of that given ion present in a sample that is injected into the instrument. While the detection of all the ions that are present within a given sample seems useful, the complexity of a given biological sample most likely will

contain multiple compounds that can generate ions of the same mass to charge ratio as the analyte. Scientists were able to address this issue in part with the development of the tandem mass spectrometer. In tandem mass spectrometry (MS/MS) the principle of separation of ions with the assistance of an electric field is applied multiple times for increased selectivity. Ions pass through a field selecting for a specific charge to mass ratio. These ions are called precursor ions which are then sent through a collision cell where an inert gas fragment the ions generating product ions that are unique in mass to charge ratio. Finally, the product ions are passed through an additional field, which separates these ions based on the mass to charge ratio. If the product ion's mass to charge ratio matches the selected value, the ion's trajectory sends it to collide with an electron multiplier generating the signal. This process can include a single fragmentation step, as was used for the studies described throughout this project. Other instruments that are able to trap ions in an electromagnetic field, such as an ion trap mass spectrometer (MS^n), are able to do multiple instances of fragmentation for further selectivity and structural information[36].

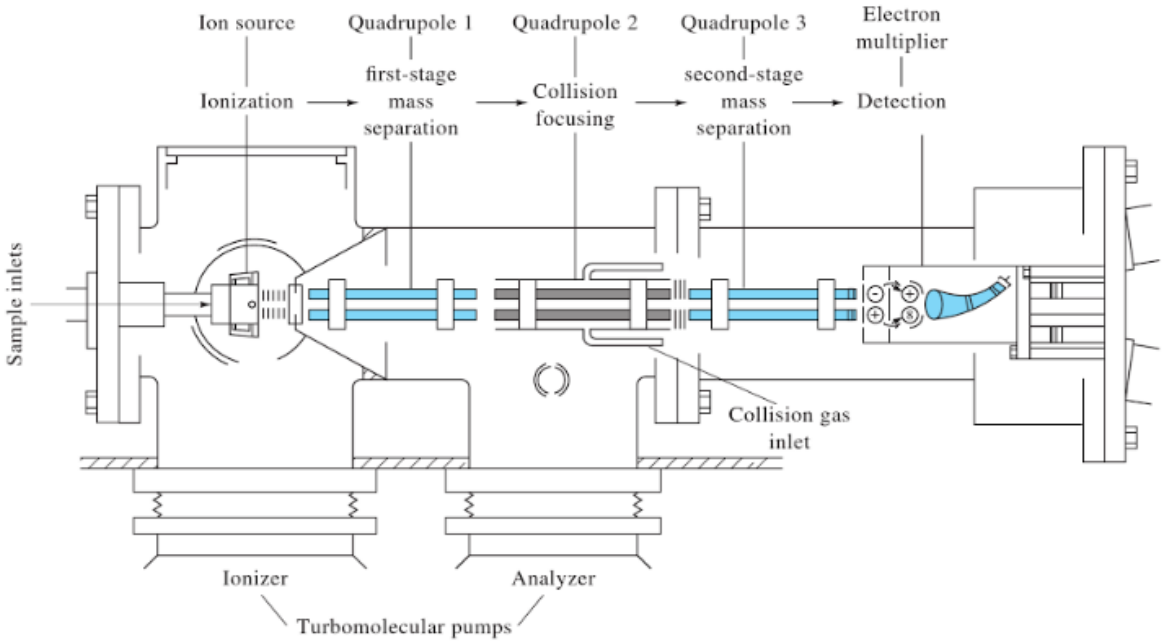

Schematic 4 – Schematic representation of a triple quadrupole mass spectrometer. Often an exterior vacuum is present to reduce the strain on the interior vacuums shown[35].

2.2.2 Introduction to Ionization Source

While the separation of ions within an electromagnetic field is the heart of the mass spectrometer, first the instrument must convert neutral species into ions for separation. There are several different methods which are utilized for the generation of ions for the interface of the instrument. The first method that was developed is electron impact (EI) ionization[37]. In this method a "curtain" of electrons is produced between two electrodes and the sample is passed through. As electrons collide with compounds passed through the electrodes, the compounds are imparted with a charge[38]. This interface is a hard ionization source. The reasoning behind this title is that collision with an electron often will cause fragmentation of the species before it reaches the electromagnetic field. Therefore, when a scan of the ions that are present in each

sample is displayed in a spectrum based on mass to charge, the spectrum reflects the fragments of the initial molecules that were introduced into the ionization source. This can be a benefit in some situations, as discussed previously with tandem mass spectrometry, but in this case all the ions that are generated in an instance within the interface are present withing a single mass spectrum. Another disadvantage to this interface is its inability to ionize large quantities of material. With the presence of a diluent in large quantities this interface quickly would become overwhelmed and diminished ionization would occur on the analyte. Due to this limitation the most optimal species for electron ionization interfaces are highly volatile species that can avoid the presence of solvents reaching the ionization source. For the first chapter of mass spectrometry's history this was a limitation that carried through to all analysis done with this method. Chemical derivatization was an option to improve ionization for mass spectrometry but carried with it a reliance on the efficiency of the reaction to the measurement that was collected. Then a novel concept changed the field bypassing the issue of overwhelming the interface.

Electrospray ionization (ESI) was a method that allowed for the interface of a mass spectrometer to take liquid samples into a mass analyzer opening new opportunities for sample analysis. The electrospray ionization interface creates fine charged droplets. The charge is imparted onto these droplets by passing the liquid samples through a fine charged capillary. A drying gas is then passed over the stream of droplets as they migrate towards the mass analyzer. The drying gas removes the solvent from the droplets causing their size to decrease and bring the imparted charge closer within each droplet. As these charges become closer, there is a point where the coulombic interactions of the ions exceed the surface tension of the droplet causing it to dissociate and transfer the charge from the solvent onto the compounds. The point at which

the imbalance in these forces causes the surface tension to break is known as the Rayleigh limit. The remaining solvent is then removed with a skimmer that filters for charged species. Through this method liquid samples can be directly interfaced with the mass analyzer. This interface in comparison to electron ionization is a soft ionization method. The ionization of species in the interface predominantly generates ions resembling the precursor structure of the compounds introduced to the interface. The most common types of ions that are generated with this type of ionization are protonated or deprotonated species. If there are small ions such as sodium ions or ammonium ions, adducts between compounds and these species are also commonly observed.

Like the electrospray ionization interface, atmospheric chemical ionization (APCI) is a useful method that allows for the interface of liquid samples to a mass analyzer. The method uses an external electrode called the corona needle that allows for the charge to be transferred onto the drying gas that then interacts with the compounds introduced to the interface and transfers that charge. Both methods are best suited for different types of compounds and could be selected for depending on the analytes of each study. APCI has been well established as an ideal ionization source for conjugated systems and working with generating negative ions.

2.2.3 Mass Spectrometric Optimizations for Calcitroic Acid Analysis

The initial conditions that were selected for the interfacing of calcitroic acid for the mass analyzer were atmospheric pressure chemical ionization based on its structure but with poor ionization observed, further optimization of the interface was required. Calcitroic acid has both a conjugated system that runs a portion of the opened ring structure as well as a carboxylic acid

functionally. These two predominant features were considered when selecting the initial conditions for measurement of calcitroic acid. Through the incorporation of a buffer into diluent and mobile phase, the pH of the matrix was adjusted to be higher than the pK_a of calcitroic acid shifting that equilibrium in favor of the deprotonated carboxylic acid form. Standard samples were run on a Shimadzu 8040 triple quadrupole mass spectrometer. A dual source ionization of atmospheric chemical ionization and electrospray ionization (DUSI) was utilized for the interface of the instrument. Direct injections with no liquid chromatography and a single quadrupole scan were conducted to determine the quality of ionization in the interface. It was found that there was moderate ionization of the analyte but diminishing returns of the fragment product ions that were generated from the $[M-H]^-$ precursor ion. Further optimization on the collision energy was conducted but only minor improvements on the signal intensity were observed. Under the current conditions calcitroic acid could be monitored under simplistic matrix conditions with a strong precursor ion signal but the method was not robust enough to allow for measurements to be taken on *in vivo* samples.

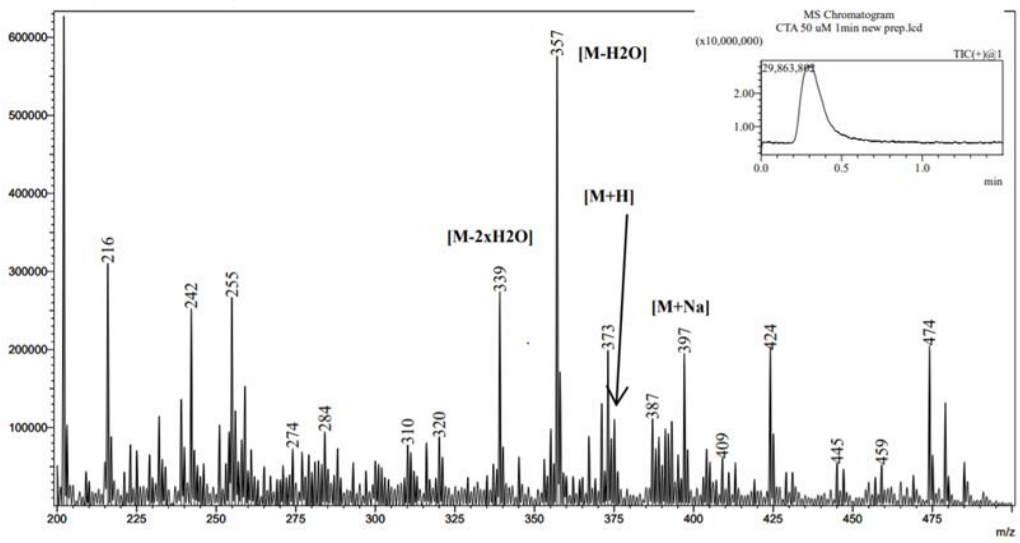

Figure 1 – Mass Spectrum of a 50 µM standard solution of calcitroic acid. The peaks that are labeled are attributed to the analyte of the study. Ions below 200 m/z remain within this spectrum but were also present within blanks on the sample instrument and were considered background signal.

Alternatively, positive mode ionization was conducted on the same standard samples with an adjusted buffer system to explore if protonation of calcitroic acid would provide greater signal of the daughter ions that would be used to identify and quantify calcitroic acid within complex matrices. **Figure 1** shows a mass spectrum of a high concentration, 50 µM, calcitroic acid sample collected on the Shimadzu 8040 tandem mass spectrometer. The mobile phase was methanol with 0.1% formic acid. The instrument was run using DUIS and event speed was set to 7500 scan/sec. The dominant peaks that appear in the spectrum were 339 m/z, 357 m/z, 397 m/z and were identified as $[M - 2H_2O + H]^+$, $[M - H_2O + H]^+$, $[M + Na]^+$ respectively. A modest peak was observed for the protonated form of calcitroic acid, $[M+H]^+$ with 375 m/z. The distinguishing feature of this peak when compared with the deprotonated form, was the improvement in the product ions that were generated in the collision cell. The dominant peaks that were observed in the product ion mass spectrum of standard solutions of calcitroic acid were characterized. Their speculated structures are shown in **Schematic 5**. Both the 357.10 m/z and 339.30 m/z represent

peak that are attributed to the dehydration of the analyte. This type of transition is not ideal for a “fingerprinting” product ion identification due to its lack of specificity but when combined with another ion, such as the 121 m/z transition that is more unique to calcitroic acid can be used for quantification of the analyte. The additional signal that was available through these peaks was enough for the optimization of a method that allowed for the measurement of calcitroic acid *in vitro* during the microsomal stability assays (MSA) **Chapter 2, Figure 14**. A multiple reaction monitoring (MRM) method was then developed to allow for measurement of the ions assigned to calcitroic acid reducing the scan length and allowing for higher resolution.

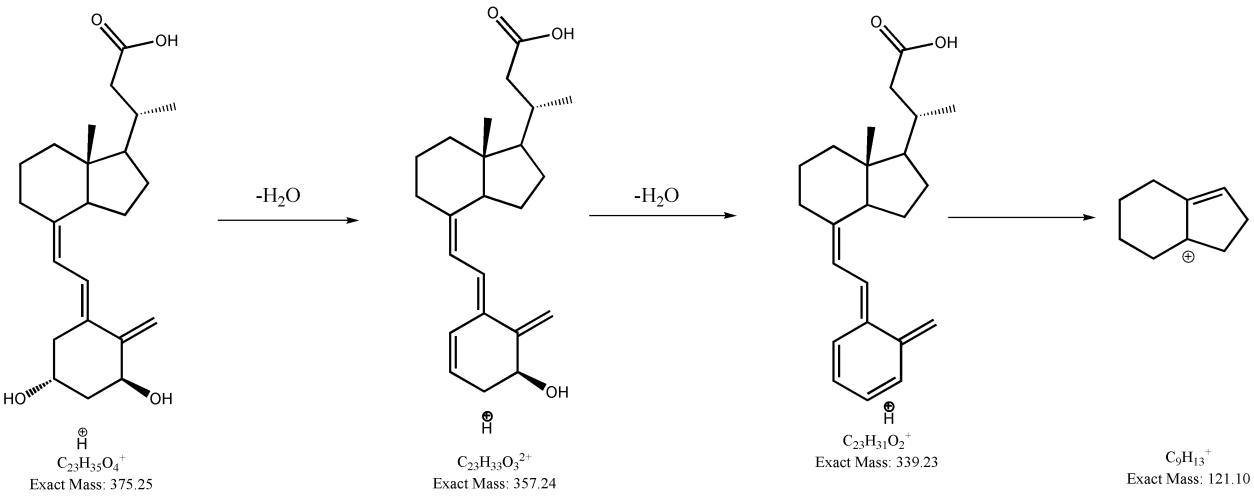

Schematic 5 – The proposed structures of the transitions of calcitroic acid generated within the collision cell. The ions 339.23 and 121.10 were used as the quantification ion and finger printing ion, respectively.

Once the initial determination of calcitroic acid’s metabolic activity was assayed, the exploration of the calcitroic acid’s biological distribution led to revisiting the parameters of the mass spectrometric analysis. The detection limit of the developed method based on the calibration curve shown in **Figure 2B** were 6.1 nM. The initial findings of the biological samples run under the developed method were unable to distinguish blanks from samples where calcitroic acid was hypothesized to be present. Adjustments were made to improve the lower

limit of detection to avoid large quantities of preconcentration of samples before analysis. The first step taken was to see whether the conditions could be modified to shift the dominant form to the $[M+H]^+$ ion. It was found that the change of the ionization to solely ESI provided only a marginal gain in signal, but the change was kept for the remainder of the analysis. Further review of the mass spectrum shown in **Figure 1** showed the option of optimizing a method of one of the dehydrated forms that was present in a single quadrupole scan. As previously mentioned, ESI is considered a soft ionization interface. Some fragmentation can occur for molecules that would lead to ions other than the protonated and deprotonated forms of the analyte. In the case of calcitroic acid, the fragment ion intensity far surpassed the signal from the protonated form under the current conditions. A product ion scan was conducted on the single dehydrated form of calcitroic acid, shown in **Figure 2A**, and three ions 339.30 m/z, 121.15 m/z, and 157.15 m/z were optimized for quantification or qualification. The hypothesized structures for each of these ions are shown in **Schematic 6.** Two of the previously identified ions for calcitroic acid were present in this mass spectra.

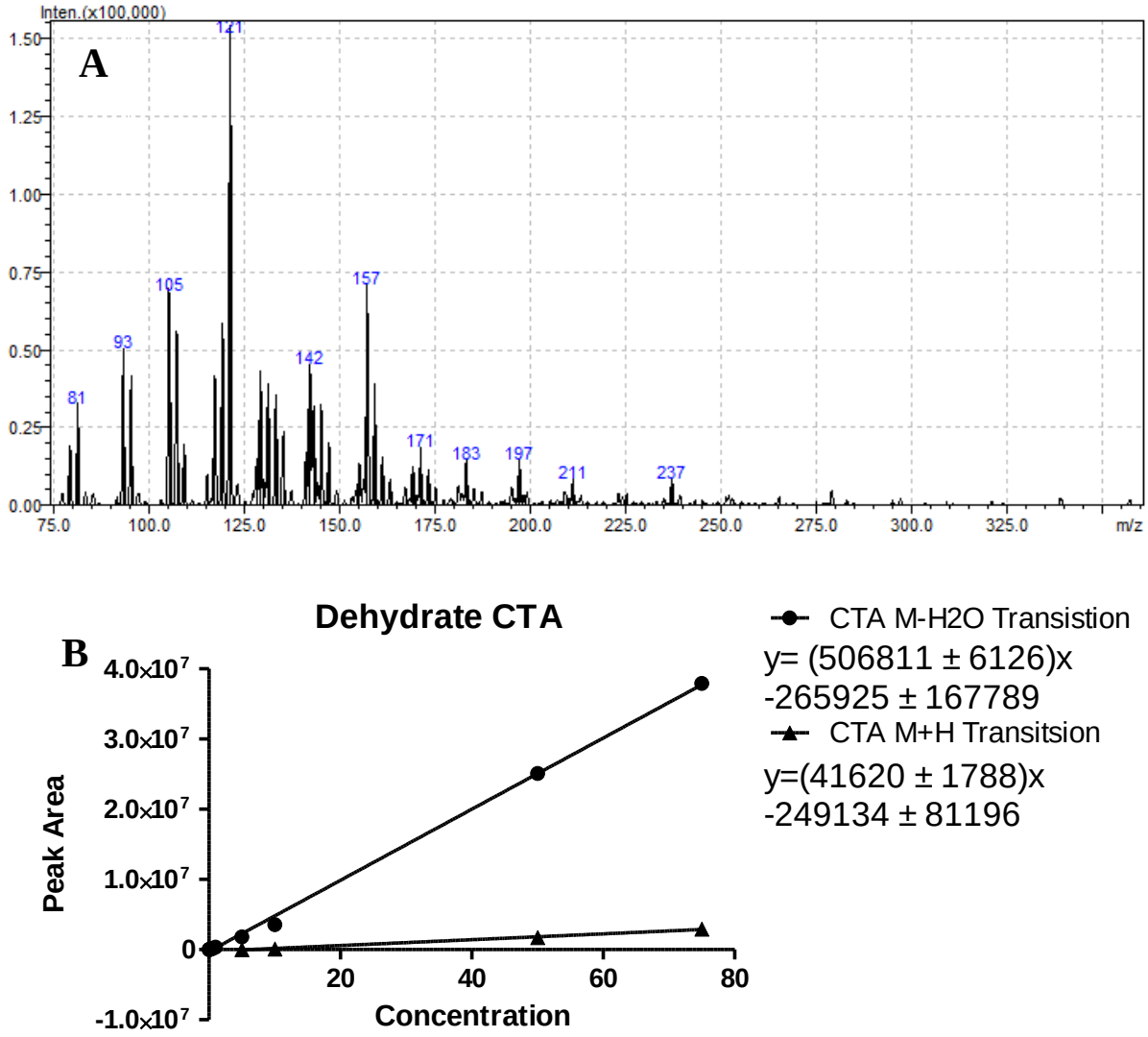

Figure 2 – The initial product ion scan for the dehydrated form of calcitroic acid standards is shown in A. after adjustments to the collision energies, the ion 339 m/z appeared at higher intensity. Overlay of two calibration curves of calcitroic acid based on the precursor ion for the method are shown in B. The circles represent the dehydrated form and the triangles the protonated form. The sensitivity as well as the lower limit of detection was greatly improved working with the dehydrated form.

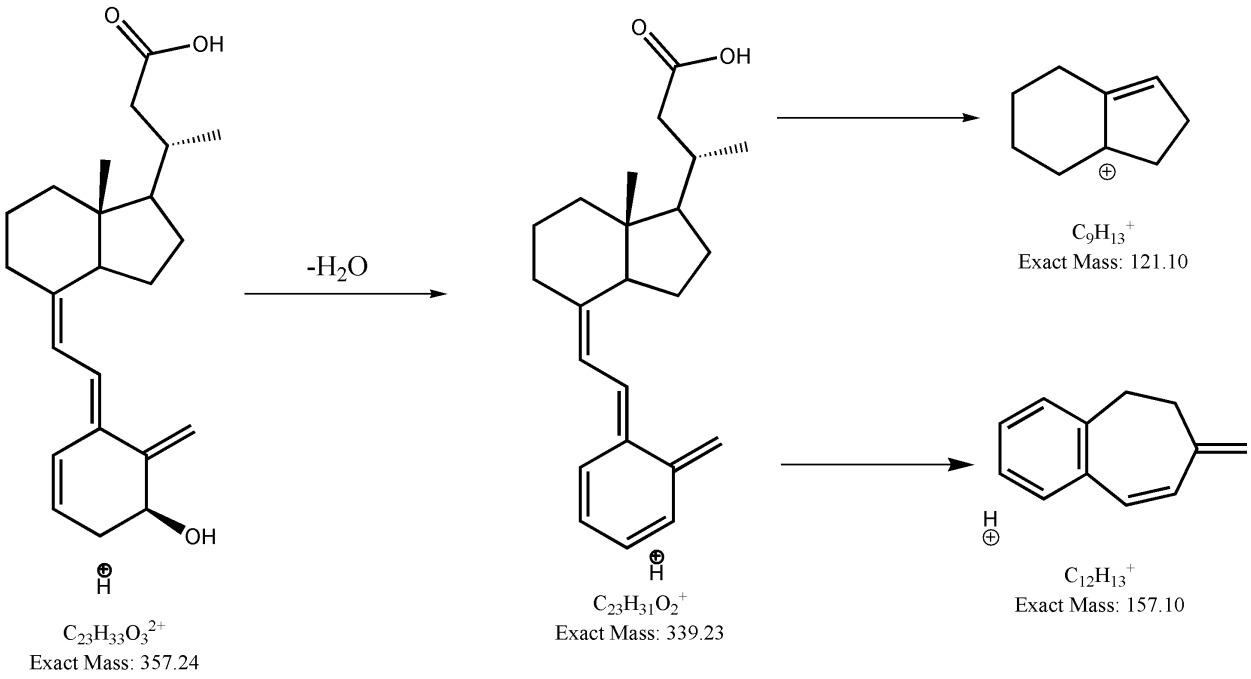

Schematic 6 – Proposed product ion transitions of the dehydrated form of calcitroic acid. Two of the structures are based on the speculations made on the $\{M+H]^+$ product ions.

Confirmation of the interface generating the dehydrated form of calcitroic acid was done to prevent the development of a method dependent on the characteristics of a single standard solution sample. To assure that no sample degradation occurred during the storage of the calcitroic acid a standard of calcitroic acid prepared from solid stocks was run under the same conditions. The chromatograms of both standards are shown in **Figure 3**. We observed that the stock solution standard previously used had a higher purity than the new sample, but the ions of interest were intact and had a retention time corresponding to the initial sample. In addition to this, **Figure 4** shows a thin layer chromatogram (TLC) of the two materials run in 1:9 ethyl acetate: methanol suggesting that no degradation was observed on a large scale in the dissolved stock solution that was initially used. For both these reasons, the 357 m/z peak concluded to originate from the starting material and fragmentation was attributed to the ionization source as the

retention times of the peak assigned to calcitroic acid matched one another.

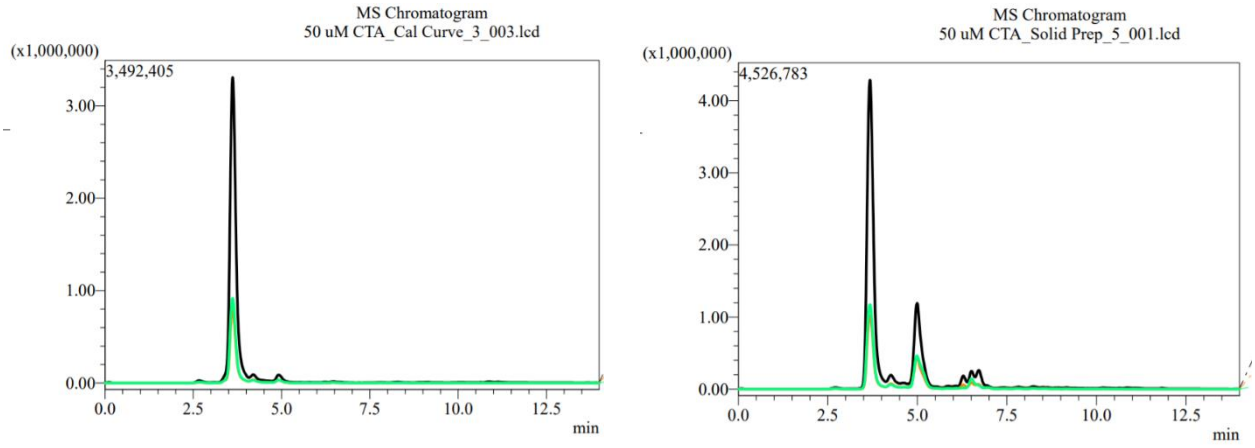

Figure 3 – Chromatograms of 50 µM standard solutions of calcitroic acid. Sample A was a working stock solution of calcitroic acid that was used for the initial development of the dehydrated CTA method. Sample B was a crude solid stock that was prepared to confirm no degradation was behind the ratio of ions observed in the original sample. The chromatogram of the working sample contains few impurities will maintaining the same retention time of the solid samples predominant peak.

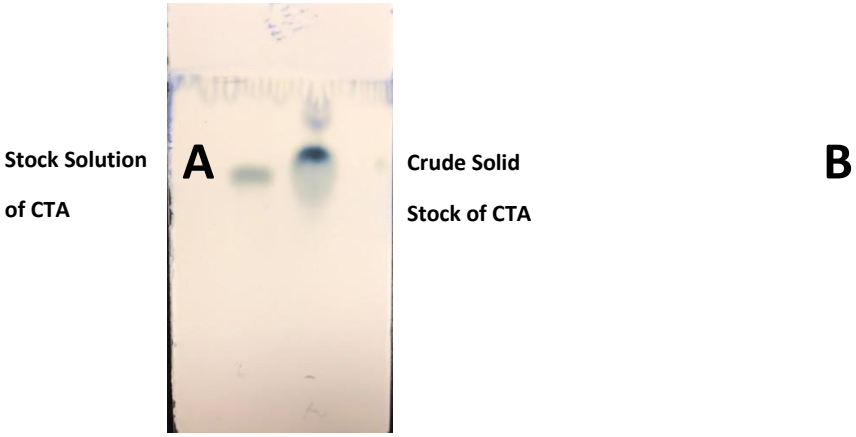

Figure 4 – TLC plate of standard solutions of calcitroic acid. The left lane was the working stock solution of calcitroic acid used for the dehydrated calcitroic acid method. The right lane was the crude solid stock calcitroic acid.

2.3.1 Introduction to Liquid Chromatography

While the specificity of the mass spectrometry is impressive in comparison to many forms of spectroscopy, the true advantage of this method is observed when paired with a separation method such as chromatography[39]. Chromatography is a method that has its roots in some of the

initial separations conducted by Mikhail Tsvet to separate out chlorophyll from plants in petroleum ether with sodium carbonate[40]. The differential migration of species through a media based on its interactions with a stationary phase of the system allowed of the separations of materials without the requirement of a volatile mixture, preventing the exposure to high temperatures, and allowing for novel chemical characteristics to be the differentiating feature[41].

A common theoretic explanation of this method can be seen in the van Deemter model[42]. This model uses a carryover from the method of distillation, theoretic plate count, that remains will the field today. The number of theoretical plates speaks towards the quality of the separation with high theoretical plate counts representing the better separations of species, leading to higher resolution in chromatograms. The model is outlined in **Equation 1**. The A term of the equation represents the Eddy diffusion coefficient. This value is independent of the flow rate and reflects inhomogeneous nature of pathlengths for molecules as they move through a column. Longitudinal diffusion is expressed with the B coefficient of the function. This is a function of Brownian motion within a liquid or gas sample. As the time that the sample can disperse within the column increases this term will increase making it inversely proportional to the flow rate of the mobile phase. Finally, the C term is a partitioning coefficient that describes both the time that is required for migration of species from the mobile phase into the stationary phase and a second term C, with describes the resistance to migration from the stationary phase back into the mobile phase. The sum of each of these terms provides a reflection on theoretical plate height, H. By taking the length of the column and dividing it by the height of an individual plate the number of theoretical plates is found. This model represents the fundamental parameters that must be considered in any chromatographic separation.

$$H = A + \frac{B}{\bar{u}} + C\bar{u} \qquad \textit{Eq. 1}$$

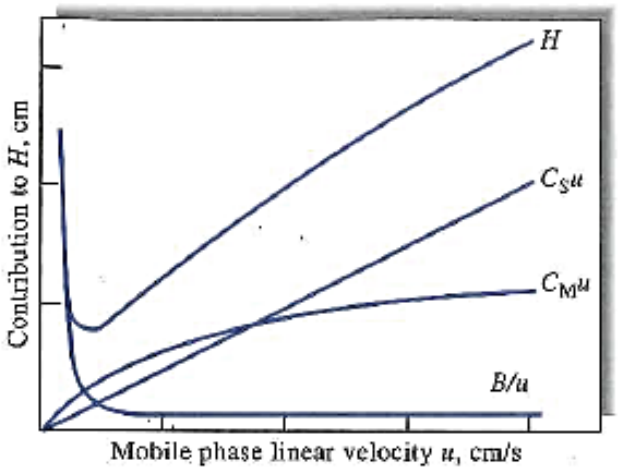

Schematic 7 – Overlay of the three terms of the van Deemter model. Each curve can be summed to find the optimal conditions for a chromatographic separation[38].

Due to the length of gas chromatographic columns in comparison to liquid chromatographic columns the number of theoretical plates has consistently surpassed liquid chromatographic separations. The decrease in the compressibility of mobile phase has not allowed for the same lengths of columns without generating an undesirable pressure gradient across the length of the column. This disadvantage prevents the same quality of resolution of be achieved with liquid chromatographic conditions. Although, working with liquid samples prevents the requirement for volatile species and can avoid incorporation methods of drying of the sample before introduction into the detector. For these reasons liquid chromatography was used for the analysis of calcitroic acid.

This initial method of passing a non-polar solvent over a polar stationary phase with unique migration of compounds was set as a precedent of the normal phase. The separation of non-polar species could be conducted by substituting the stationary phase for a hydrophobic species and a hydrophilic mobile phase to allow for the separation of more non-polar species is considered a reverse phase (opposite of normal phase) separation.

2.3.2 Liquid Chromatographic Optimization for Calcitroic Acid Analysis

The protonated form of calcitroic acid is a bulky structure with a seco-steroidal backbone allowing for the separation under acidic conditions to be conducted using a reverse phase column. The starting conditions for the separations of calcitroic acid took this into account when developing the initial separation for standards. The standard of verapamil HCl was used for the normalization of the ionization of the instrument and INT–777, a synthetic bile acid, was used as an extraction efficiency internal standard. **Figure 5** shows the separation that was achieved once the mass spectrometric parameters for each of these compounds conducted and a short gradient used. A Waters 2.5 µm particle 2.1 x 100 mm C18 bridged ethylene hybrid (BEH) column was used for the separation. Methanol and water were used as the mobile phase with a 0.1% formic acid buffer. The flow rate was set to 0.600 mL/min and the gradient went from 50% organic to 99% organic over 4 minutes. The high organic phase was held and then returned to initial mobile phase composition to maintain column integrity. This method was crude in comparison to the later developed methods for the liquid chromatography but was able to handle the separation that was required for the *in vitro* microsomal stability assays that are described in chapter 4 of this thesis.

While beginning the extraction procedure described in chapter 4, the sample diluent composition became of interest for this analysis and required optimization for tissue sample measurements to be made. The initial conditions that were utilized for a strong anion exchange extraction included a dilution into 5% formic acid. These conditions proved too harsh for the structure of calcitroic acid, causing degradation to occur and the biproducts produced separate peak within the chromatograms collected shown in **Figure 6**. Several different conditions for the concentration and type of acid were explored to prevent this degradation from occurring in the sample. By lowering the concentration and changing to the weaker acid of acetic acid, the ratio of peak area was shifted back to resembling chromatograms previously collected. It was found that the substitution for 0.1 % acetic acid as a buffer proved best suited for the analysis without jeopardizing the solid phase extraction efficiency that is explored in **Chapter 4.** Future extractions of tissue samples utilized this method to prevent degradation of calcitroic acid before the chromatographic analysis.

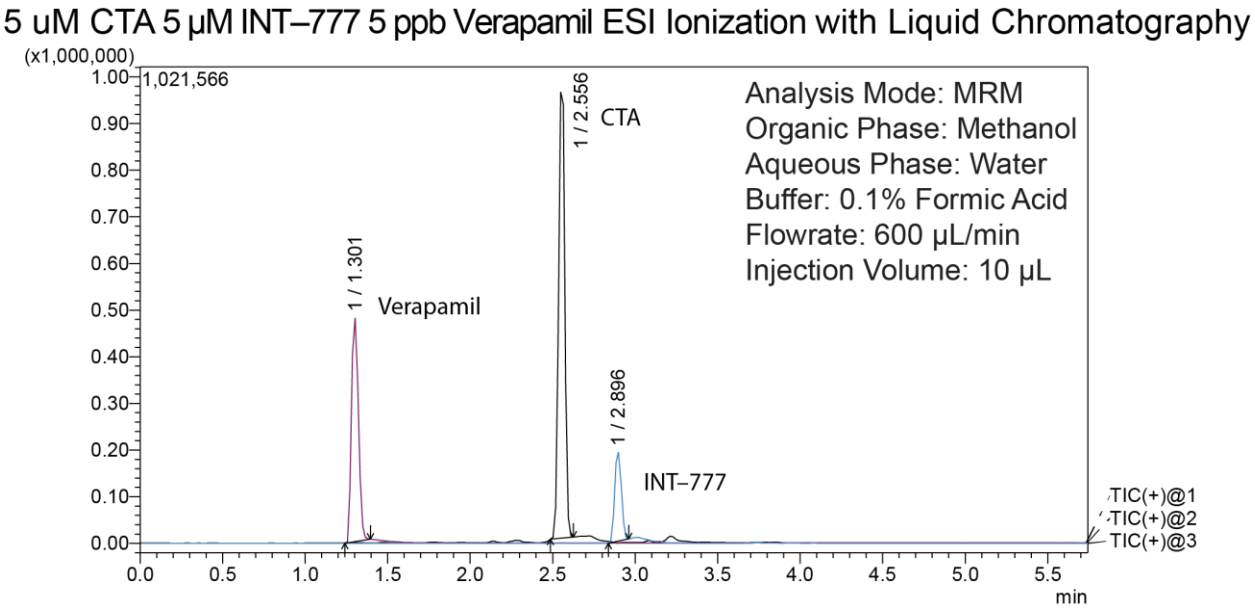

Figure 5 – Chromatogram of calcitroic acid separated from two internal standards Verapamil and INT–777. This method demonstrating proper separation. Note the concentration of CTA is quite high in this sample allowing this method only to be used in samples with high concentrations.

During the procedure development for the extraction of calcitroic acid from biological matrices, the transition from high performance liquid chromatography to ultra-high-performance liquid chromatography became of interest. Previously the column that was used for the separations of calcitroic acid from standards was a Restek C18 column with 5 µM particle size and internal dimensions of 50 x 4.6 mm. By changing this column for a UHPLC column the same level of separation was achieved while removing time from the method allowing for higher sample throughput, ideal for future microsomal assays as well as large batches of tissue samples. The downside to this change was the need to revisit the instrumental standards during the chromatographic optimization.

Instrument: 8040

Detector: MRM

Daughter Ions: 357.10 >> 339.30; 157.15; 121.15

Sample Solvent: MeOH : Acid Listed on Chromatograms

Mobile Phase: MeOH : H_2O 0.1% formic acid

Flow Rate: 0.500 mL/min

Liquid Chromatography: Restek C18 5 µm 50x4.6 mm

Gradient: 0.0 min: 70% MeOH; 0.5 min: 70% MeOH; 7.5 min: 99% MeOH; 10.5 min: 99 % MeOH; 10.75 min: 70 % MeOH;

Oven: 40 °C

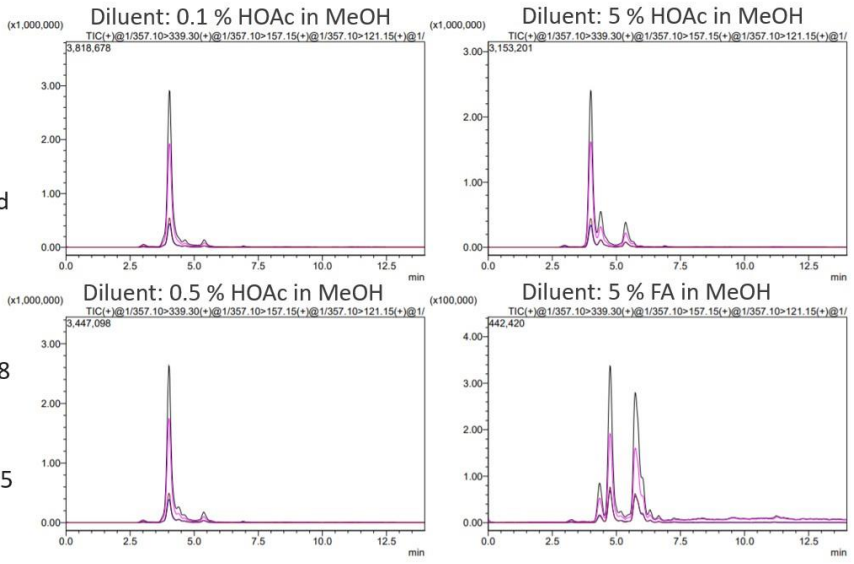

Figure 6 – Comparison of diluent composition on the chromatography of calcitroic acid samples. Chromatogram A, B, C, and D are diluted in 0.1% acetic acid, 5% acetic acid, 0.5 % acetic acid, and 5 % formic acid, respectively. We observed that as the concentration and strength of the acid was decreased, the number of peaks that attributed to degradation products decrease.

Verapamil, the initial instrumental standard, was found to have variable retention times throughout sample batches, making the integration of the peaks in chromatograms unreliable. Since the instrumental internal standard is one of the more interchangeable portions of the method, other alternatives were explored. The potential compounds shown in **Schematic 8** were considered. A majority these standards did not have optimal logD values for proper retention by a reversed phase column. Several other standards had issues with poor ionization within the interface and antipyrine formed dimer ions posing questions of the signal consistency. Of the compounds that were screened for mass spectrometry signal and chromatographic retention, 4,5 diphenylimidazole (4,5–DPI) was identified as the best option for the instrumental internal standard. Once the mass spectrometric method was optimized for this standard, chromatography with the UHPLC column was conducted. The initial chromatogram is shown in **Figure 7**. There was a significant amount of the 4,5–DPI that was not being retained on the column and coming out in the void peak preventing consistent integration of the retained species

among samples. The other standards were then run under the same chromatographic conditions to see if they presented better retention under these conditions. All the instrumental internal standards showed the same peak splitting effect. Further optimization of the chromatographic parameters was then made to address the signal splitting.

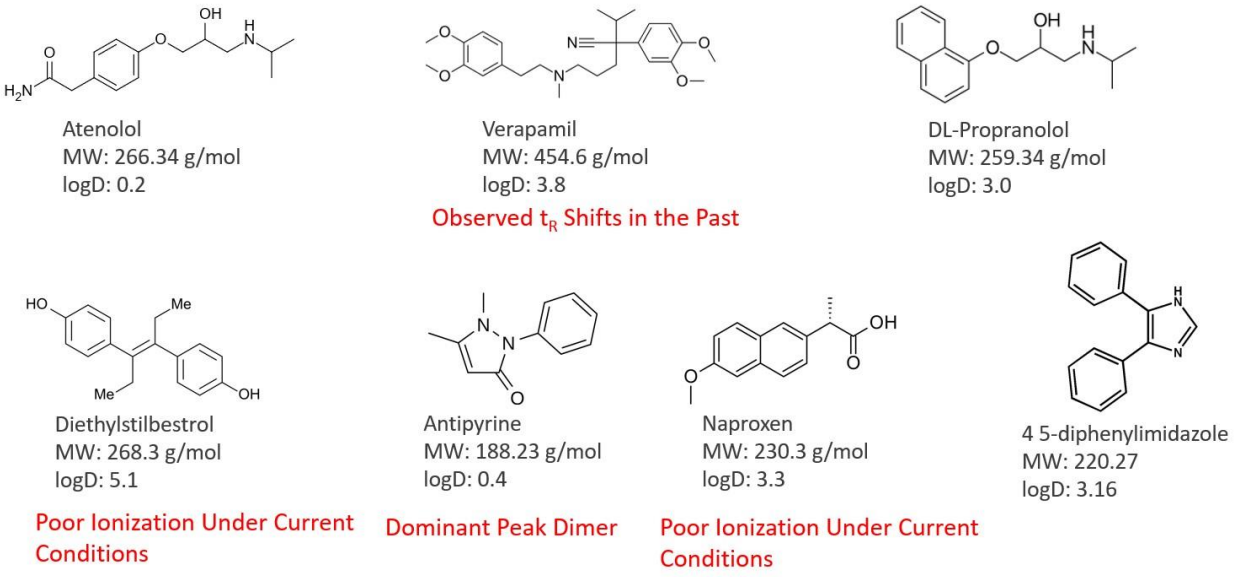

Schematic 8 – Structures of the screened molecules for instrumental internal standards for the UHPLC–MS/MS method.

Instrument: 8040

Detector: MRM (Just showing TICs of Events)

CTA –357.10>> 339.30; 157.15; 121.15

Atenolol –267.15>> 145.15; 190.20; 56.05

Verapamil – 455.25>> 165.15; 150.15; 303.30

Propranolol –261.20>> 56.05; 116.20; 184.15

Sample Diluent: MeOH 0.1% HOAc

Mobile Phase: MeOH : H_2O 0.1% formic acid

Flow Rate: 0.500 mL/min

Liquid Chromatography: Agilent Extend-C18,2.1x50mm

Gradient: 0.0 min: 50% MeOH; 0.5 min: 50% MeOH; 3 min: 99% MeOH; 4 min: 99 % MeOH 4.1 min: 50 % MeOH;

Oven: 40 °C

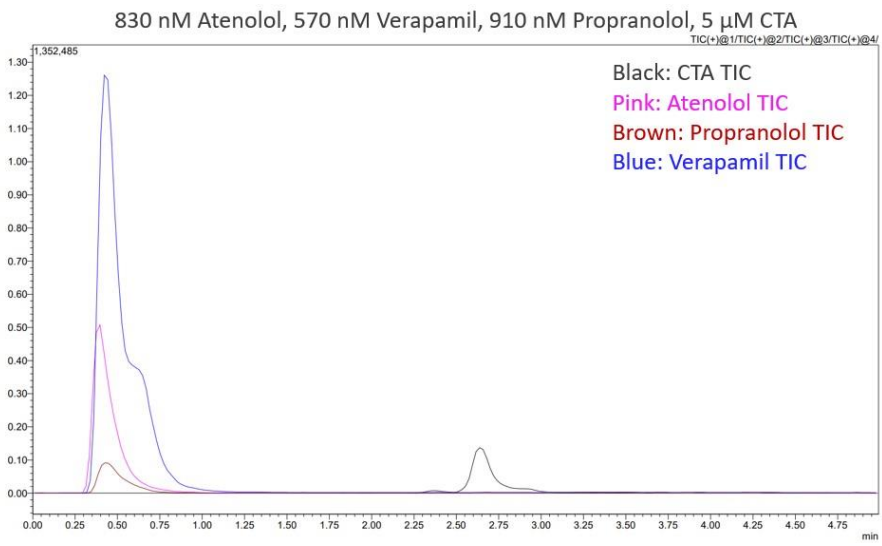

Figure 7 – Initial chromatographic overlay of the instrumental internal standards screened with strong enough ionization for mass spectrometric optimization. All three of the internal standards had poor retention on the column under the initial conditions and further optimization was required to improve retention.

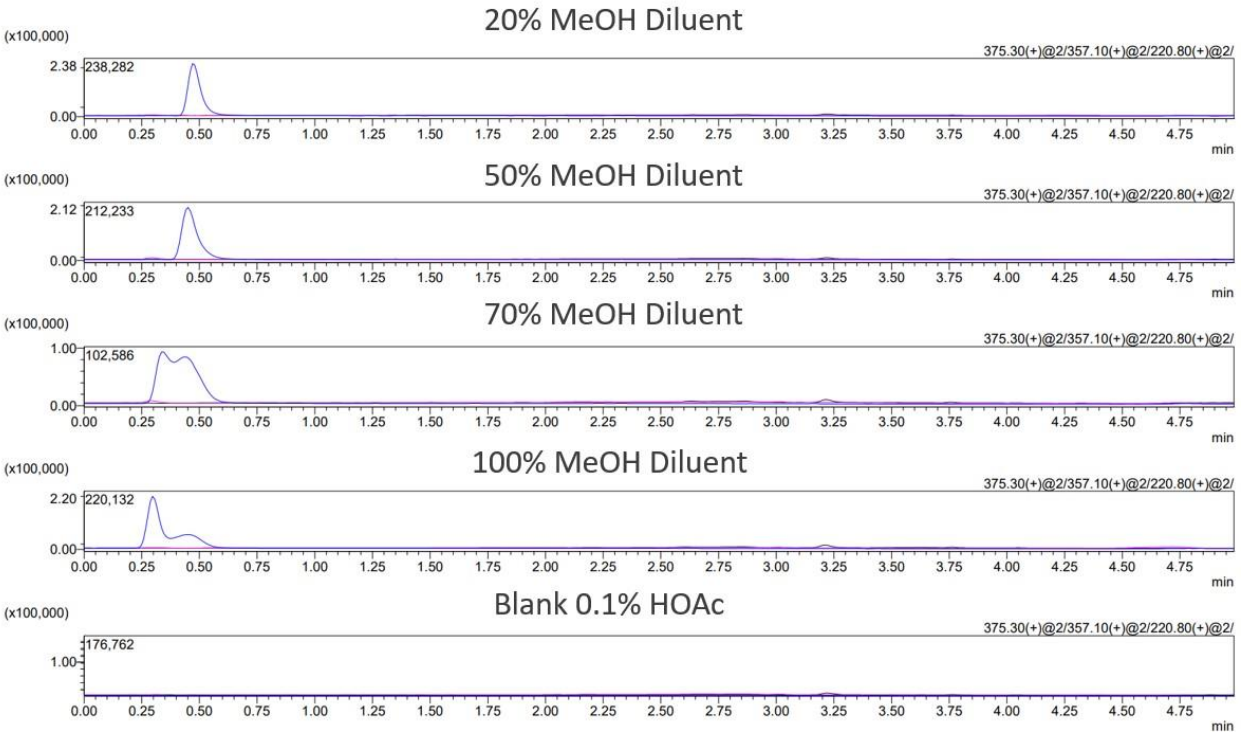

Figure 8 – Chromatograms of 1 µM 4,5–DPI standard solutions prepared with different diluent compositions. The diluent composition has consequences for the extraction procedure that is described in chapter 4.

Through changes made to the chromatographic parameters, an UHPLC method was developed with appropriate separation of calcitroic acid from the instrumental internal standard.

First, the starting composition of the mobile phase was adjusted to explore if the hydrophilicity of the standard was causing the void peak. A comparison between different diluent compositions affects upon the retention of 4,5–DPI standard solutions shown in **Figure 8**. Different column temperatures were also explored to rule out some form of sample degradation occurring on the column. The area between the peaks remained consistent suggesting that the change in retention times was chemical. The initial method for the separation included a hold at the initial mobile phase composition to allow for polar species to be eluted in the void peak to simplify the collected chromatograms. This hold was removed from the method and the gradient started at the initial time of the run, unifying the signal of 4,5–DPI in the chromatogram into a single peak. The final resulting gradient was as follows, the aqueous and organic mobile phases were optima grade water with 0.1% formic acid and methanol with 0.1% formic acid, respectively. Samples were prepared through serial dilution in methanol 0.1% acetic acid. The flow rate was set to 0.500 mL/min and the mobile phase composition started at 20% organic (MP B) and increased to 80% over 2 minutes. The gradient then continued to increase the organic composition to 99% over 1 minute. The high organic composition was then held for 1 minute before returning to 20% organic and holding for 1 minute. The time of each separation was 5 minutes. The final resulting method was conducted on a standard sample of calcitroic acid and 4,5–DPI and the resulting chromatogram is shown in **Figure 9**. The instrument standards appear as a single peak and calcitroic acid has a retention time closer to the tail end of the gradient but not retained after the gradient is complete. The remaining two minutes after the gradient was intended to prevent buildup of highly hydrophobic matrix species within the column. The final return to 20 % mobile

phase B allows for the mobile phase composition within the column to match the start of the gradient on any subsequent runs.

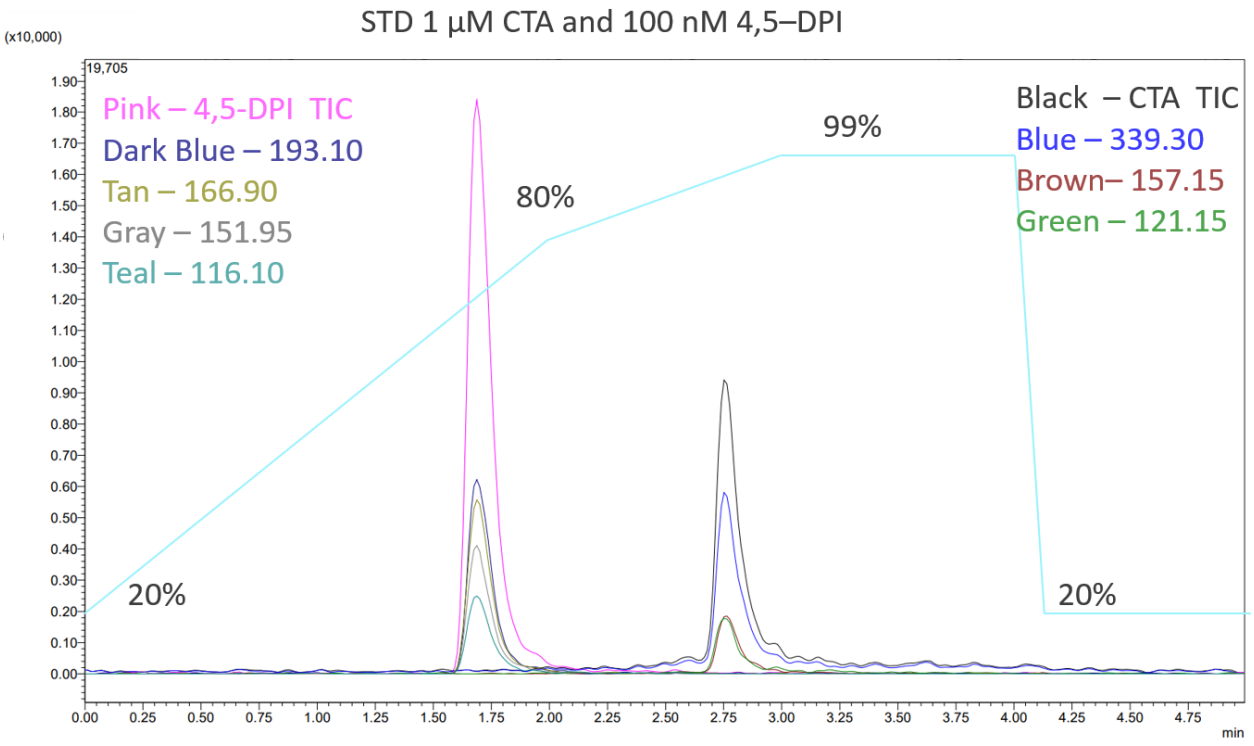

Figure 9– A chromatograph of a standard solution of calcitroic acid and 4,5–DPI using the developed separation. The gradient is overlayed in light blue in concentration of organic mobile phase as a percentage.

2.4 Conclusion

The measurement of calcitroic acid has been of interest for many decades. At the time of its initial discovery the goals of the researchers that conducted those studies had very different questions in mind. The quantification of *in vivo* calcitroic acid would have been a challenging prospect before the innovations in mass spectrometry that allowed for the interface of liquid samples. The lack of nonspecific derivatizing agents to allow for GC–MS or HPLC–UV Vis detection come with a series of challenges that will be further discussed in chapter 5. Though every method that was developed for this study was not optimal for all calcitroic acid measurements, the early

methods were simple allowing for samples with simple matrices to be properly separated. Later after further consideration of the conditions, further improvements were achieved that allowed for the decreasing of the lower limit of detection to 6.1 nM. In addition to the improvements to the mass analysis, the liquid chromatographic separation that was achieved allowed for a high throughput method for the measurement of calcitroic acid in complex matrices. The separation was more robust than the initial method and when paired with the extraction procedure described in chapter 4, certainty on the distribution of calcitroic acid was determined.

References

1. Onisko, B. L.; Esvelt, R. P.; Schnoes, H. K.; DeLuca, H. F., Metabolites of 1 alpha, 25-dihydroxyvitamin D3 in rat bile. *Biochemistry* **1980,** *19* (17), 4124-30.
2. Skoog, D. A.; West, D. M.; Holler, F. J., *Fundamentals of Analytical Chemistry*. 9th ed.; Saunders College: New York, 1988.
3. Eliuk, S.; Makarov, A., Evolution of Orbitrap Mass Spectrometry Instrumentation. *Annu Rev Anal Chem (Palo Alto Calif)* **2015,** *8*, 61-80.
4. Griffiths, J., A brief history of mass spectrometry. *Anal Chem* **2008,** *80* (15), 5678-83.
5. Skoog, D. A.; Holler, F. J.; Crouch, S. R., *Principles of Instrumental Analysis*. 7th ed.; Saunders College Pub.: Philadelphia, 1997.
6. Loos, G.; Van Schepdael, A.; Cabooter, D., Quantitative mass spectrometry methods for pharmaceutical analysis. *Philos Trans A Math Phys Eng Sci* **2016,** *374* (2079).
7. Tswett, M., Physical-chemical studies of chlorophyll. Adsorption. *German Botanical Society* **1906,** *3-10*, 384-393.
8. Martin, A. J.; Synge, R. L., Separation of the higher monoamino-acids by counter-current liquid-liquid extraction: the amino-acid composition of wool. *Biochem J* **1941,** *35* (1-2), 91-121.
9. van Deemter, J. J.; Zuiderweg, F. J.; Klinkenberg, A., Longitudinal diffusion and sesistance to mass transfer as causes of nonideality in chromatography. *Chemical Engineering Science* **1956,** *5* (6), 271-289.

3 Metabolic Stability of Calcitroic Acid

The metabolic conversion of a compound speaks towards its bioavailability and half-life within an animal. Pharmacokinetic studies can be used for this purpose but are challenging due to the interplay between absorption and elimination. Alternatively, *in vitro* metabolic stability assays can model the metabolic pathway of a compound and allow for information of key enzymes to be identified[43]. The liver and kidneys are responsible for the conversion of most xenobiotics and native ligands into more hydrophilic species and priming molecules for further conjugation for excretion and circulation. liver, hepatocytes, can be collected, homogenized, and centrifuged to isolate membrane bound enzymes responsible to metabolism. The corresponding fraction of the centrifuged samples are called liver microsomes, a fraction containing the highest concentration of the endoplasmic reticulum[44]. By incubation of compounds with the appropriate cofactor, NADPH, the metabolic activity of the oxidative pathway was explored in this study.

3.1 Phase I Metabolism of Calcitroic Acid

The oxidative metabolism is classified as phase I metabolism and encompasses many known modifications made to compounds that enter the body. The primary class of enzymes that conduct these modifications are P450 enzymes[44]. The oxidation of a compound leads to the improvement in its hydrophilicity allowing for it to be circulated through the bloodstream and finally excretion from the bile ducts, or kidneys into the bladder. There are many novel ways in which xenobiotics have been developed to control the release or activity of a compound that take advantage of this conversion. While P450 enzymes are predominantly expressed within hepatocytes, these enzymes are also expressed within renal cells.

Calcitroic acid has long been identified as an end product to the oxidative metabolism of 1,25-dihydroxyvitamin D[45, 46]. This assumption was made based on the absence of other oxidation products using *in vivo* and *ex vivo* studies.

Calcitroic acid was incubated with human and mouse hepatocytes microsomes in two sets of replicates along with the two precursors to generate NADPH, G6PGH and $NADP^+$ with the cofactor Glc-PO_4. A reduction is done upon the $NADP^+$ converting it to the proper oxidation state for the assay. The limited stability of the NADPH during storage and even during the enzymatic reaction prevents oxidative microsomal activity assays over one hour. The microsomal mixtures were buffered with a 0.5 M phosphate buffer and microsomes were stored at -80 °C before the study and allowed to come to room temperature 30 min before the study began. The mixtures were incubated at 37 °C for the course of the study. Calcitroic acid and microsomal mixture were combined in the absence of NADPH and an aliquot for the zero time point of the study was taken. Then, the assay was initiated with the introduction of the NAPDH and 50 µL aliquots were collected in 10 min intervals for 1 hour. Each of these time points was collected and immediately quenched when added to a 96 well plate containing 100 µL of methanol containing internal standard verapamil. The quenched samples were stored on ice throughout the assay. The plate was then transferred, and vacuum filtered to remove precipitated proteins due to the percentage of methanol. 100 µL of the filtered samples were diluted to 500 µL in methanol and the resulting samples analyzed through the previously described mass spectrometric analyses for the microsomal stability assay.

The assay was conducted and analyzed using the method outlined in **Chapter 2**. The integration was automated based on the retention time determined for standard samples. The

339.30 m/z was used for the quantification of calcitroic acid throughout the procedure. This signal was normalized to a signal that was observed with the instrumental internal standard, verapamil. Finally, the time points were normalized to the starting concentration of calcitroic acid in the microsomal mixture and the natural log was taken of these values were plotted in **Figure 10** to demonstrate the first order kinetic conversion of the analyte. The assay was replicated to confirm the results of the assay.

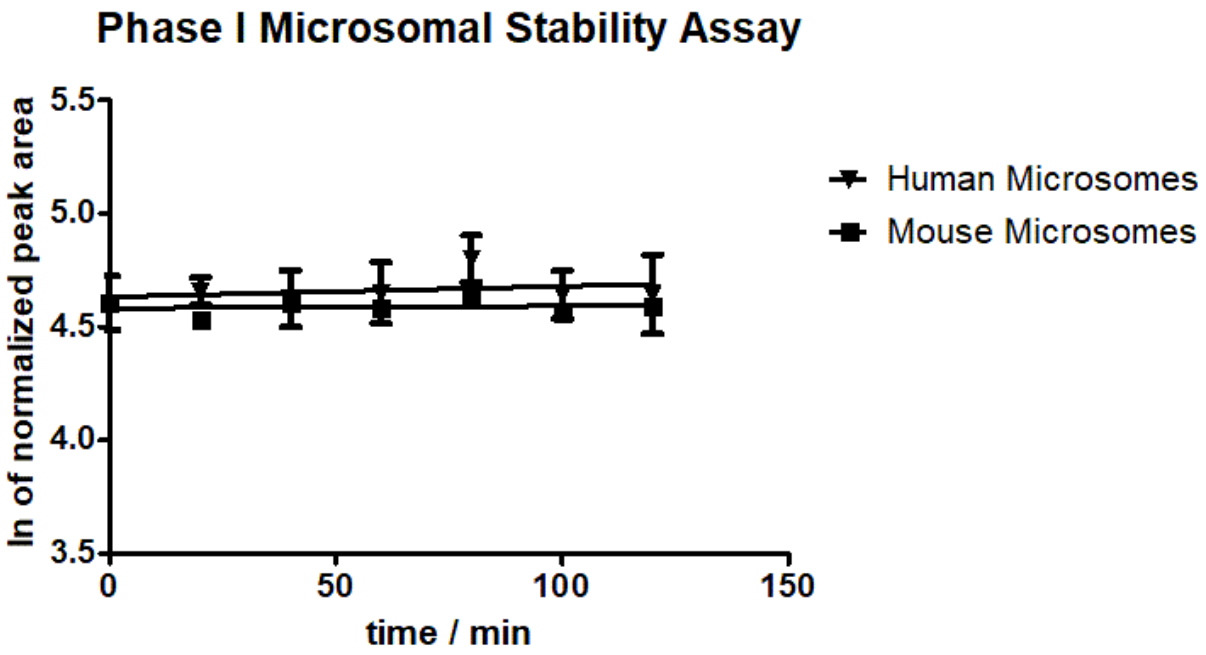

Figure 10 – Oxidative microsomal stability assay of calcitroic acid conducted with both human (triangles) and mouse (squares). The slope of the natural log of each assay was determined to not significantly deviate from zero suggesting no activity.

It was found that the slope of the linear regression of the nature log of the time points did not significantly deviate from zero. This suggested that the activity of P450 enzymes on calcitroic acid was negligible. These findings were further confirmed with a positive control conducted with a compound JDP–107 under the same conditions which was found to have half–

life of 135.9 min. These findings confirm the assumption that was previously made, that calcitroic acid is the phase I metabolic end product of vitamin D through the 25 oxidative pathways.

3.2 Phase II Metabolism of Calcitroic Acid

While phase I metabolism serves as a mechanism for increased solubility to allow for the transport, change in activity and final excretion of metabolites, phase II metabolism further increases the solubility of compounds to increase the clearance and prevents passive cellular membrane transport. Phase II metabolism is a class of enzymatic reactions in which a conjugate is added onto a molecule to further increase solubility for its excretion through the bile ducts or in urine through the bladder. The general title for these enzymes is transferase enzymes with each type of moiety addition having a sub–class title. Transferase enzymes of interest are localized within hepatic and renal cells. A common property of each of the possible conjugates is that they increase aqueous solubility of these compounds in. Some of the most abundant forms of conjugates include glucuronic acid, glucose, sulfate, and amino acid (glycine, and taurine). Cellular localization of the enzymes responsible for cellular reactions vary depending on the class. For example, the uridine 5'-diphospho-glucuronic acid transferase (UDPGA) enzymes[47] are present within the endoplasmic reticulum while the sulfotransferase (SULTs) enzymes[48] are present in the cytosol. This difference needed to be accounted for along with the cofactors of each reaction when modeling the process in the *in vitro* assays. The appropriate centrifugal fraction was utilized to account for the cellular distribution of the enzymes of interest.

Bile acids, a structurally similar class of molecules to calcitroic acid, have been shown to undergo phase II metabolism in the liver before secretion through the bile ducts[49]. In addition,

vitamin D's predominant circulating form, 25-hydroxy vitamin D or calcifediol, is shown to undergo sulfate conjugation further suggesting possible conjugation of calcitroic acid[50]. The goal of this set of assays was to determine whether similar metabolic processes govern the final excretion of vitamin D metabolites that undergo the 1,25 metabolic pathways.

3.2.1 Glucuronic Acid Conjugation of Calcitroic Acid

The first group of activities that was assayed was the conjugation of calcitroic acid with glucuronic acid. This was speculated to be the most likely form of conjugation that would occur with this analyte. The proposed reaction is shown in **Schematic 9** The conditions were modeled after the phase II microsomal stability assay described in Shimada *et al.* (1997)[51]. Later the assay conditions were adjusted further to account for the weak initial metabolism of calcitroic acid. A positive assay control was an established compound that our group had previously found to undergo this form of conjugation.

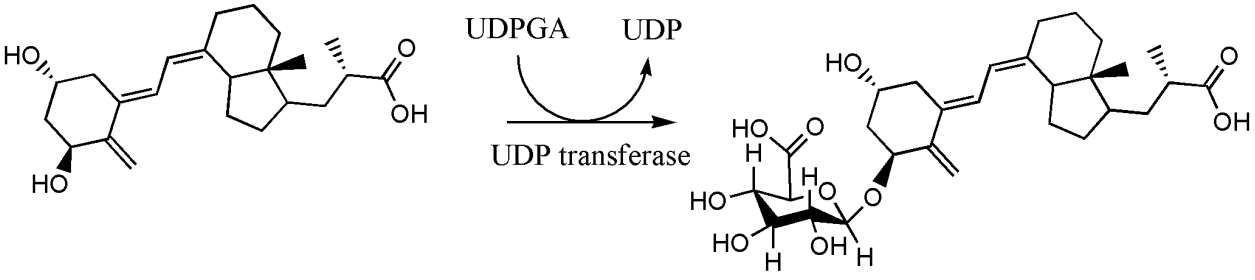

Schematic 9 – A proposed reaction for the formation of a glucuronic acid conjugate. Other possible sites for this conjugation could occur on the 3-hydroxyl position as well as the carboxyl.

The conditions for the assay were as follows. A microsomal mixture was prepared in a 0.5 M concentration of phosphate buffer with a pH of 7.4. 1 mM of $MgCl_2$ was added to the mixture for a final concentration of 0.1 M. The surfactant alamethicin[52] was added to the mixture to disturb the endoplasmic reticulum to insure availability of the uridine phosphotransferase in the solution. D-Saccharic acid 1,4-lactone[53] was used as an inhibitor to the reverse reaction to prevent the loss of any of the conjugate that may have been formed. Calcitroic acid was then added to the mixture to the final concentration of 10 µM. The cofactor of UPDGA was added to a final concentration of 5 mM to start the reaction. Six replicates of both human and mouse microsomes throughout this study were collected. Microsomes came to room temperature for 1 hour before their addition to the reaction vials. A summary of the final reagent concentrations is shown in **Table 1**. The reactions were performed for 2 hours with time point aliquots collected every 10 min. Each aliquot was quenched in a solution of methanol containing the instrumental internal standard of (4,5–DPI). Samples were then vacuum filtrated and diluted in methanol 5-fold. The samples were then placed in the autosampler of the Shimadzu 8040 for HPLC–MS/MS analysis following the procedure outlined in **Chapter 2**.

Table 1 – A summary of the reagents and their respective concentrations for the phase II microsomal stability assay of hepatic glucuronidation.

Reagent	Conc	unit
0.5 M PO4 Buffer	0.1	M
50 mM UDPGA	0.005	M
50 mM D-saccharic acid 1,4-lactone	0.005	M
0.1 M MgCl2	0.001	mM
1 mM Analyte	0.01	mM
5 mg/mL Alamethicin in DMSO	0.0225	mg/mL

Human Liver S9 (20mg/mL)	0.44	mg/mL

Flurbiprofen, and analog of ibuprofen, was used as a positive control for the assay. Flurbiprofen has previously been reported to form a glucuronide conjugate[54]. The final ionization of flurbiprofen was unpromising for the activity of the enzyme under these conditions. Alternatively, activity was observed with both the disappearance of the native species and the formation of the glucuronic acid conjugate of the lead compound of another project of our group, MIDD0301. A replicate of the assay was conducted and used as a confirmation of the assay conditions for calcitroic acid. The results are shown in **Figure 11**. MIDD0301 was found to have a half–life of 110.7 min under these conditions.

A replicate of the study was conducted with calcitroic acid with the conditions shown above. The results are shown in **Figure 12**. Calcitroic acid was found to have a metabolic assay slope that did not significantly deviate from zero suggesting stability under hepatic phase II glucuronic acid metabolism. These findings could be further confirmed with synthesis of the glucuronic acid conjugated form of calcitroic acid, a project that our group is exploring. Using a standard sample of the glucuronic acid conjugate of calcitroic acid, would allow for the monitoring of the formation of the conjugate in the assay in addition to the disappearance of starting material. The necessity of this type of method development appeared minor as the current finding suggests that calcitroic acid does not undergo glucuronidation. Futher studies into renal glucuronide metabolism would allow for a greater understanding of this form of conjugation on calcitroic acid.

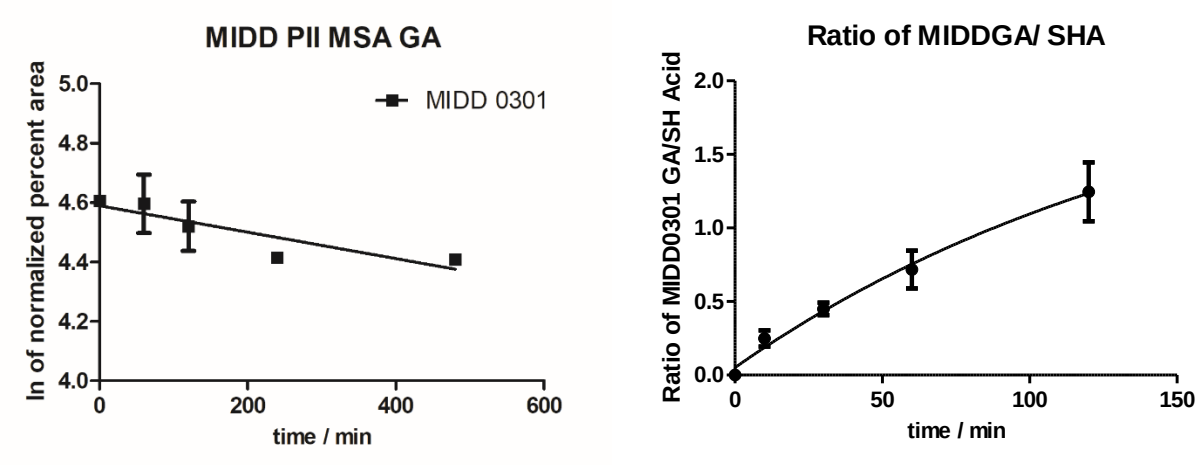

Figure 11 – Glucuronidation metabolic stability assay using human liver microsomes n = 6 for MIDD 0301. The monitoring of the loss of MIDD 0301 is reflected on the left while the right shows the normalized signal of its glucuronide increasing during the assay. The half-life was determined to be 110.7 min.

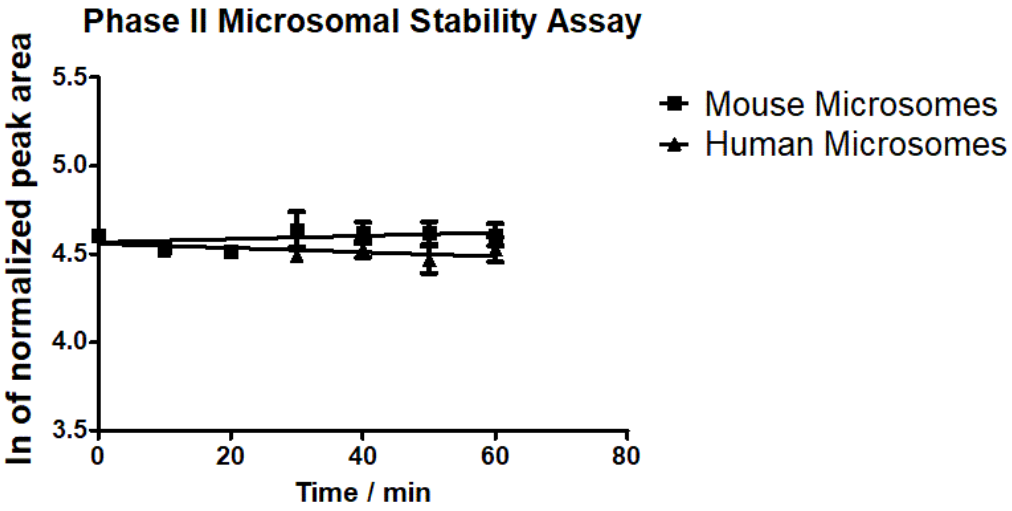

Figure 12 – The metabolic stability assay of calcitroic acid normalized against an instrumental internal standard. The linear regression of the natural log of the signal did not significantly deviate from zero suggesting no activity. For this reason, no metabolic values were assigned for this assay.

3.2.1 Sulfate Conjugation of Calcitroic Acid

Other vitamin D metabolites have been shown to undergo sulfate conjugation leading to the interest in calcitroic acid's availability for this moiety addition[55]. The enzymes responsible for this conjugation are sulfotransferase (SULTs). They use the cofactor 3'-phosphoadenosine-5'-phosphosulfate (PAPS) as a source of sulfate to increase the solubility of both endogenous and

exogenous compounds. The conjugation can occur at similar sites on the analyte's structure including hydroxyl, carboxyl, and amine functionalities[56]. **Schematic 10** is a representation of the proposed reaction. Incubation with calcitroic acid and hepatic and renal cytosol centrifugal fractions paired with the cofactor, PAPS, still needs to be explored within our group to confirm the stability of calcitroic acid. Synthesis of the mono- and di- sulfates of calcitroic acid were prepared for standard solutions for the development of a HPLC–MS/MS analysis. It was found that the ionization of these compounds was limiting for the development of a method that would monitor the formation of the metabolite throughout the study.

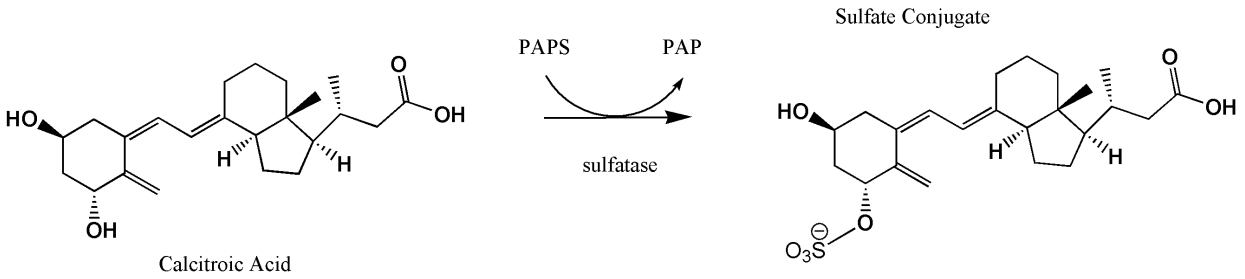

Schematic 10 – A representation of the conversion of calcitroic acids conjugation with a sulfate. Both hydroxyl groups could potentially undergo this conjugation as well as the carboxyl moiety.

The disappearance of the calcitroic acid under the assay conditions may prove to be more reliable for measures conducted with HPLC–MS/MS. Alternatively, GC–MS was successfully utilized for the characterization of the synthesized sulfate conjugates. With modifications to the workup procedure for the metabolic stability samples, a method could be developed with this instrument for measurements. Once the metabolic stability is determined under these conditions, a more specific identification of enzymes may be available. By incubation with individual enzymes under the same reaction conditions the metabolic variables of K_m and V_{max} will be determined.

3.2.2 Amino Acid Conjugation of Calcitroic Acid

Like a previously discussed phase II metabolic processes, conjugation with amino acids is a mechanism that animals utilize to increase solubility of exogenous and endogenous compounds for circulation and clearance. The amino acid that is commonly utilized by animals to metabolize compounds is glycine. The other molecule that will be discussed in this section is taurine, a small sulfonic acid with a terminal amine. Taurine is present in large quantities in bile and is used as a substrate in the biological synthesis of taurochenodeoxycholic acid[57]. Due to the localization and hepatic circulation of calcitroic acid, the possibility of these forms of conjugation were of interest to this project. A hypothesized reaction of calcitroic acid is shown in **Schematic 11**.

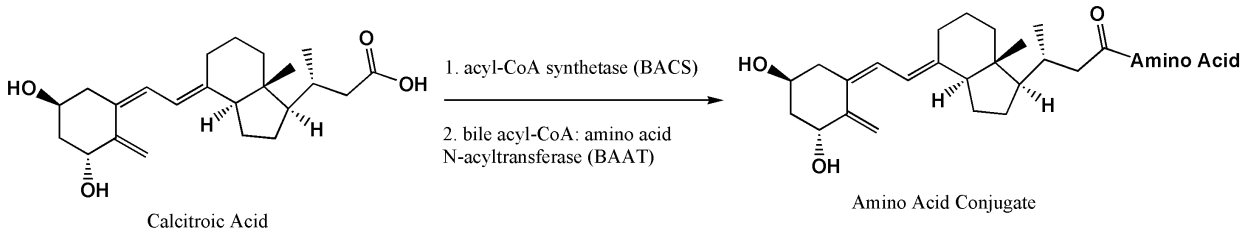

Schematic 11 – The representation of the proposed reaction of the calcitroic acid conjugate formation with amino acids and taurine. Unlike the previous conjugation reactions this reaction would be localized to the carboxyl functional group.

The class of enzymes that are expected to be responsible for this form of conjugation are acyl-CoA synthetase (BACS) and acyl-CoA: amino acid N-acyltransferase (AAT). When provided with the cofactor, ATP, BACS can conjugate the coenzyme A with an acetyl moiety (in this reaction attaching calcitroic acid). Then, the BACS substitutes the CoA with the second cofactor, glycine or taurine, forming the final product and releasing CoA[49].

To monitor the second step of this metabolism calcitroic acid will first need to be modified into a thioester with CoA. This molecule would then allow for the activity and kinetics of the

amino acid N-acyltransferase to be determined. Alternatively, to the use of human liver microsomes, purified BACS will be used for this set of assays. Biological pH and temperature will still be utilized. Currently the synthesis of CoA-calcitroic acid is still in progress and future members of this project will conduct this assay. If activity is observed in the assay relevant kinetic values will be determined and assigned. While the dominant location of this form of conjugation occurs within the liver, renal phase II metabolism and excretion may be a part of the process. Each assay will be replicated with the corresponding renal fractions and enzymes to speak towards the total metabolism.

It has been shown that a series of bile acids that underwent phase II metabolism have the process reversed by bacteria within the intestine[49]. Our group is interested in determining if a similar process occurs. If it is found that phase II metabolism occurs upon calcitroic acid future assays, conjugated calcitroic acid will be incubated with isolated hydrolases from C. *welchii*. to monitor the deconjugation.

3.3 Conclusion

Calcitroic acid was initially determined to be the end product of vitamin D within animals. This conclusion was determined based on a method of radiolabeling and derivatization reaction GC–MS which would not be able to discern calcitroic acid from other possible metabolites that may form. In this study we have shown no significant activity of P450 enzymes occurs upon calcitroic acid. This suggests calcitroic acid is the true final oxidative metabolite of 1,25 dihydroxy-vitamin D. It was also found that a glucuronic acid conjugation assay shown to work on a positive control of MIDD0301 did not show significant conversion of calcitroic acid into a conjugate in hepatic conditions. Further assays in this study will continue to explore the possibilities of other

common phase II metabolism in both hepatic and renal conditions to determine if calcitroic acid truly is the 1,25 dihydroxy-vitamin D final metabolite.

References

1. Paolini, M.; Bauer, C.; Corsi, C.; Del Carratore, R.; Nieri, R.; Bronzetti, G., Stability of microsomal mono-oxygenase during incubations for the liver microsomal assay with S9 fractions of mouse liver under various inductions. *Mutat Res* **1983,** *110* (2), 221-30.

2. Nelson, D. L.; Cox, M. M., *Principles of Biochemistry*. Fifth ed.; Sara Tenney 2008; p 1158.

3. Zimmerman, D. R.; Reinhardt, T. A.; Kremer, R.; Beitz, D. C.; Reddy, G. S.; Horst, R. L., Calcitroic acid is a major catabolic metabolite in the metabolism of 1 alpha-dihydroxyvitamin D(2). *Arch Biochem Biophys* **2001,** *392* (1), 14-22.

4. Onisko, B. L.; Esvelt, R. P.; Schnoes, H. K.; Deluca, H. F., Excretion of metabolites of 1 alpha, 25-dihydroxyvitamin D3 in rat bile. *Arch Biochem Biophys* **1980,** *205* (1), 175-9.

5. Meech, R.; Hu, D. G.; McKinnon, R. A.; Mubarokah, S. N.; Haines, A. Z.; Nair, P. C.; Rowland, A.; Mackenzie, P. I., The UDP-Glycosyltransferase (UGT) Superfamily: New Members, New Functions, and Novel Paradigms. *Physiol Rev* **2019,** *99* (2), 1153-1222.

6. Gamage, N.; Barnett, A.; Hempel, N.; Duggleby, R. G.; Windmill, K. F.; Martin, J. L.; McManus, M. E., Human sulfotransferases and their role in chemical metabolism. *Toxicol Sci* **2006,** *90* (1), 5-22.

7. Hofmann, A. F.; Hagey, L. R., Key discoveries in bile acid chemistry and biology and their clinical applications: history of the last eight decades. *Journal of Lipid Research* **2014,** *55* (8), 1553-1595.

8. Epstein, E. H., Jr.; Han, A.; Shackleton, C. H., Failure of steroid sulfatase to desulfate vitamin D3 sulfate. *J Invest Dermatol* **1983,** *80* (6), 514-6.

9. Shimada, K.; Mitamura, K.; Nakatani, I., Characterization of monoglucuronides of vitamin D2 and 25-hydroxyvitamin D2 in rat bile using high-performance liquid chromatography-atmospheric pressure chemical ionization mass spectrometry. *Chromatography B* **1997,** *690*, 348-354.

10. Vollmer, M.; Klingebiel, M.; Rohn, S.; Maul, R., Alamethicin for using in bioavailability studies? - Re-evaluation of its effect. *Toxicol In Vitro* **2017,** *39*, 111-118.

11. Oleson, L.; Court, M. H., Effect of the beta-glucuronidase inhibitor saccharolactone on glucuronidation by human tissue microsomes and recombinant UDP-glucuronosyltransferases. *J Pharm Pharmacol* **2008,** *60* (9), 1175-82.

12. Kuehl, G. E.; Bigler, J.; Potter, J. D.; Lampe, J. W., Glucuronidation of the aspirin metabolite salicylic acid by expressed UDP-glucuronosyltransferases and human liver microsomes. *Drug Metab Dispos* **2006,** *34* (2), 199-202.

13. Axelson, M., 25-Hydroxyvitamin D3 3-sulphate is a major circulating form of vitamin D in man. *FEBS Lett* **1985,** *191* (2), 171-5.

14. Shimada, K.; Mitamura, K.; Saito, K.; Ohtake, Y.; Nakatani, I., Enzymatic hydrolysis of the conjugate of vitamin D and related compounds. *J Pharm Biomed Anal* **1997,** *15* (9-10), 1207-14.

15. Falany, C. N.; Johnson, M. R.; Barnes, S.; Diasio, R. B., Glycine and taurine conjugation of bile acids by a single enzyme. Molecular cloning and expression of human liver bile acid CoA:amino acid N-acyltransferase. *J Biol Chem* **1994,** *269* (30), 19375-9.

4 Identification and Quantification of Calcitroic acid in Biological Settings

4.1 Introduction

The determination of calcitroic acid's distribution and concentration were of interest to determine its biological role within humans. Therefore, mice were first explored due to the availability of tissue samples and the ability to administer mice with samples of calcitroic acid. The robust method that was designed for the liquid chromatographic separation and mass spectrometric measurement of calcitroic acid was the starting point of the detection of calcitroic acid in biological samples. The method was initially designed employed an organic solvent induced precipitation of large biological molecules followed by filtration and detection. Methods have been designed with a procedure like this in mind by Reddy *et al*[28]. The method described in **Chapter 2** summarizes what was initially used for the mass spectrometric parameters of the initial findings.

The goal of this research was to determine if calcitroic acid was present in a concentration that was sufficient to be biologically active. Previous members of our group have reported that calcitroic acid is able to bind to the vitamin D receptor (VDR) receptor and form the retinoid-X receptor (RXR) complex. Understanding the localization of calcitroic acid will speak towards its ability to induce this complex that is responsible for gene transcription.

4.2 The need for Separation Methods Beyond Liquid Chromatography

The initial studies that were conducted were unable to separate calcitroic acid from the matrix generated by the background in the respective chromatograms. Previous groups had

reported a simple liquid–liquid extraction for the separation of bile acids from liver and bile samples for LC–MS analysis[58]. The analysis began at this point due to the ease of sample preparation under similar conditions.

Swiss Webster mice were used during this study. Livers were collected during necropsy and transported to the lab on ice before homogenization with 1.0 g to 1 mL of MeOH. These homogenates were centrifuged and passed through a 0.2 µm nylon filter to remove remaining particulates. The procedure for this instrumental analysis is described in chapter 2. In **Figure 13** the generated chromatogram is shown along with the corresponding instrumental parameters. The chromatogram of the sample was more complex than what was initially expected under these conditions. No peak with corresponding retention time and product ion ratios was observed in the initial samples collected.

Instrument: 8040

Ionization: Positive

Mode: MRM

CTA Transitions: 375.30>357.25; 339.25; 121.15

Sample Solvent: 50 % MeOH 50% H_2O 0.1% formic acid

Mobile Phase: MeOH: 0.1% formic acid H_2O

Flow Rate: 0.600 mL/min

Liquid Chromatography: 130 Å, 2.5 µm, 2.1 x 100 mm BEH–C18

Gradient: 0.0 min: 50% MeOH; 0.5 min: 50% MeOH; 4.0 min: 99% MeOH; 4.75 min: 99 % MeOH; 5.0 min: 50 % MeOH;

Oven: 45 °C

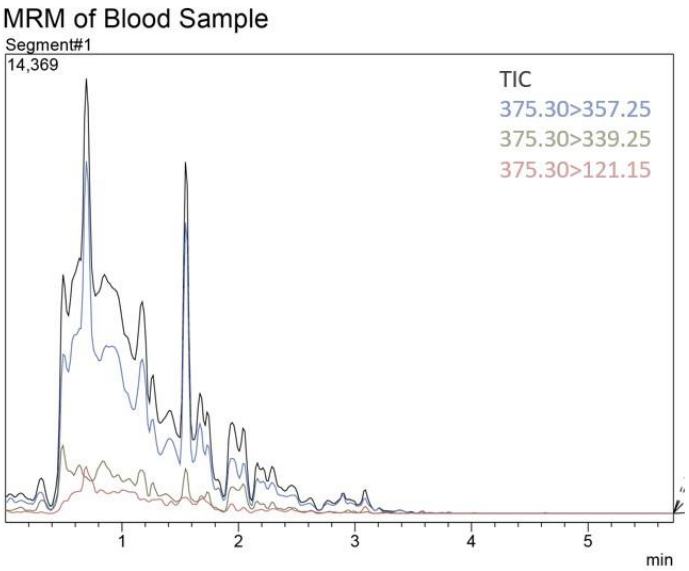

Figure 13 – Initial method to explore the simplest form of sample preparation for chromatographic separation. It was found that the background signal was too high, and the chromatographic separation did not allow for the quantification of calcitroic acid.

It was thought that the sample preparation conditions could be improved by the removal of matrix that may be suppressing the ionization of the analyte. Forms of additional separation were then explored to try and address these concerns.

4.3 Liquid–Liquid Extraction

The conditions that were used in the beginning of this extraction were closer to an organic crash than a liquid–liquid extraction. A liquid–liquid extraction was thought of as a possible method and researched for this application although was not part of the final implemented method.

Liquid–liquid extraction operates on the principle that two non–miscible phases allow for the exchange of compounds at the interface of the phases. The root of this type of exchange is proportional to the amount of surface area that is generated between these phases. The partitioning between the two phases will operate on a similar equilibrium as what is observed in the equilibrium term in the van Demeter model [38].

The most common model of a liquid–liquid extraction is a water:hexane model in which the logD represents the equilibrium of concentration observed between the two phases. Based on the calculated logD value of calcitroic acid the partitioning into an organic phase would be minimal in a water non–miscible solvent. For this reason, liquid–liquid extraction was not optimized for this study. Another barrier for the incorporation of liquid-liquid extractions would have been the low through put of samples not allowing for this method to be scaled to larger numbers of samples.

4.4 Solid Phase Extraction

Solid phase extraction (SPE) was a logical alternative for the extraction procedure to minimize the quantity of solvents used and maintain a high throughput of samples through the procedure. Another advantage of solid phase extraction comes from the ability to utilize unique interactions such as ionic interactions for the extraction of calcitroic acid. Selectivity based on hydrophobic interactions was already implemented within the chromatographic separation. If a new property of calcitroic acid was selected for in the extraction, the method could remove many structurally similar compounds to simplify the final chromatographic separation. The preconcentration of the samples was also an option that was explored in the extraction procedure as the final eluent does not need to match the loading volume of the sample placed on the solid phase cartridge. The decrease in the amount of diluent led to a final increase concentration of the sample upwards of 8-fold.

Solid phase extraction can be conducted in an on–line or off–line method. While on–line methods allow for the high throughput of samples, optimization of extraction methods can be more cumbersome than off–line methods. The general procedure for the solid phase extractions is outlined in **Schematic 12**. Each of the following sections will describe the optimization of solvents used during the extractions and the effects on the homogenization steps, as well as chromatographic analysis.

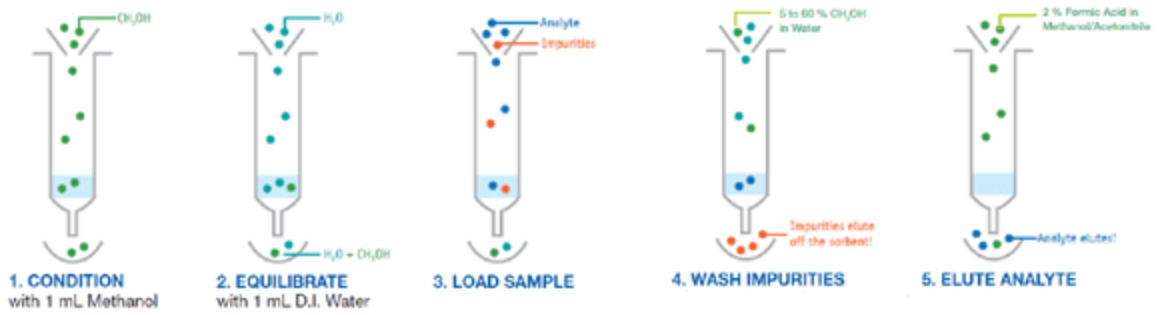

Schematic 12 – A representation of the basic procedure of a solid phase extraction. Solvents would be matched with the type of analyte and stationary phase for the best performance[59].

4.4.1 Reverse Phase Solid Phase Extraction

The initial conditions that were explored for the separation of calcitroic acid from biological systems were based on reverse phase interactions. The intermolecular forces that govern the partitioning and adsorption into a solid phase in these methods rely on the van der Waals interactions, and π–π stacking dependent on the structure of the analyte and stationary phase. Other interactions that molecules in the solution may outweigh the energy gained from these interactions preventing them to be held in the stationary phase. This difference in functional groups allows for selectivity for hydrophobic species preventing many the large charge species from interfering with the detection. The disadvantage of this method was that no additional properties of the analyte beyond its hydrophobicity were selected for in this analysis, so the simplification of the chromatographic separation were not observed.

To determine the parameters of this extraction, pipette tips affixed with a C18 stationary phase were explored for this portion of the study. The extraction procedure for this part of the study is shown in **Schematic 13**. MilliporeSigma ZipTips™ pipette tip cartridges were used for this study paired with aqueous and MeOH eluents for the wash and elution steps of the procedure. Standard solutions of calcitroic acid were prepared and used for the determination of the

extraction efficiency through the procedure. For higher throughput in measurements, a Tecan plate reader is used for the measurements of the sample extracted with the SPE. First a spectrum from 200 – 700 nm of the calcitroic acid standard solution was collected and is shown in the **Figure 14**. The wavelength of 264 nm was selected and used for spectrometric measurement throughout the study. The diluent's absorption was measured in parallel to these samples and subtracted from the total absorbance to accurately determine the absorption of calcitroic acid at this wavelength. The pipette cartridges were pretreated with methanol then water before aspiration of the samples in an aqueous load solution. The loaded cartridges were then washed with an aqueous solution to remove hydrophilic species from the cartridge. Finally, the cartridges were treated with 500 µL of MeOH to elute off the sample into a solution for detection. This method with standards was found to have a high recovery rate of 95% shown in **Figure 15**. This was thought to be promising as it would correspond to a low loss of sample through the extraction allowing for a low limit of detection for the final extraction procedure. In addition to these finding the low standard deviation on this extraction prevented the introduction of variance into the extraction procedure maintaining the accuracy of the measurements.

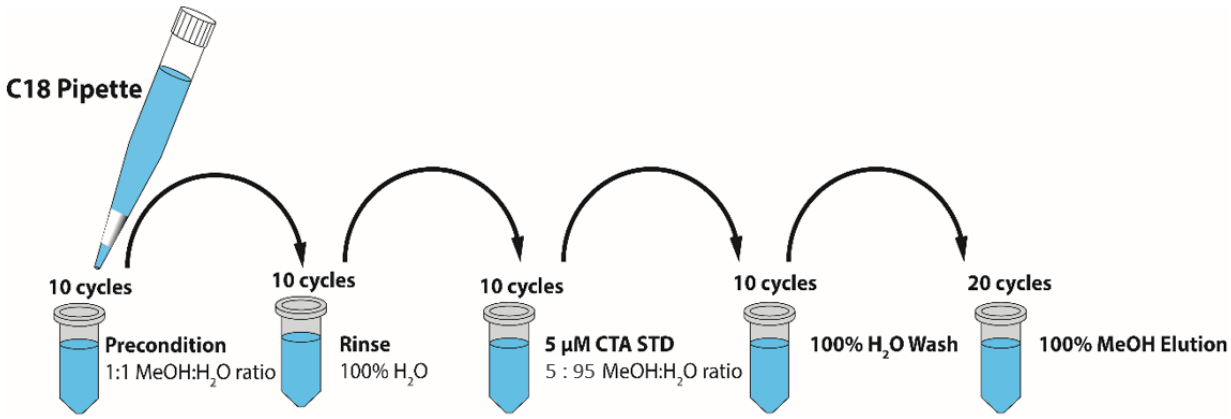

Schematic 13 – A representation of the reverse phase extraction procedure of calcitroic acid tissue extraction. The solvent composition of the load solution was adjusted by the evaporation of the samples and reconstitution in the appropriate solvent.

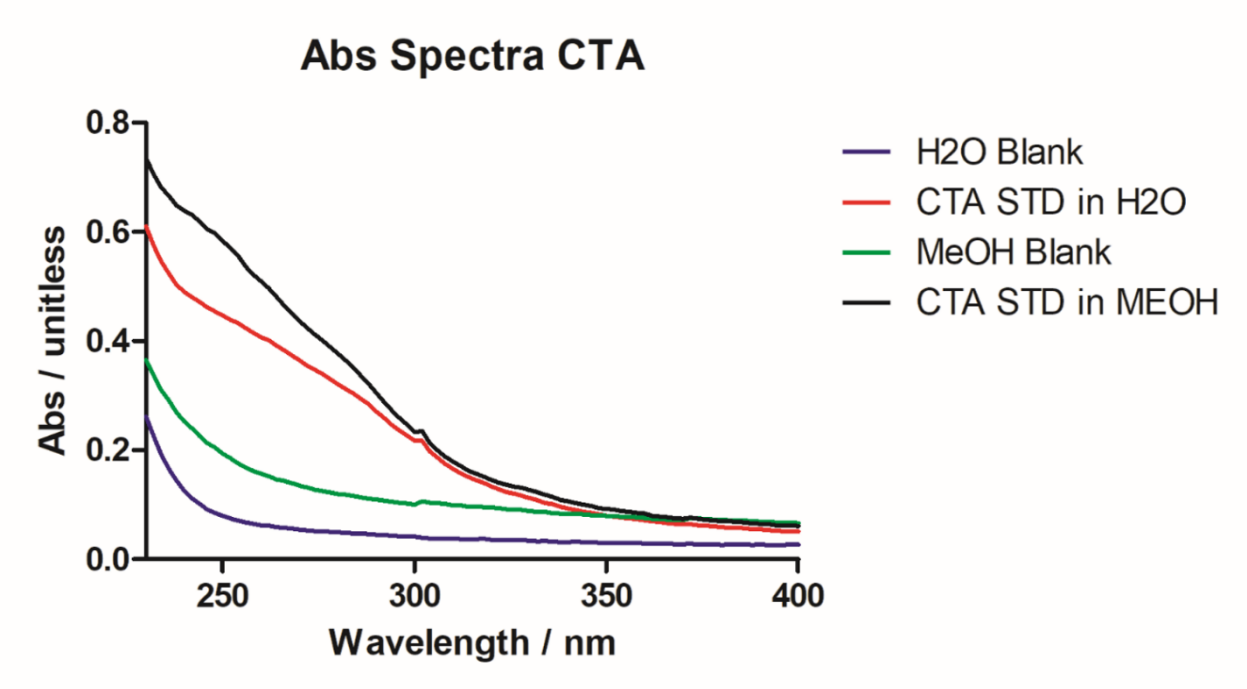

Figure 14 – An absorbance spectrum of calcitroic acid and two separate solvents of the determination of the optimal intensity of the detection during the extraction optimization. This was paired with a PDA contour and it was determined that accounting for impurities, 264 nm would be used as the wavelength for detection.

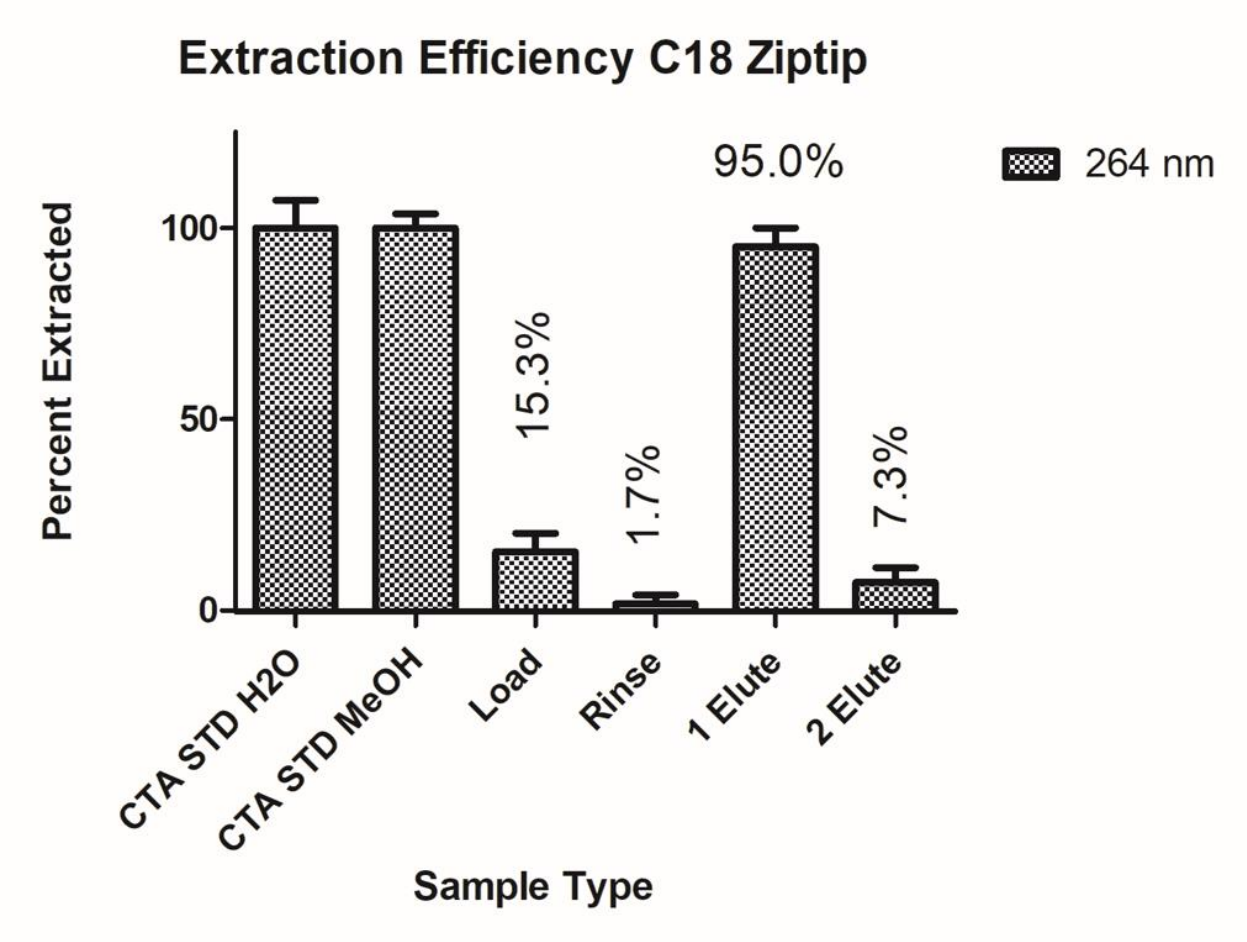

Figure 15 – The calculated extraction efficiency through the reverse phase extraction and the expected losses at each step of the procedure. This method had the highest recovery rate of calcitroic acid standards out of any of the explored solid phase extractions.

The method was then applied to a series of mouse plasma samples and then analyzed by mass spectrometry for determining the circulating concentration of calcitroic acid. Mice were provided supplemental vitamin D in their diet. The mass spectrometry analysis was implemented again to gain the selectivity over other similar species that may still be present after the extraction. A representative mass chromatogram of mouse plasma spiked with calcitroic acid to determine the extraction efficiency in this matrix is shown in **Figure 16**. It was found that while there was a high recovery of calcitroic acid through the standard solutions, once plasma samples were used, the recovery through the procedure was minimal. Figure 4 shows a comparison

between samples of plasma that had a standard of calcitroic acid added before the reverse phase solid phase extraction compared to after the extraction procedure. Due to the very poor recovery through the method and the lack of increased specificity that this extraction provided ion-exchange solid phase extractions were alternatively explored.

Instrument: 8040

Detector: MRM

Daughter Ions: 357.10 >> 339.30; (Omitted other two ions for legibility)

Sample Solvent: 100% MeOH

Mobile Phase: 75 % MeOH 25% H_2O 0.1% formic acid

Flow Rate: 0.500 mL/min

Liquid Chromatography: Restek C18 5 µm 50x4.6 mm

Gradient: 0.0 min: 70% MeOH; 0.5 min: 70% MeOH; 10.5 min: 99% MeOH; 12.9 min: 99 % MeOH; 13.0 min: 70 % MeOH;

Oven: 40 °C

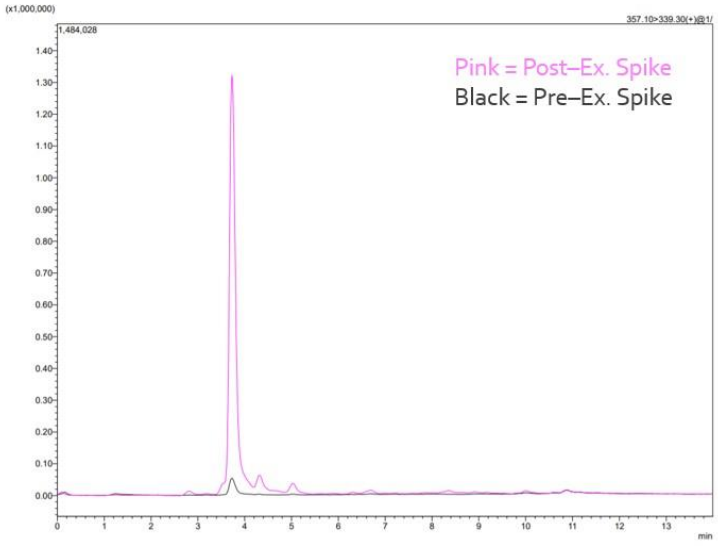

Figure 16 – A comparison of the recovery during a spiked sample of calcitroic acid that had undergone the reverse solid phase extraction procedure to a sample that underwent the extraction and then was spiked with calcitroic acid at the same concentration. The observed loss of calcitroic acid was too large to move forward with this method.

4.4.2 Weak anion exchange Solid Phase Extraction

Weak anion exchange solid phase extraction (WAX–SPE) is a subset of solid phase extraction that uses the ion–ion interactions between components of a sample and a stationary phase. Weak anion cartridges have pH dependent charged stationary phase that allow for the adherence of charged species. This adds an additional property to the extraction procedure. When the pH of the diluent changes the protonation of the stationary phase removes the charge from the charge allowing the solubilization of the analyte and elution into the final sample.

Pipette tips with WAX–SPE cartridges were used for high throughput in the samples for optimization of the method. The spectrometric measurement and background subtraction of the reversed phase extraction was used for determining the extraction efficiency through the cartridges. The findings are shown in **Figure 17**. The extraction efficiency of the method was significantly lower than what was observed for the reverse phase method. This suggested that the interaction with the stationary phase was not as strong for calcitroic acid. The poor loading of the samples onto the cartridges prevented moving forward with tissue samples under these extraction conditions. While the weak anion exchange was explored for the extraction procedure, the more promising strong anion exchange was tested for extraction efficiency.

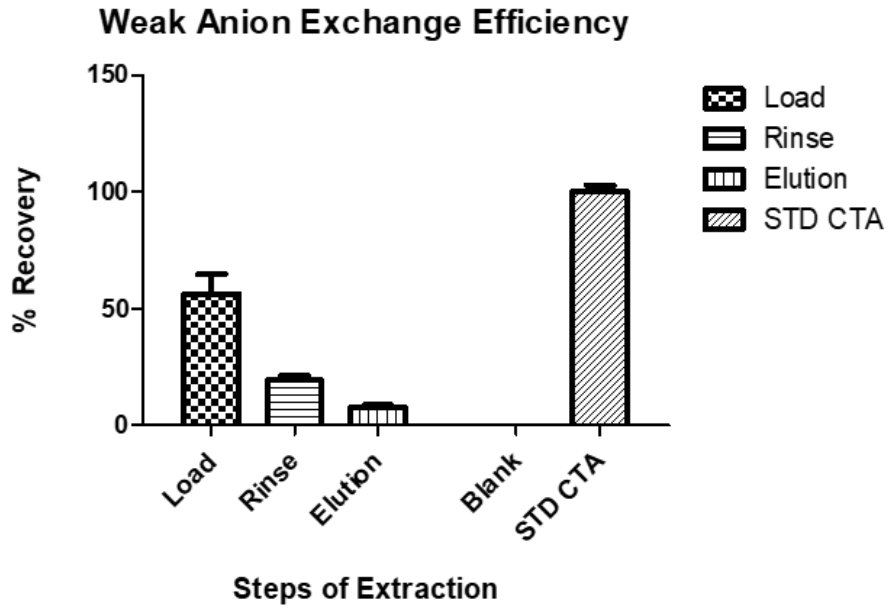

Figure 17 – A comparison of calcitroic acid present in solvents of the weak anion exchange procedure. It was observed that a majority of the calcitroic acid remained within the initial load solution not properly interacting with the stationary phase.

4.4.3 Strong Anion Exchange Solid Phase Extraction

Strong Anion Exchange Solid Phase Extraction (SAX–SPE) operates similarly to weak anion exchange reversing the role of weak electrolyte onto the analyte. While this part is shifted the

use of ion–ion interactions for the adsorption of the charged species from a solution onto a stationary phase for later elution based on ion displacement remains. The primary difference between a strong and weak anion exchange method is weak anion exchange works more as a displacement of ions where the analyte is best suited if it has a permanent charge. The stationary phase then binds with an energetically more favorable ion displacing the charged analyte into the solution. In a strong anion exchange, the stationary phase has a permanently positively charged moiety that is better suited for the pairing of ions that have a pKa that can be used to change from a charged to neutral state[35]. Calcitroic acid's pKa made it well suited for this type of extraction method.

Phenomenex HyperSep™ SAX Strong Anion Exchanger SPE Cartridges were used for this solid phase extraction. The cartridges utilized for this analysis were a more traditional tube cartridge in which solvents would be loaded and eluted in a single direction. These cartridges reduced the throughput of the method but allowed for the higher accuracy in flow rate over the cartridges. In future studies, the implementation of a solid phase extraction manifold could further increase the accuracy of flow rates for the procedure and the parameter could be more accurately optimized. Another property of these cartridges was the phenyl moiety in the stationary phase shown in **Schematic 14**. This functional group allowed for π–π stacking a hydrophobic effect that increased the selectivity even greater.

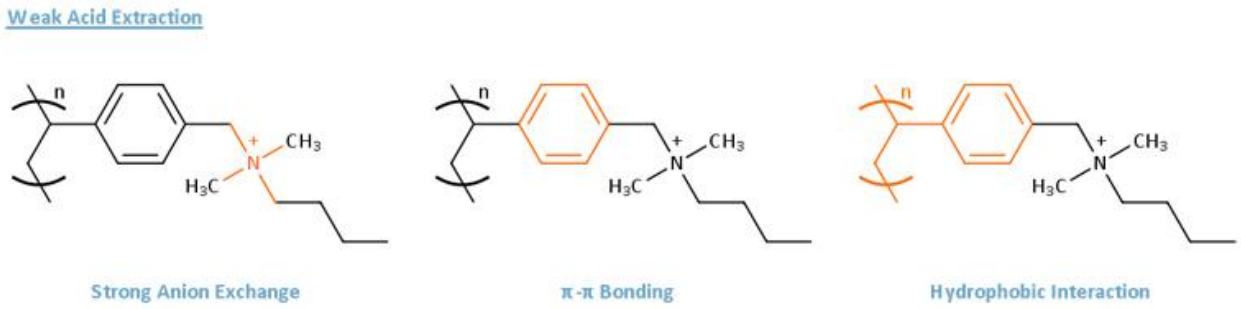

Schematic 14 – A summary highlighting the selectivity gained through a strong anion stationary phase.

The method that was developed for determination of the extraction efficiency of cartridges for the reverse phase method was once again utilized for the SAX–SPE. Measurements of standard samples of calcitroic acid that underwent extraction through the SAX–SPE were measured with the Tecan plate reader. The findings were reported in **Figure 18**. It was found that calcitroic acid through the initial procedure exhibited 82% recovery. This was a decrease in the recovery of the sample suggesting that some of the calcitroic acid remained on the stationary phase based on the absorbance observed of each solution. While the recovery was lower for this method when compared to the reverse phase extraction the sample lower standard deviations were observed once again preventing high variance in the final reported concentrations of calcitroic acid in the initial samples. The quantity recovered spoke towards a more productive interaction between calcitroic acid and the stationary phase than what was observed with the weak anion cartridges. The strong anion exchange for this reason was further explored over the weak anion exchange for the extraction of calcitroic acid from tissue samples.

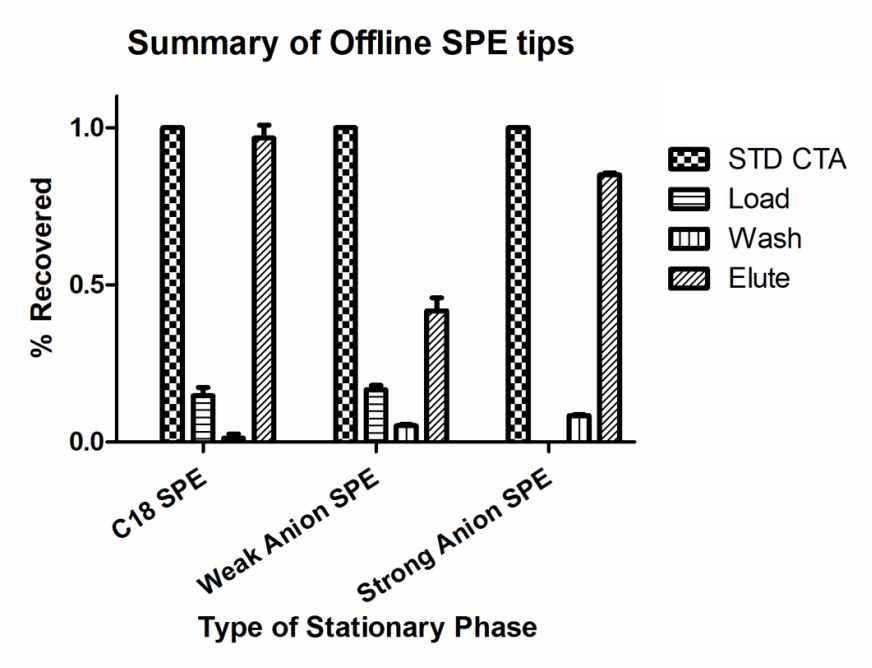

Figure 18 – A comparison of the three different types of solid phase extraction explored within this study. It was found that the greatest recovery was observed in standard solutions with the C18 stationary phase, but the strong anion exchange method provided greater amounts of selectivity than the other stationary phases.

Standard samples that underwent this procedure had an unexpected peak splitting pattern that were consistent with previous observations in samples that had degraded under low pH conditions. This pattern was missed on the plate reader due to its lack of a chromatographic separation and lower selectivity when compared to mass spectrometry. This was first seen for calcitroic acid that was prepared synthetically. This suggested that the conditions for the final elution may be too harsh for calcitroic acid. A chromatogram of a standard calcitroic acid solution that underwent SAX–SPE is shown in **Figure 19**. The use of acetic acid (a weak acid with a pK_a of 4.75, higher than formic acid, 3.75) at a lower concentration was explored to prevent the degradation of calcitroic acid in the eluent. Mass chromatograms of the standard solutions prepared under different concentrations of acetic acid and formic acid were collected to see if a reduction in degradation was available under milder conditions. The different eluent conditions

were used for extraction of calcitroic acid out of standard samples. The ratios of the three peaks under each set of conditions are summarized in **Figure 20**. A mild reduction in extraction efficiency when 0.1% acetic acid was observed but the variance of the measurements remained consistent allowing the procedure to move forward for tissue sample extraction.

Instrument: 8040

Detector: MRM

Daughter Ions: 357.10 >> 339.30; 157.15; 121.15

Sample Solvent: 95% MeOH 5% Formic acid

Mobile Phase: MeOH : H_2O 0.1% formic acid

Flow Rate: 0.500 mL/min

Liquid Chromatography: Restek C18 5 µm 50x4.6 mm

Gradient: 0.0 min: 70% MeOH; 0.5 min: 70% MeOH; 7.5 min: 99% MeOH; 10.5 min: 99 % MeOH; 10.75 min: 70 % MeOH;

Oven: 40 °C

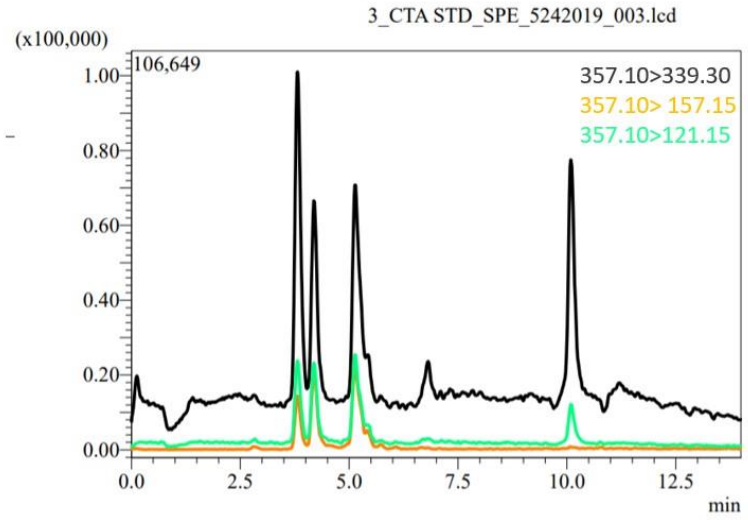

Figure 19 – A chromatogram of a standard sample of calcitroic acid that underwent the strong anion exchange method. It was found that there was unexpected signal from the standard sample that was attributed to the degradation of the sample under acidic conditions.

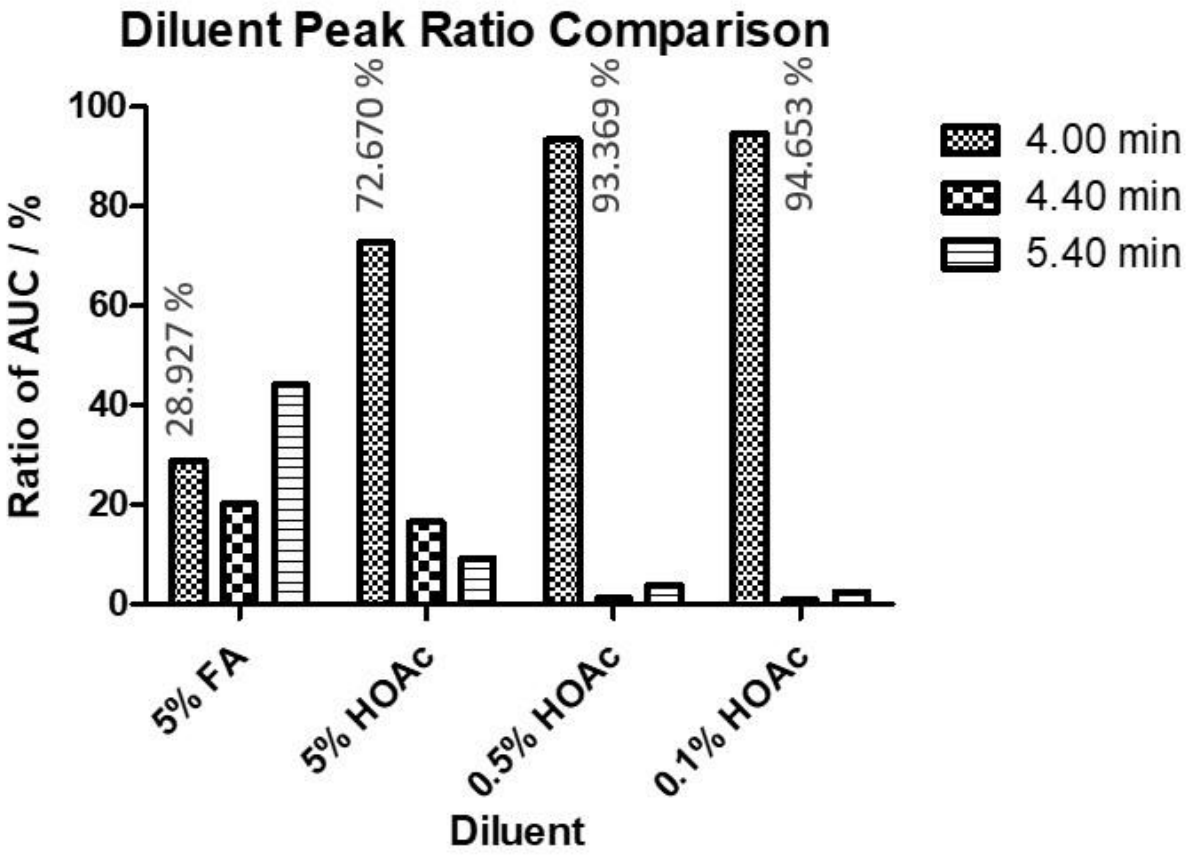

Figure 20 – A comparison of the ratio of the peaks observed in chromatograms of standard solutions of calcitroic acid dependent upon the concentration and type of acid during the final elution step. It was found that the type of acid as well as its concentration significantly contributed to the ratio of the observed peaks in the chromatograms.

Tissue samples were harvested from non-treated mice collected by necropsy and underwent the optimized procedure removing large biological molecules. Samples were homogenized in 1 mL of aqueous 0.1 M phosphate buffer pH 7.4 and centrifuged at 10000 rpm. The supernatant was then collected and passed through 0.2 µm nylon filters to remove remaining particulates. The samples were then evaporated by vacuum centrifugation for 24 h set to 30 °C. The dried samples were then solvated in water, filtered through 0.2 µm nylon filters loaded onto the liquid solid phase cartridge for extraction. The final eluent was 0.1 % acetic acid. The samples

were then placed in the autosampler for HPLC–MS/MS measurement following the procedure outlined in chapter 2. A summary of the extraction procedure is outlined in **Schematic 15**.

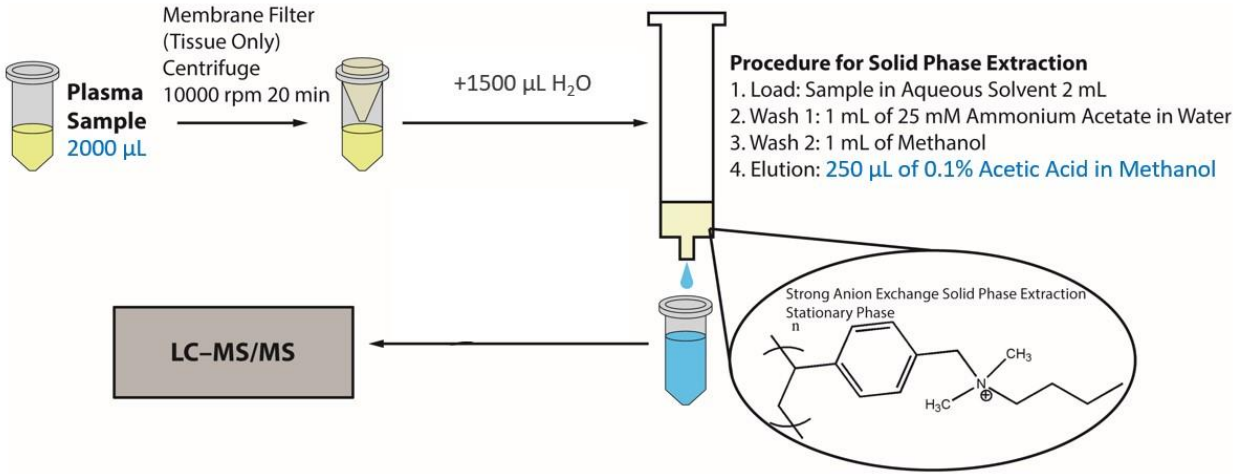

Schematic 15 – The workflow of the sample extraction procedure incorporating the strong anion exchange solid phase extraction. The concentration of the acid used in the final elution was lowered from the initial 5% to make the method compatible with calcitroic acid.

In the strong anion exchange extraction, the final eluent was able to be decreased in volume from the initial 2 mL for loading to 250 µL. This decrease allowed for the preconcentration of remaining species giving a signal increase in the final chromatograms. This effectively lowered the limit of quantification by 8-fold during the procedure. This proved useful as is discussed below.

4.5 On–Line Solid Phase Extraction

On–line solid phase extraction follows the same principles of an off–line method but allow for a high throughput of samples that would be challenging in an off–line procedure. The manifold interface of the autosampler to the liquid chromatographic column in our system allows

for the incorporation of a SPE cartridge and methods for direct sample analysis were explored to allow for utilization of this kind of high throughput system. The cartridge is placed in line with the column and loaded in a slow flow rate step before the analysis. Then the valve position is changed to allow for the eluent to pass over the cartridge disturbing the interactions of the species that remain on the cartridge and pass them onto the column for the HPLC-MS/MS analysis. The principles are identical to an off–line system but come with new parameters which must be properly optimized for the analysis. The flow rates of the loading time, and wash step on the cartridge have a similar counterpart but the elution becomes more challenging to account for the dead volume between the SPE cartridge and column. In addition to this the elution conditions become the initial conditions for the gradient that is used during the chromatographic separation. For this reason, much of the optimization was conducted with the off–line extraction method. The thought was that once a method was developed for the extraction procedure it could be transferred to an on–line system if higher throughput were needed.

The initial solid phase extraction that was explored for the extraction of calcitroic acid, an on–line reversed phase cartridge was used for the separation to remove background species from the final mass chromatograms. The chromatograms of tissue samples that underwent homogenization in methanol and centrifugation at 10000 rpm at 4 °C. The supernatants were collected, filtered, and placed in the autosampler for analysis. This procedure used the initial product ions for detection of calcitroic acid in its measurements. The chromatograms shown in **Figure 21** were collected using this method. An increase in the retention time from the initial samples shown at the beginning of this chapter were observed due the dead volume between the solid phase cartridge and the liquid chromatographic column. The complexity of the

chromatograms was surprising after the extraction procedure. Much of the initial signal that was observed in the samples that had only undergone an organic crash procedure remained in these samples. The chromatograms contained peaks that corresponded individual product ions but not the correct ratio that would be expected based on the fragmentation observed in the standard samples. It was speculated that structurally similar compounds may share some of the transitions that were used in the identification of calcitroic acid. The signal that was most unique (not a dehydration of the precursor ion) 121.15 m/z was seen in very low intensity throughout the procedure. This high amount of background after the extraction procedure suggested that an alternative extraction procedure may be required for the simplification of the chromatographic separation to prevent signal suppression or misidentification.

Instrument: 8040

Ionization: Positive

Mode: MRM

CTA Transitions: 375.30>357.25; 339.25; 121.15

Sample Solvent: 50 % MeOH 50% H_2O 0.1% formic acid

Mobile Phase: MeOH : 0.1% formic acid H_2O

Flow Rate: 0.600 mL/min

Liquid Chromatography: 130 Å, 2.5 µm, 2.1 x 100 mm BEH–C18

On–line SPE: 0.3 mL/min flow; 10% MeOH Load; 20% MeOH Wash; Total Time: 1.25 min

Gradient: 0.0 min: 50% MeOH; 0.5 min: 50% MeOH; 4.0 min: 99% MeOH; 4.75 min: 99 % MeOH; 5.0 min: 50 % MeOH;

Oven: 45 °C

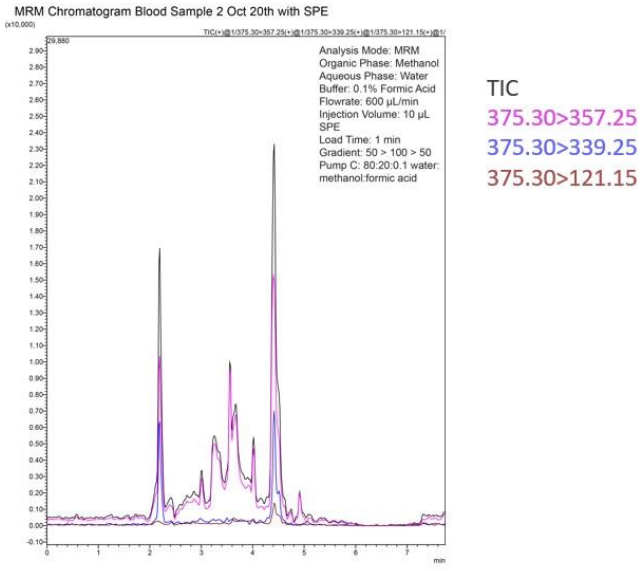

Figure 21 – A representative chromatogram of the separation that was achieved with an online solid phase extraction of calcitroic acid. No peaks observed in the chromatogram corresponded with the expected retention time of calcitroic acid standard solutions suggesting the reported signal was background.

With the development of a strong anion exchange method for the separation of calcitroic acid proving more promising that the reverse phase method, further exploration into on–line solid phase extraction may be useful to increase the consistency of the extraction procedure and reduce the manual labor currently present in the procedure. Substituting the cartridge of the on–line solid phase extraction would allow for an increase in compatibility with the chromatographic conditions. Additionally, a union introducing an aqueous mobile phase after the cartridge could allow for minimal changes to the solid phase extraction eluent.

4.6 Molecular Filtration

The addition of methanol to tissue samples during homogenization was able to precipitate many of the large proteins that are present in the matrix of the solution. Eliminating large, charged biomolecules was still a concern for the strong anion solid phase extraction. Large negatively charged species like deoxyribonucleic acid may make it through the proposed extraction procedure and damage the column lowering its longevity. The introduction of a 10 kDa molecular filter was added as a final filtration step before the evaporation. Ultracel-10 membrane filters were purchased from Fisher Scientific. The extraction efficiency through the membrane was explored. The extraction efficiency that was initially measured was far lower than expected.

It was observed that mouse plasma samples spiked with calcitroic acid did not contain a quantity of calcitroic acid above the limit of detection after the molecular filtration. A representative chromatogram of the findings is shown in **Figure 22**. It was speculated that unspecific binding proteins may interact with calcitroic acid and then during the filtration step of the procedure cause calcitroic acid to be removed from the filtrate. To explore this possibility the

addition of the organic crash with MeOH instead of the phosphate buffer used in the previous procedure was implemented. The thought processes being that the MeOH might be able to disturb this interaction, dissociating calcitroic acid into the solution before the filtration. Acetonitrile was also considered as a more nonpolar solvent that could be used during precipitation and protein interaction disruption but was not compatible with the filters under the desired solvent composition. The extraction efficiency of the spiked plasma samples that were homogenized in methanol is shown in **Figure 23**. While substantial loss of the analyte was observed the variance through the procedure would allow for precise calculation of the initial calcitroic acid within tissue.

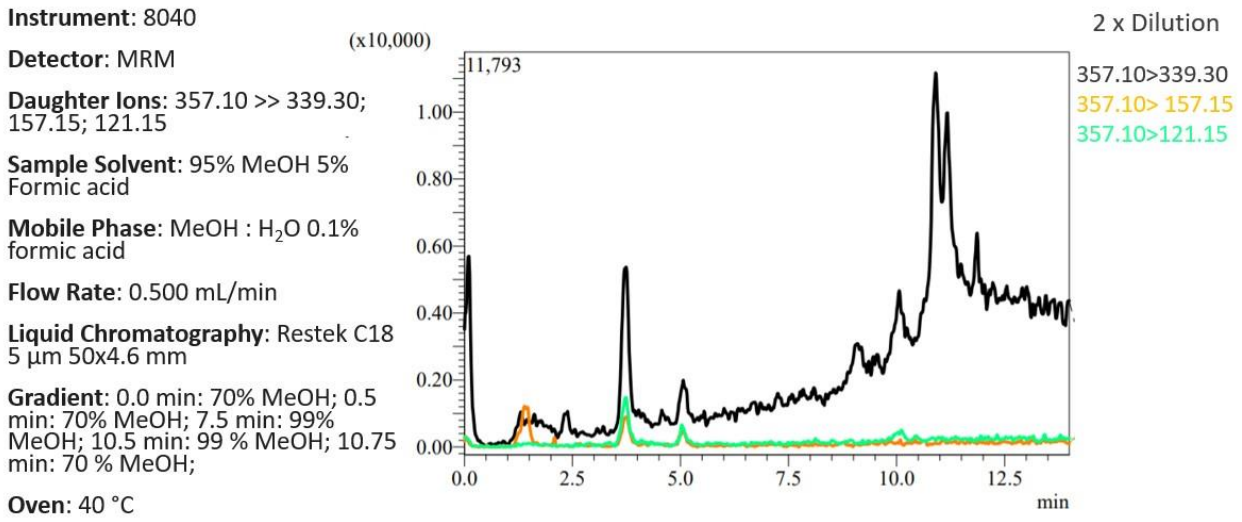

Figure 22 – A chromatogram of a spiked mouse plasma extract through the SAX-SPE method. The sample had a negligible peak that came from the spiked standard. It was speculated that the signal was lower than expected due to unspecific protein binding preventing the analyte from reaching the solid phase extraction method.

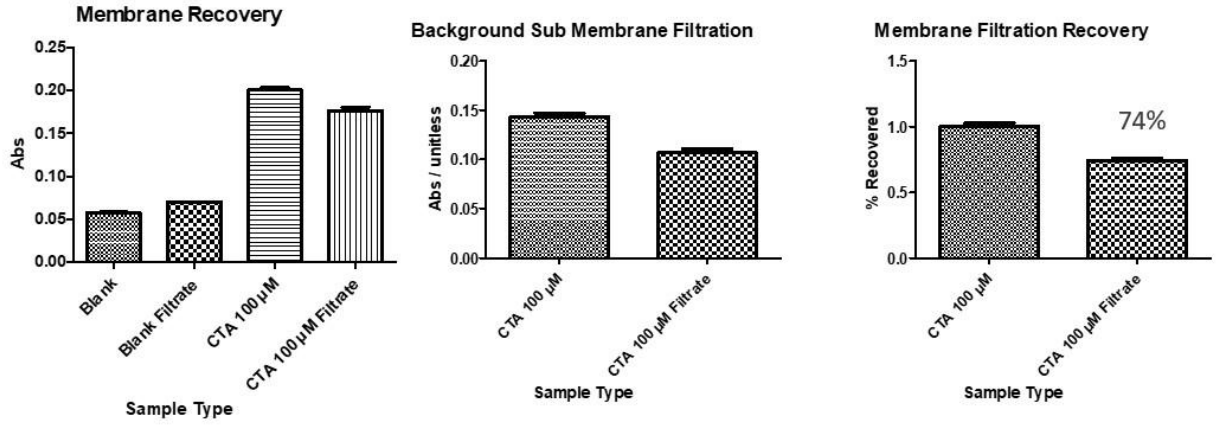

Figure 23 – A comparison of A calcitroic acid sample with a standard solution that did not undergo membrane filtration. It was found that there were significant losses during the process but due to the low standard deviation between the samples these could be accounted for in the calculation of the initial concentrations of calcitroic acid in samples.

With the addition of the molecular filtration the final extraction procedure for calcitroic acid in biological samples was finalized as the following procedure outlined in **Schematic 16**. Tissue samples were homogenized in 1 g/mL methanol and centrifuged at 4 °C, 10000 rpm. The supernatants were then collected and filtered through 0.45 µm then 0.2 µm and final 10 kDa filters. The filtrates were then evaporated in a vacuum centrifuge over 24 h. The samples were then reconstituted in water and filtered through 0.45 µm and 0.2 µm filter. The strong anion exchange procedure described above was then used to extract calcitroic acid into 0.1% acetic acid in MeOH. The samples were then diluted with water to match the starting composition of the mobile phase composition. The extracts were then placed in the autosampler for LC–MS/MS analysis.

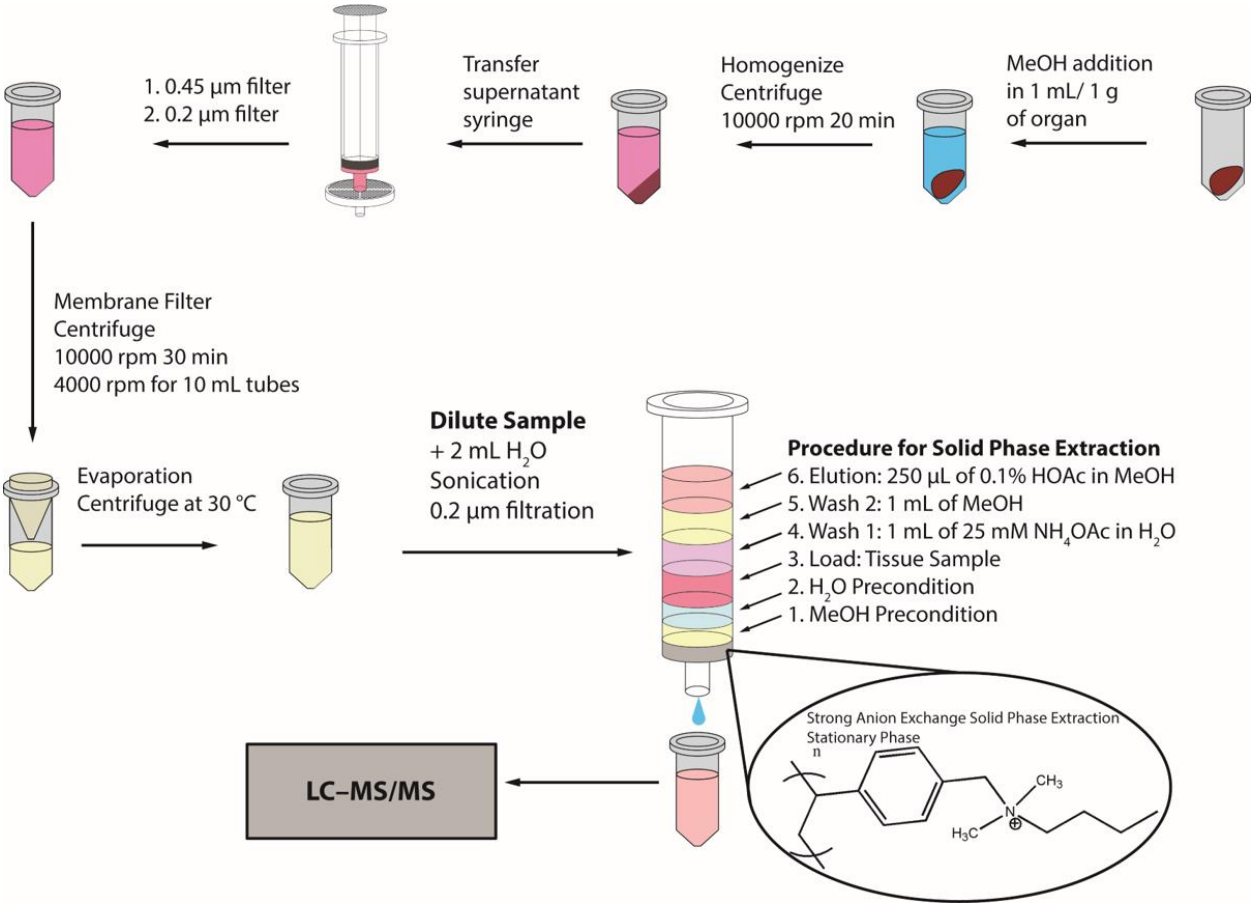

Schematic 16 –A final summary of the extraction procedure with the membrane filtration step. Samples were evaporated between the membrane filtration and the SAX-SPE to allow for matching of the loading step solvent.

4.7 Stability of Calcitroic Acid Under Extraction Procedure Conditions

This study was confronted on multiple occasions with the instability of calcitroic acid under acidic conditions. Samples were evaporated in the first designed procedure with just an organic crash present. Depending upon the temperature of the evaporation it was seen in some tissue samples the formation of other species in the final chromatogram than the expected retention time and product ion peak ratio of calcitroic acid. Its procedure was then adjusted to have a condenser added onto the vacuum to allow for the lower temperature of 30 °C. This was not the end of the issues with calcitroic acid stability. Similar chromatographic peak splitting was observed in the crude stock calcitroic acid used in the optimization of the new product ions in

Chapter 2. This pattern arose again in later observations when the initial organic crash used in the tissue extractions contained 0.1% formic acid. It was speculated, as the solvent is evaporated from the filtrate, the pH of the solution becomes lower causing the degradation of the analyte, interfering with its liquid chromatographic mass spectrometric measurement.

The final omission of formic acid was adopted for the remainder of the studies conducted once this was observed. A similar acid instability was reported by the member of our group who conducted the synthesis of calcitroic acid. The exact byproducts of this degradation were not determined to be relevant for the goals of this project but are suspected to maintain major portions of the initial analyte's structure due to the chromatographic, and mass spectrometric similarities. The increase in the retention time in the chromatograms also suggested an increase in hydrophobicity during the degradation.

4.8 Quantification of Calcitroic Acid Concentration is Tissue Samples

Throughout the optimization of the extraction of calcitroic acid, measurements were collected that informed the parameters for the analysis. The initial sample of interest was of mouse plasma to determine the levels of circulating calcitroic acid. Understanding the concentration that was present in the plasma would speak toward the localization that could be expected in other tissue samples if the primary site of the metabolism were the hepatocytic cells. Mouse plasma samples were explored using the final method described above in **Schematic 16**. A representative chromatogram of the plasma samples is shown in **Figure 24**. It was observed that even with the preconcentration gained with the solid phase extraction, and background suppression from the separation methods, calcitroic acid was not present at a concentration

above the determined limit of detection in plasma samples. This suggests that the circulating concentration of calcitroic acid would be lower than the determined biological active concentration. This would suggest that if any site downstream of the liver in the intestinal track does not utilize the biological activity of calcitroic acid. To assure that calcitroic acid was not being suppressed by the final matrix of the samples, calcitroic acid as a spike to the concentration of 10 µM was added to the sample. The results can be seen in **Figure 25**. The peak associated with calcitroic acid was observed in these chromatograms suggesting minimal signal suppression was occurring.

Instrument: 8040

Detector: MRM

Daughter Ions: 357.10 >> 339.30; 157.15; 121.15

Sample Solvent: 99.5% MeOH 0.1% Acetic Acid

Mobile Phase: MeOH : H_2O 0.1% formic acid

Flow Rate: 0.500 mL/min

Liquid Chromatography: Restek C18 5 µm 50x4.6 mm

Gradient: 0.0 min: 70% MeOH; 0.5 min: 70% MeOH; 10.5 min: 99% MeOH; 12.9 min: 99 % MeOH; 13.0 min: 70 % MeOH;

Oven: 40 °C

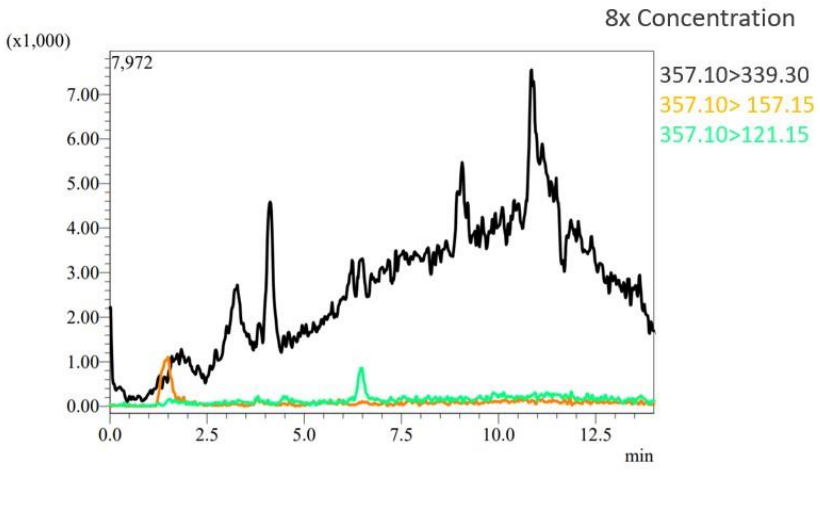

Figure 24 – A chromatogram of a native mouse plasma sample worked up through the SAX-SPE extraction procedure. Several peaks of a single product ion at retention times not matching standard solutions of calcitroic acid were observed. It was concluded that calcitroic acid was not present in theses samples at a concentration above the limit of detection.

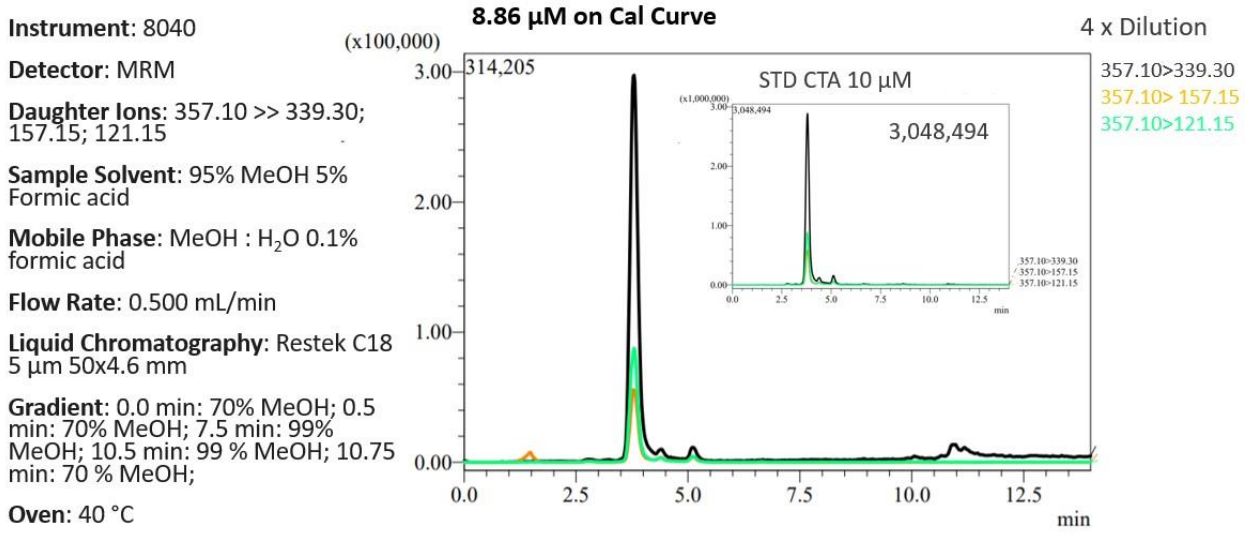

Figure 25 – A chromatogram of a calcitroic acid spiked solution mouse plasma to measure the extraction efficiency through the procedure. It was found that when a sample was spiked to a concentration of 10 µM the measured concentration after the extraction was 8.86 µM giving an 88.6 % recovery through the procedure.

To further explore the activity and localization within the intestinal tract of calcitroic acid, liver, large and small intestinal samples were collected and worked through the extraction procedure the determine the native concentration of calcitroic acid. A collection of representative chromatograms is shown in **Figure 26**. It was observed that no signal with the corresponding product ion ratios and retention time corresponding to standards of calcitroic acid was observed within the study. While no signal for the corresponding retention time was observed several other peaks came through in high intensity during. The large intestinal samples appeared to have high signal at a later retention time than would be expected for the native form of calcitroic acid. Due to the high specificity of the extraction and separation method it was postulated that the molecules responsible for this signal were most likely closely related to calcitroic acid in structure and may be unidentified metabolites of calcitroic acid, possibly a conjugate. If calcitroic acid was in a conjugated form that could have consequences to the

retention time as well as the fragmentation through the measurement. A spike of calcitroic acid to assure that the retention time was not shifted due to the matrix conditions was conducted. **Figure 27** shows the corresponding spiked liver sample after the extraction procedure. It was observed that the spiked sample did not have a tangible change in retention time that would account for the signal that was observed in the chromatograms. To further explore this hypothesis, mice were supplemented with cholecalciferol (vitamin D_3) and a second set with ergocalciferol (vitamin D_2) to see if quantities of Vitamin D affected the circulation of calcitroic acid.

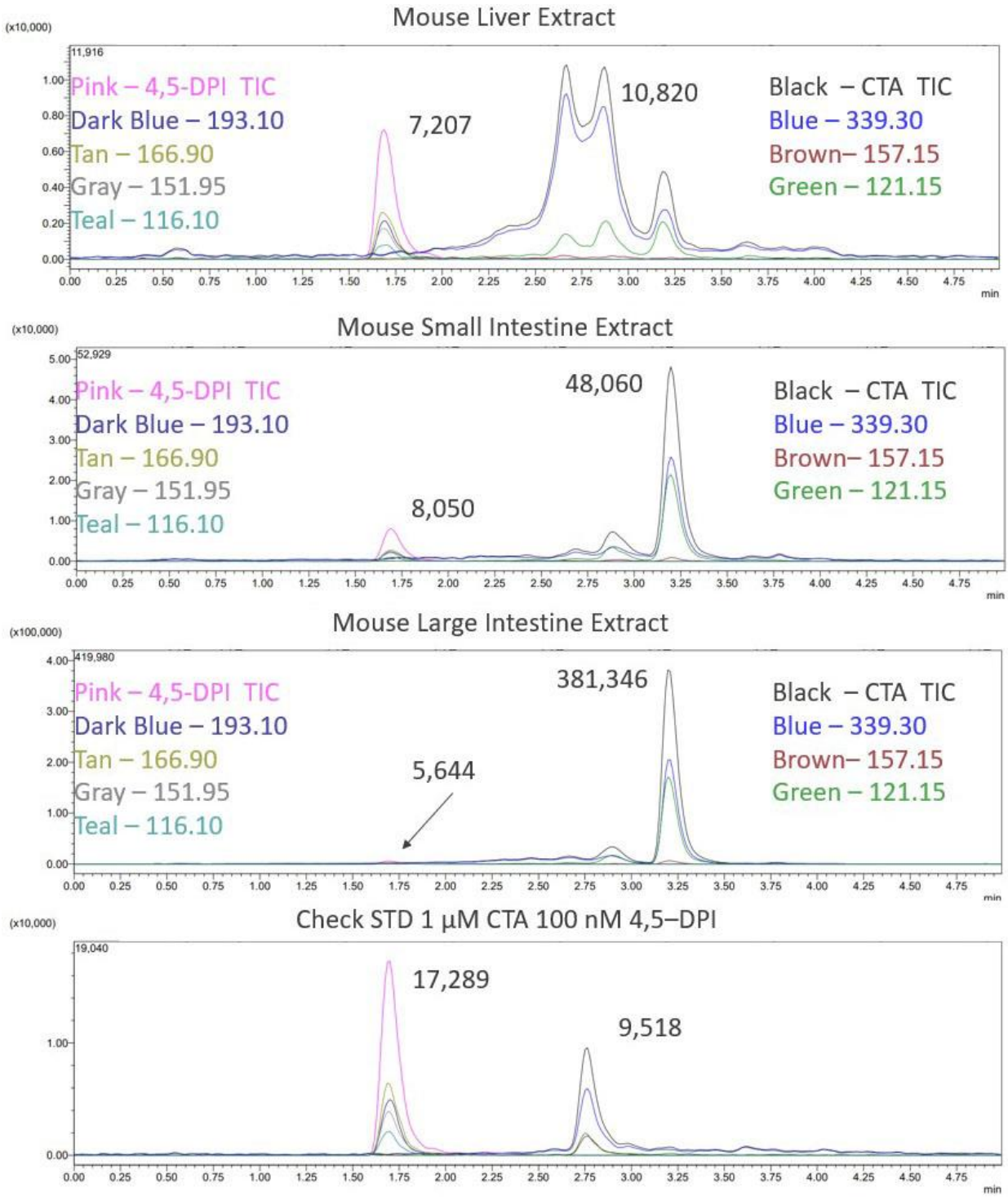

Figure 26 – A collection of chromatograms of tissue samples that underwent the described strong anion exchange extraction procedure. Several peaks were observed in the chromatograms that contained fragmentation seen in calcitroic acid. The retention time as well as the product ion ratios did not match what had previously been seen in chromatograms of calcitroic acid standards. A standard sample of calcitroic acid is shown at the bottom for comparison of the retention times and a sense of scale of the signal intensity.

Instrument: 8040

Detector: MRM

Ions: 357.10 >> 157.15;

220.80>>193.10;

Sample Diluent: 99.5% MeOH 0.1% Acetic Acid

Mobile Phase: MeOH : H_2O 0.1% formic acid

Flow Rate: 0.500 mL/min

Liquid Chromatography: Agilent Extend-C18,2.1x50mm

Gradient: 0.0 min: 20% MeOH; 2.0 min: 80% MeOH; 3 min: 99% MeOH; 4 min: 99 % MeOH; 4.1 min: 20% MeOH;

Oven: 40 °C

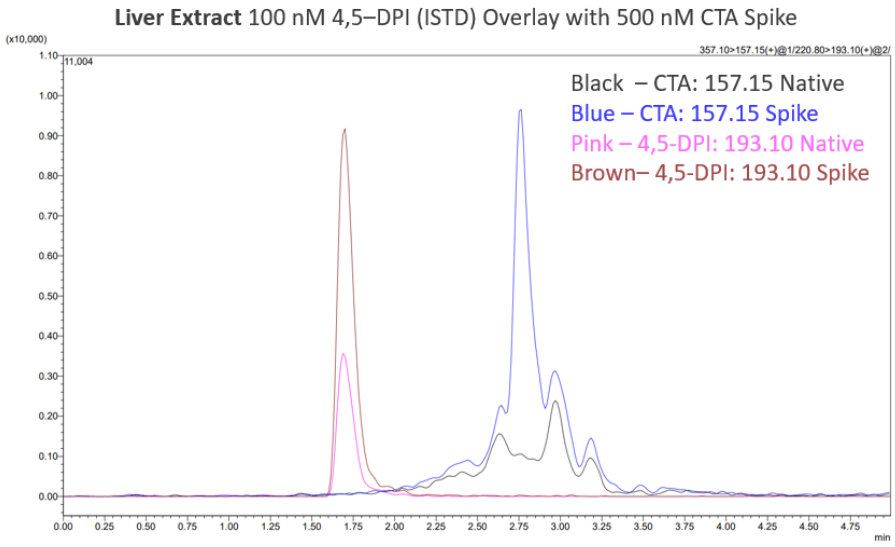

Figure 27 – A chromatogram of a liver extract sample that was spiked with calcitroic acid after the extraction procedure to compare the retention time of the native signal with the standard under these matrix conditions. It was observed that the retention time of calcitroic acid was not affected by the biological matrix in an of the samples measured.

To explore the possibility of high levels of excretion of calcitroic acid, a mouse was provided with a dose of vitamin D_2 to monitor the effect of catalysis of calcitroic acid. One set of mice were provided with a 5 mg/kg intraperitoneal (IP) injection, and feces collected over of 24 h. Afterwards samples were worked up through the described extraction procedure before HPLC–MS/MS quantification. A set of representative chromatograms are shown in **Figure 28**. The top chromatogram in the figure represents the HPLC–MS/MS method that was developed based on the fragmentation of $[M+H]^+$ and below the fragments of the dehydrated form of calcitroic acid. It was observed that the fecal samples of the mice appeared comparable to large intestinal samples that were collected of the untreated mice. This suggests that predominant signal that is observed in these samples comes from the contents of the intestinal tract and that the signal is independent of the vitamin D exposure of the animal. To confirm this finding feces and urine samples of mice given cholecalciferol were explored.

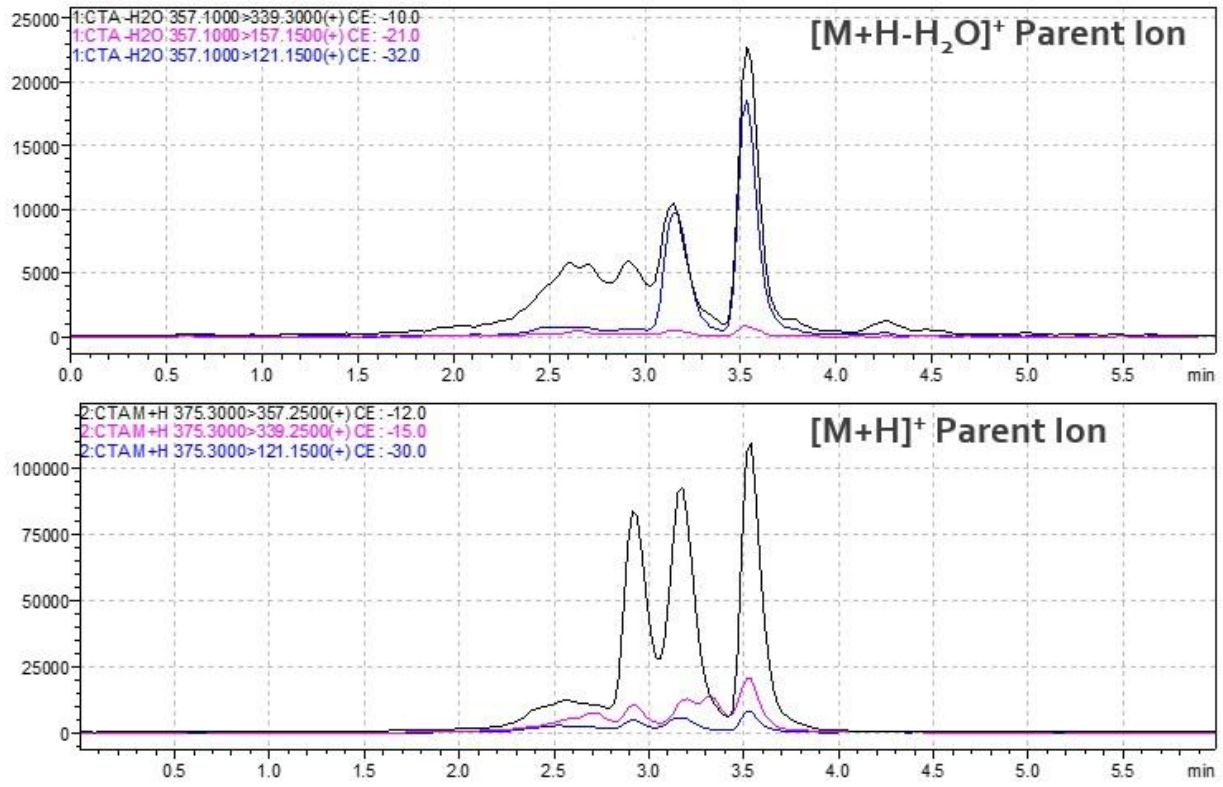

Figure 28 – A set of two chromatograms showing both the $[M+H]^+$ (bottom) and the dehydrate product ions (top). Several peaks were observed in both chromatographic methods thought the ratio of intensity seems to change between the two methods of detection.

Mice were given a 2.0 mg/kg of cholecalciferol orally in vegetable oil. Urine and feces samples were then collected in two 24 h fractions over 48 h. the samples underwent the described extraction procedure before HPLC–MS/MS analysis. The corresponding mass chromatograms are shown in **Figure 29**. Consistent to the previous set of organ samples, no calcitroic acid was observed above the limit of detection in either set of samples. What was found is a similar pattern in the chromatographic peaks between the feces samples and the large intestinal samples. The previous colon sample did not have the feces removed before the extraction and thus contained feces in the samples. The resulting chromatogram seems to reflect this design choice in the inclusion of compounds in the final chromatograms that is attributed to the feces. This suggests that the peak that was present in the colon samples that was thought to

be structurally similar to calcitroic acid is truly present in the feces samples and its concentration is independent of the concentration of vitamin D in the mouse's diet.

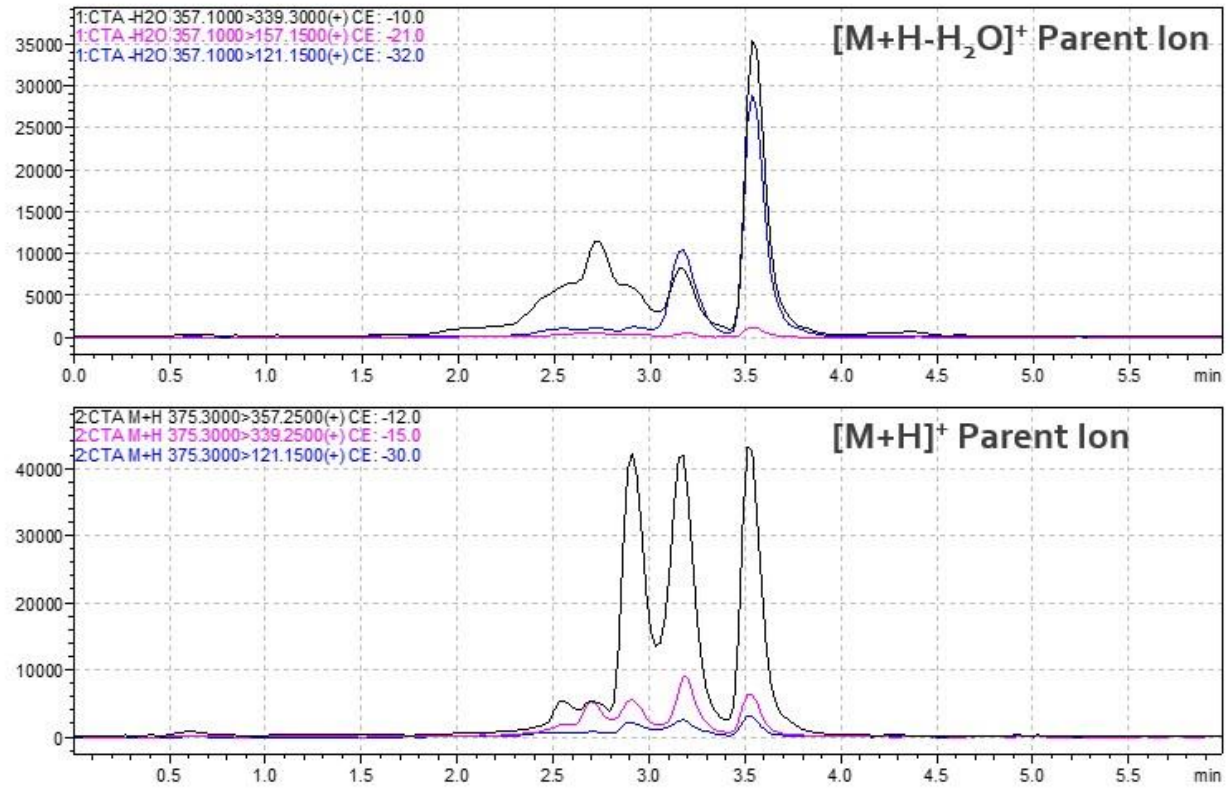

Figure 29 – A set of two chromatograms of the same fecal sample from a mouse given an oral dose of vitamin D3. The sample follows a similar pattern to what was seen in the mouse given vitamin D2. The sample's chromatogram contained similar peaks as the large intestinal sample collected in non-treated mice.

Future studies that would build upon these finding could incorporate a direct dose of calcitroic acid provided to the studied mice. This would eliminate the possibility of vitamin D excretion through other pathways and would allow our group to speak more directly towards the circulation of calcitroic acid before excretion. Including this dose of calcitroic acid would more directly measure the possibility of conjugation of calcitroic acid leading to changes in the signal that was speculated to be corresponding to other structurally similar species. If it were found that a strong link between the previously measured signal and calcitroic acid was observed

carbon labeled calcitroic acid could be substituted into the procedure to affect the mass spectrometry and allow for a comparison of the native calcitroic acid and the supplemented quantity of calcitroic acid.

4.9 Conclusion

The quantification of calcitroic acid within tissue samples provide more challenging than other molecules that our group has explored in the past. Several separation methods were included beyond the initial method of liquid chromatographic separation paired with the selectivity gained from the tandem mass spectrometric detection to allow for the avoidance of forms of signal suppression or misidentification due to structural similarity. Several additional extraction procedures were explored to improve the chromatography during this study. Optimization was done on a strong anion exchange method to allow for eluent conditions that were compatible with the stability of calcitroic acid. A working method of separation was determined for calcitroic acid that accounted for hydrophobic species that may have previously been reaching the liquid chromatographic separation. In addition, the incorporation of a small molecule membrane filtration when paired with an organic crash allowed for the removal of proteins and other larger charged species from interfering with the solid phase extraction. The final method was implemented on a series of tissue and biological samples and found that calcitroic acid was not present in a form that was above the limit of detection for the developed method. Mice that were provided with vitamin D before the samples were collected showed similar negligible levels of calcitroic acid.

Further optimization to the conditions used for the solid phase extraction can be conducted to further lower the limit of detection of the method as well as modify the method for the implementation of an on–line extraction, drastically increasing the throughput of the study. To first determine if the additional optimization is necessary for greater insight into calcitroic acids localization, the identification of the later retention time peaks within the large intestinal samples will need to be confirmed as related to calcitroic acid. A study where mice are provided with calcitroic acid and biological samples and tissues are collected and undergo the extraction procedure will provide insight into the vitamin D clearance process. Previous studies suggest that the expected product of vitamin D excretion would be calcitroic acid. This study adds to that body of work suggesting that due to improvements in the chromatographic separation that our method provides we may be separating out conjugated forms of calcitroic acid that have not been previously identified by the scientific community. Further confirmation with calcitroic acid *in vivo* and *in vitro* studies will explore these finding.

References

1. Reddy, G. S.; Omdahl, J. L.; Robinson, M.; Wang, G.; Palmore, G. T.; Vicchio, D.; Yergey, A. L.; Tserng, K. Y.; Uskokovic, M. R., 23-carboxy-24,25,26,27-tetranorvitamin D3 (calcioic acid) and 24-carboxy-25,26,27-trinorvitamin D3 (cholacalcioic acid): end products of 25-hydroxyvitamin D3 metabolism in rat kidney through C-24 oxidation pathway. *Arch Biochem Biophys* **2006,** *455* (1), 18-30.

2. Makin, G.; Lohnes, D.; Byford, V.; Ray, R.; Jones, G., Target cell metabolism of 1,25-dihydroxyvitamin D3 to calcitroic acid. Evidence for a pathway in kidney and bone involving 24-oxidation. *Biochem J* **1989,** *262* (1), 173-80.

3. Skoog, D. A.; Holler, F. J.; Crouch, S. R., *Principles of Instrumental Analysis*. 7th ed.; Saunders College Pub.: Philadelphia, 1997.

4. Inc, P. Sample Preparation. (accessed March 29th).

5. Skoog, D. A.; West, D. M.; Holler, F. J., *Fundamentals of Analytical Chemistry*. 9th ed.; Saunders College: New York, 1988.

5 Derivatization Reactions of Calcitroic Acid

5.1 Introduction to Vitamin D metabolite derivatization

Derivatization reactions have long been a part of the measurement of vitamin D in assays. Radiolabeled vitamin D was integral for many of initial studies which identified vitamin D metabolite[60, 61]. Different types of derivatization reactions have been able to adjust the properties of vitamin D to match the needs of the type of measurement being conducted[62]. Often the modifications changed the retention with in a chromatographic separate, adjusted the volatility for gas chromatography, shifted the absorbance to allow for the measurement with absorbance spectroscopy, or increased the molecular mass and increased the ionization for mass spectrometry[63, 64]. This chapter summarizes the studies performed to explore advantages of derivatization reactions for calcitroic acids detection. Methods that have incorporated derivatization reactions into the analysis of vitamin D species have reported the benefit of 10-fold to 100-fold increase in signal intensity[62, 65]. Our work explored if these advantages could simply be applied to our method of measurement.

While the advantages of a derivatization reaction seem quite appealing for any chemical analysis, there are significant downsides that can hamper the ability of a quantitative analysis. When a chemical reaction is included into an analysis the efficiency of the reaction now governs the measurements that are made on the reaction. Matching the exact reaction conditions during replication can cause variance from scientist to scientist or interday variance. Additional time and labor are also needed to do these analyses. While some level of specification is expected with the different classes of derivatization reactions, side reactions are also very common in samples

with high matrix complexity like biological samples. Other species can undergo similar reactions causing excess reagent to be required for each sample[63]. Depending on reagent use and the load capacity of columns used during the analysis, and volatility of derivatization reagents, this can have ramifications in the column longevity and the quality of chromatography.

The class of derivatization reagents that were explored in this portion of the study were called dienophiles. These types of molecules were first reported by Cookson *et al.* as a derivatizing agent[66]. The general form Cookson reagent reaction can be seen in **Schematic 17**. The final structure retains some of the conjugation of the starting reactant but allows for additional moieties to be included in the final structure, bestowing the red shift that is desired for absorbance spectroscopy[67]. Alternatively, the shift in the m/z ratio that these molecules provide can move the analysis of an analyte into a lower background region of a mass spectrum. The amide functionalities also can assist in the ionization of derivatized products[65].

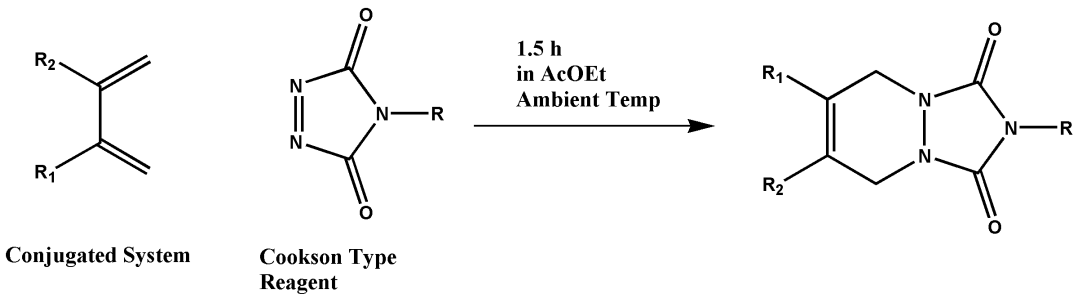

Schematic 17 – A representation of the dieneophile reagent acting upon the analyte through a Diels-Alder reaction.

5.2 Instrumental Considerations Metabolite Analysis

One trait that is commonly adjusted in these derivatization reactions, is the volatility of analytes allowing for gas chromatographic analysis. The column dimensions of gas chromatography led to an improvement in the separation over liquid chromatography. While the

separation of our method could be improved, the goal was to explore removing molecules that shared a precursor ion with calcitroic acid but did not contain the diene motif. To accomplish this derivatization, reagents were explored that would not only change the mass of calcitroic acid but the red shift in absorbance to allow for a simple spectrometric detection. Being able to use an UV-VIS spectrometer would allow for less optimization during the analysis, which at this point in the study was still underway. While calcitroic acid has several unique functional groups, the hope would be to operate upon the conjugated system. This functionality unlike the carboxylic acid or hydroxide moieties was far less common among other molecules, adding a layer of selectivity to the analysis.

5.3 Applications of Derivatization Reactions on Calcitroic Acid

The specific dienophile that was used for this study was 4-[2-(3,4-Dihydro-6,7-dimethoxy-4-methyl-3-oxo-2-quinoxalinyl) ethyl]-3H-1,2,4-triazole-3,5(4H)-dione (DMEQ-TAD). The proposed reaction between calcitroic acid and this species is shown in **Schematic 18**. The absorbance of calcitroic acid had previously been measured at the wavelength of 264 nm as reported in **Chapter 4**. With the addition of the DMEQ-TAD tag, the absorbance was expected to shift higher, close to the λ_{max} of the DMEQ-TAD, 370 nm.

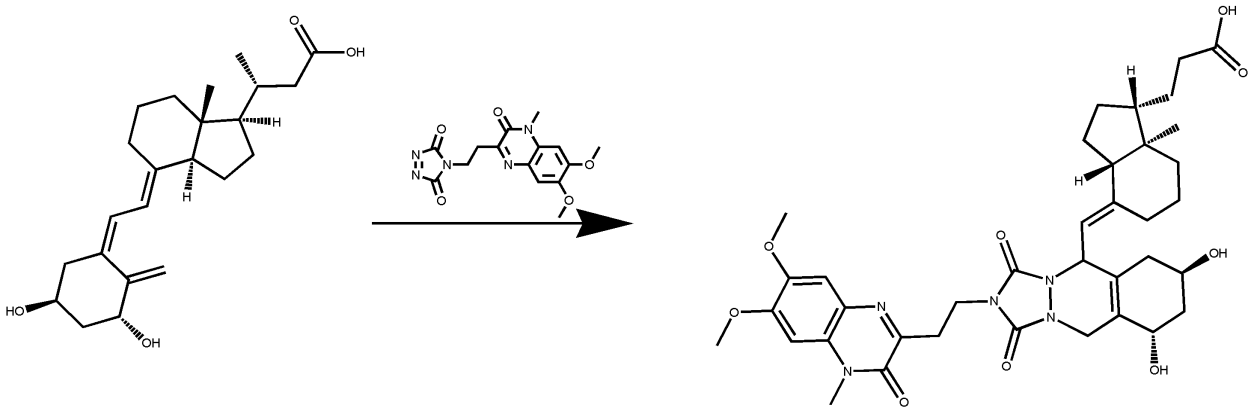

Schematic 18 – A representation of speculated reaction between calcitroic acid and the DMEQ-TAD forming the fluorescent derivative used for UHPLC measurement.

The reaction conditions were taken from the work of Hagashi *et al*.[68]. The reaction was monitored over 3 h and ran at room temperature with a large excess of the DMEQ-TAD to assure conversion to the final product. TLC was performed with the starting materials as well as the reaction at 30 min and 3 h. The TLC is shown in **Figure 30**. The derivatization reaction formed two fluorescent products in addition to the starting material (**Figure 30A**). Detection at 254 nm also showed the conversion of calcitroic acid. ^{1}H-NMR spectroscopy and HPLC–UV/VIS were conducted for further analysis. The ^{1}H-NMR spectra are shown in **Figure 31**. We monitored for the disappearance of the diene peaks which are visible between 5.0 - 6.3 ppm for calcitroic acid. While this change seemed to occur, the aromatic protons for the adduct were missing, which brings concerns on material stability. However, limited stability of the adduct in deuterated chloroform might has influenced the analysis.

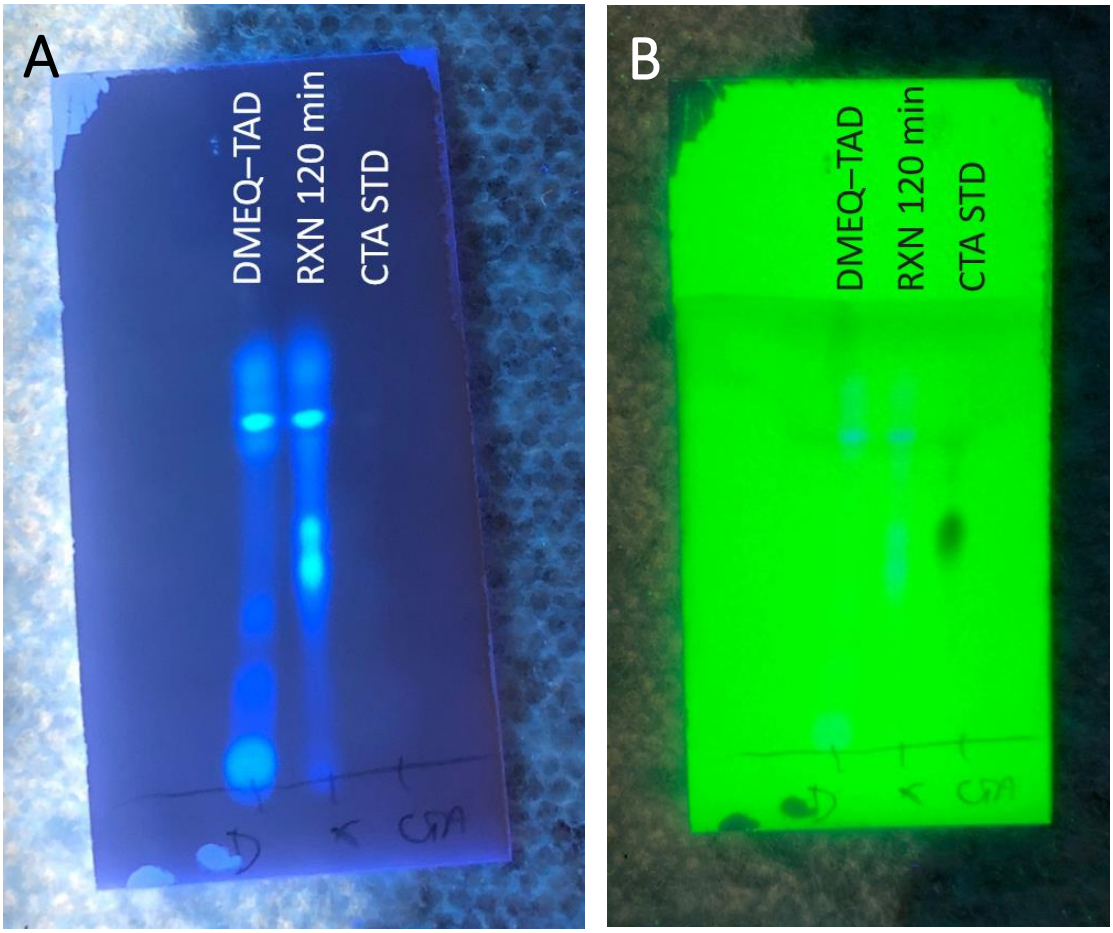

Figure 30 – Thin layer chromatogramphy in 1:9 MeOH:EtOAc comparing the starting materials to the shwon on the right and left under 365 nm, and 254 nm light respectivily. The loss of the starting material and the formation of a central peak between the retention of the starting materials suggested the reaction had occurred.

Figure 31 – A set of spectra reflecting Calcitroic Acid, Reaction after 2 h, and the Cookson reagent, DMEQ-TAD, top, middle, and bottom, respectively.

To further confirm these findings, HPLC analysis was conducted on the derivatized sample of calcitroic acid as well as the starting materials using the indicated conditions in **Figure 32**. An overlay of the collected UV chromatograms shows that the starting materials contained all the peaks observed within the reaction mixture. The starting DMEQ-TAD reagent contained several

peaks that suggested low purity and possible degradation of the sample before its use in the reaction. This may have led to a loss in activity and product yield during the reaction.

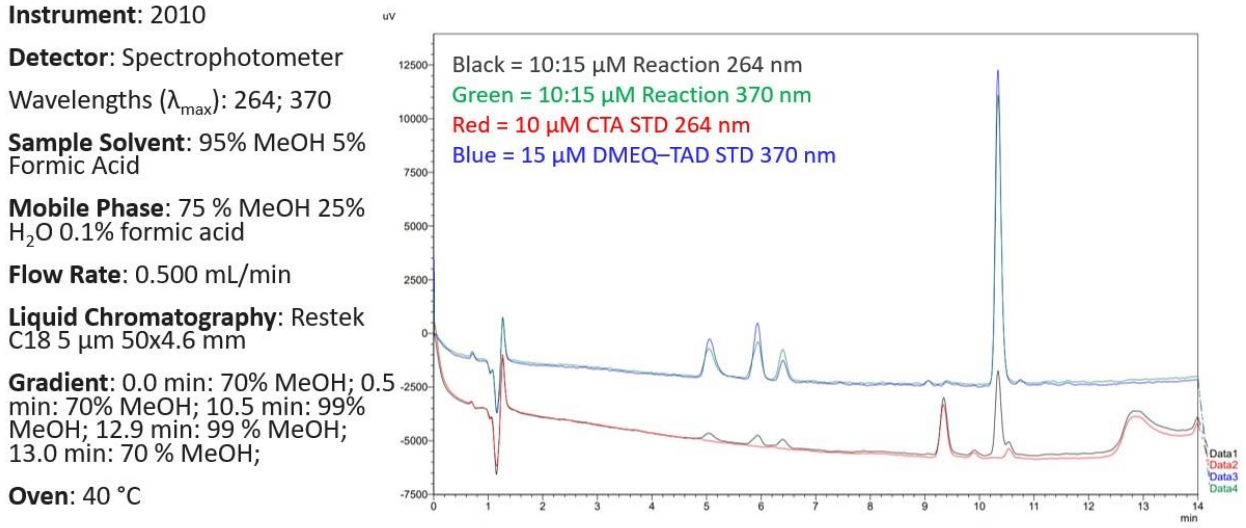

Figure 32 – An overlay of the starting materials of the reactions with the reaction mixture sample run for 2h. No peaks that were seen the reaction mixture were unaccounted for in the starting material chromatograms.

Interestingly, the overlay of spectra from calcitroic acid and the reaction mixture showed the starting material in both samples. At this point the derivatization of calcitroic acid with DMEQ-TAD was inconclusive. Further optimization has not been conducted but the mild reaction conditions for this reaction make it an ideal candidate for its use with calcitroic acid. The relatively short reaction time would allow for this type of reaction to be well utilized with large sets of samples. While these advantages paired with the simplicity of spectrometric measurement may prove useful, further optimization needs to be conducted on the reaction conditions and the controls in place to assume conversion to the red shifted product.

5.4 Isotope Labeling of Calcitroic Acid

Calcitroic acid is a naturally occurring biological species. Its natural occurrence can make the choice for standards to use in its analysis challenging. Selecting of other biologically available

compounds can be affected by the endogenous concentration. At the same time working with samples where calcitroic acid may already be present in some concentration can prevent the measurement of the quantity that is present after administrating into an animal during a study[63, 69]. One clever method for addressing these issues is to use heavy isotope labeling paired with the mass spectrometric detection. Mass spectrometers can distinguish ^{13}C-labeled calcitroic acid from natural occurring calcitroic acid. Heavy isotope labeling can prevent ionization differences between the analyte and internal standards. They allow extraction efficiency of procedures to be identical allowing a high accuracy in the correction done to the initial concentration of the native analyte. Chromatographically, there is a disadvantage to these standards. Ultra-high-performance liquid chromatographic separations are not typically able to well resolve compounds separated by a single mass unit.

Our group synthesized isotope labeled calcitroic acid for the use as an internal standard for the studies that would be conducted within animal models. The synthesis route follows previously published work by our group[70]. In future work isotope labeled calcitroic acid will be used to further explore the clearance pathway of calcitroic acid in mice. As discussed in **Chapter 4**, complex chromatographic patterns were observed for calcitroic acid when exploring mouse organ samples. Peaks that did not correspond to the expected retention time of calcitroic acid appeared in the chromatograms of samples that had undergone an extensive extraction procedure. It was speculated that other metabolites of calcitroic acid of structurally similar compounds could be present within the samples after the work up. To confirm the connection to the circulation concentrations of calcitroic acid, ^{13}C-labled calcitroic acid could be administered to distinguish metabolic products of calcitroic acid from other structurally similar compounds. If

peaks that had not previously been confirmed in connection to calcitroic acid increase in area, this will speak towards their relationship to vitamin D metabolism. Similar studies can be conducted with isotope labeled vitamin D to determine the clearance of the vitamin D to see if it is a structurally similar compound that could follow a different metabolic pathway than the one that leads to calcitroic acid. With the identification of metabolites through the *in vivo* studies, paired *in vitro* studies as described in **Chapter 3** will confirm the conversion of these species and metabolic rates of formation can be determined.

5.5 Conclusion

Vitamin D metabolite identification was built on a series of radiolabeling methods paired with several derivatization reactions to allow for the separation and identification of species based upon their physical properties. At the heart of these methods is radiolabeling, which allowed for low limits of detection with almost no background signal to the measurements. While these methods have many advantages the synthesis of these compounds can be time consuming and costly for research projects. New advances in mass spectrometry allow for a new view into vitamin D metabolism with selectivity from fragmentation patterns. While this is a powerful method as shown in previous chapters, the instrumentation comes with a level of sophistication and complexity to the results. Our group set out to explore alternative methods that could supplement the measurements being conducted with the mass spectrometric detection. It was found that Diels–Alder reagents could be used to shift the wavelength of compounds containing the diene motif providing selectivity for this characteristic and shifting the absorbance into a region where other biological samples do not absorb. During this reaction, Impurities in the derivatization reagent affected the reaction efficiency. Additional optimization and controls

would need to be put into place for the reaction to be utilized in routine analysis, preventing further exploration into the topic.

Heavy isotope labeling offers a unique method of the measurement of extraction efficiencies within individual samples. Improving upon the accuracy of individual measurements of calcitroic acid within a given sample. Our group synthesized ^{13}C calcitroic acid for the purpose of internal standards of studies and monitoring calcitroic acids pathway, distribution, and clearance in animal models. Future studies will use these samples paired with the developed mass spectrometric detection to determine calcitroic acids localization of possible metabolites in *in vivo* studies.

References

1. Norman, A. W.; Lund, J.; Deluca, H. F., Biologically active forms of vitamin D3 in kidney and intestine. *Archives of Biochemistry and Biophysics* **1964,** *108* (1), 12-21.

2. Mawer, E. B.; Lumb, G. A.; Schaefer, K.; Stanbury, S. W., The Metabolism of Isotopically Labelled Vitamin D3 in Man: The Influence of the State of Vitamin D Nutrition. *Clinical Science* **1971,** *40* (1), 39-53.

3. Aronov, P. A.; Hall, L. M.; Dettmer, K.; Stephensen, C. B.; Hammock, B. D., Metabolic profiling of major vitamin D metabolites using Diels–Alder derivatization and ultra-performance liquid chromatography–tandem mass spectrometry. *Analytical and Bioanalytical Chemistry* **2008,** *391* (5), 1917-1930.

4. Giera, M., Bioanalytical derivatization: is there still room for development? *Bioanalysis* **2015,** *7*, 2439-2441.

5. Shimada, K.; Oe, T.; Mizuguchi, T., Cookson-type reagents: highly sensitive derivatization reagents for conjugated dienes in high-performance liquid chromatography. *Analyst* **1991,** *116* (12), 1393-1397.

6. Kaufmann, M.; Gallagher, J. C.; Peacock, M.; Schlingmann, K. P.; Konrad, M.; DeLuca, H. F.; Sigueiro, R.; Lopez, B.; Mourino, A.; Maestro, M.; St-Arnaud, R.; Finkelstein, J. S.; Cooper, D. P.; Jones, G., Clinical utility of simultaneous quantitation of 25-hydroxyvitamin D and 24,25-

dihydroxyvitamin D by LC-MS/MS involving derivatization with DMEQ-TAD. *J Clin Endocrinol Metab* **2014,** *99* (7), 2567-74.

7. Cookson, R. C.; Gilani, S. S. H.; Stevens, I. D. R., Diels–Alder reactions of 4-phenyl-1,2,4-triazoline-3,5-dione. *Journal of the Chemical Society C: Organic* **1967,** (0), 1905-1909.

8. Higashi, T.; Shimada, K., Application of Cookson-type reagents for biomedical HPLC and LC/MS analyses: a brief overview. *Biomedical Chromatography* **2017,** *31* (1), e3808.

9. Higashi, T.; Awada, D.; Shimada, K., Simultaneous determination of 25-hydroxyvitamin D2 and 25-hydroxyvitamin D3 in human plasma by liquid chromatography-tandem mass spectrometry employing derivatization with a Cookson-type reagent. *Biol Pharm Bull* **2001,** *24* (7), 738-43.

10. Jones, G.; Kaufmann, M., Vitamin D metabolite profiling using liquid chromatography-tandem mass spectrometry (LC-MS/MS). *J Steroid Biochem Mol Biol* **2016,** *164*, 110-114.

11. Yu, O. B.; Arnold, L. A., Calcitroic Acid-A Review. *ACS Chem Biol* **2016,** *11* (10), 2665-2672.

6 Modeling Inflammatory Bowel Disease

Animal models are a powerful tool in understanding the efficacy of drugs and the biological role of endogenous molecules. *In vivo* studies account for many factors that are excluded for simplicity in an *in vitro* model such as the lack extracellular signaling pathways from a typical inflammatory response. In this set of studies our group set out to adopt a model of inflammatory bowel disease. Inflammatory bowel diseases have had a global increasing trend within the past decades[71]. Kong et al. have shown a relationship with the vitamin D receptor and inflammatory bowel disease[72]. We hoped to determine whether calcitroic acid plays a role in the mitigation of inflammation within the colon. If it were found that calcitroic acid was effective in mouse models, novel compounds could be designed with higher efficacy to help combat this disease.

6.1 Introduction to Inflammatory Bowel Disease

Inflammatory bowel disease (IBD) follows an inflammation pathway that can cause acute distress as well as chronic scar tissue formation leading to long term effects on digestion and other illnesses such as colon cancer. Inflammatory bowel disease can be broken down into two diseases, Crohn's disease, and ulcerative colitis. IBD has a multi-causational, though it is speculated that there is a genetic component that leads to induction of the inflammatory response through an overactive immune system. One aspect of the pathophysiology of the disease is the exposure of regions of the intestinal tract to bile acid acting as an irritant inducing inflammation. Common compounds currently used in the treatment of IBD include corticosteroids such as prednisone and dexamethasone[73]. These compounds were used as

positive controls in the design of the animal model below. They act by disrupting cytokine response preventing the cascade of recruitment[74, 75]. The blocking of cytokines prevents the histological signals of inflammation from occurring. Steroidal treatments cause suppression of the immune system, which leads to other applications of these drugs in treating autoimmune diseases but can have significant side effects[76]. Developing a drug based on the response of the calcitroic acids activity on the vitamin D receptor would allow for greater specificity over traditional corticosteroids.

6.2 Experimental Design

Our research in this section was designed to determine the effect of calcitroic acid on induced colitis in mice to see if there was a reduction similar to the response observed with currently used corticosteroids such as dexamethasone and prednisone. Our goal was to implement a model using swiss webster (CFW) mice, an out-bred stain, to demonstrate the robustness of the model. Outbred mice contain more genetic variance within the population leading to a more accurate representation of human populations. The initial model was based on studies that were using inbred mice, and the procedure was modified in the way described below to account for the difference in the colonies used[77].

CFW mice were purchased from Charles River for the use during the study. The mice were separated into groups of positive control (corticosteroid treated), and vehicle. The mice were housed in groups of four to accommodate for social tendencies. Bedding material was provided as an enrichment for each cage. Each set of mice that were used in the study were given seven days to acclimate to the new environment after relocation. Mice were then administered a dose

of corticosteroid, or vehicle daily depending on the group. Weights were collected for each mouse daily throughout the study. Photographs of the coat quality were taken daily and compared between the two groups. It was found that this measure seemed independent of the other measures of colitis severity during the study and thus was omitted from the findings. On the third day of each study, mice were anesthetized using isoflurane for an installation of the chemical irritant to induce colitis. This model was designed to imitate the type of inflammation that would be observed in ulcerative colitis. 2,4-dinitrobenzene sulfonic acid (DNBS) was used during the first set of these studies to serve this purpose. The number of installations and concentration varieties during the optimization of this model and is described in **Section 6.4**. The mice were monitored over the course of five days after the initial installation, or seven days after the first dose of the respective compound. On each day, the mice were given a dose of corticosteroid, or the vehicle dependent upon their group. On the final day of the study the mice were euthanized through CO_2 asphyxiation and spinal dislocation. This was followed with exsanguination for ease of the necropsy. Colons were excised, photographed, and measured in length before and after the cleaning procedure. The colons were rinsed with a PBS buffer and stored on ice in PBS before homogenization.

6.3 Quantification of Colitis

A preliminary study conducted by our group identified several markers that could be utilized for the analysis of inflammation within this model. The first measure that would be monitored throughout the study was the weight of the mice. Besides the ramifications of this measurement for the humane endpoint of the study, set to be 25% total loss of body mass, this measurement allowed for a sense of distress that the study was placing onto the animal signaling

eating and drinking pattern. Coat quality hoped to speak towards the same measure by measuring the habitual grooming pattern of mice and how this could signify the wellbeing of the animal. Movement patterns were explored during the early parts of the study and would follow the tracking of animals. Animals were placed into a container and monitored for 90 sec time intervals. Their position relative to the edge of the container suggested regular survival instinct to avoid the center of the container for predatory exposure. Finally hematological data and histology was planned for the study based on the initial finding with BALB/c mice suggesting that a difference in the recruitment of immune cells to the site of inflammation was visible. Differences were observed in the circulating concentration of granulocytes with mice that were treated with the chemical irritant. This measure was planned to be used once the activity of myeloperoxidase (MPO) expressed by granulocytes was determined. MPO activity can be determined by its ability to form perchlorate from hydrogen peroxide[78]. The perchlorate then acts as an oxidizing agent dimerizing the o-dianisidine shifting its absorbance to 460 nm for spectrometric measurement.

Each colon was transferred from the animal facility along with the blood samples when appropriate for histological and biochemical assays. Blood parameters were measured at the Medical College of Wisconsin. The colon samples were then transferred to a new vial and massed without the PBS buffer. The initial study that was conducted to determine the activity of MPO used a fragment of colon that was weighted, homogenized, and analyzed. A change to the procedure was done to account for the distal localized nature of the inflammation within the colon. The entire colon was used during the procedure and the protein concentration was

determined with a bicinchoninic acid (BCA) assay to enable a uniform protein concentration for all colon samples.

The principle of the BCA assay operates on the reduction of Cu^{2+} present in the assays reagents to control the metal chelation leading to a shift in the absorbance of the reagents. A general mechanism of the procedure is shown in **Schematic 19**. cysteine, cystine and tryptophan reduce copper ions added in the reaction changing its oxidation state[79]. The cuprous then can form a complex with the chelating agent changing the absorbance maximum to the wavelength of 562 nm. The absorbance can be compared to a calibration curve generated from standards to determine the amount of protein that was present in the original sample.

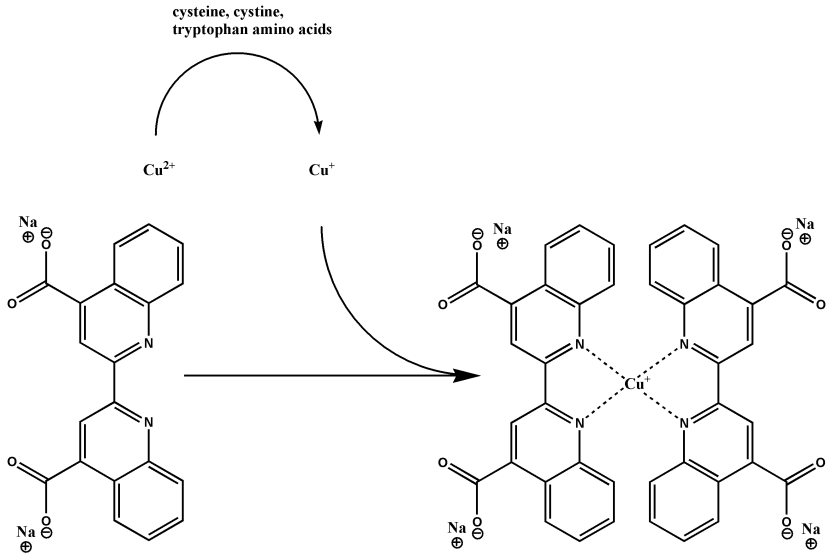

Schematic 19 – Representation of the reduction of coppric to copprous by amino acids. The reduced form is then chelated to form a redshifted complex.

A solution of 50 mM phosphate buffer at pH 6.0 with a detergent of 50 mM hexadecyltrimethylammonium bromide was used to homogenize the samples. A handheld

homogenizer was used for the homogenization step within a biological hood. Colon homogenate samples were then transferred into a centrifuge tube and centrifuged at 10000 rpm at 4 °C from 10 min. Aliquots of the supernatants were then diluted 8-fold and 16-fold in two sets and a BCA assay was conducted on each of the samples to determine the total protein concentrations of the supernatants.

In the BCA assay, a ladder of bovine serum albumin (BSA) was prepared from solid stock standards to generate a calibration curve of protein. The two reagents were then added to a 96 well plate and 4 replicates on each standard and sample were measured using the Tecan plate reader at the wavelength of 562 nm. Samples were compared to the calibration curve to calculate the protein concentration. Informed by the initial supernatant concentration in protein, each sample had an aliquot diluted to the concentration of 200 µg/mL for use in the myeloperoxidase (MPO) Assay. Diluted supernatant samples were stored at 4 °C during the solution preparation of the MPO assay.

A daily standard solution for the hydrogen peroxide solution was prepared to a concentration of 0.0024% from a 35% v/v stock. The phosphate buffer that was prepared for the BCA assay was utilized for the dilution step of this assay. O-dianisidine dihydrogen chloride was prepared at a concentration of 167 µg/mL in phosphate buffer and sonicated for 30 min to dissolve in the buffer. 8 µL of the BCA assay concentration adjusted colon supernatant was transferred to a 384 well plate containing 62 µL of the o-dianisidine solution. The reaction is initiated with the addition of 10 µL of the hydrogen peroxide solution prepared above. The conversion of the o-dianisidine was mitigated by a secondary oxidation after the hydrogen peroxide is converted into hypochlorite. The general process of this reaction is shown in

Schematic 20. The product of this reaction shifts the absorbance to the λ_{max} to 460 nm. The plate is then measured over a 15 min period in the plate reader in 30 sec intervals. Four replicates on each homogenate sample were conducted for each of the MPO assays described in this chapter.

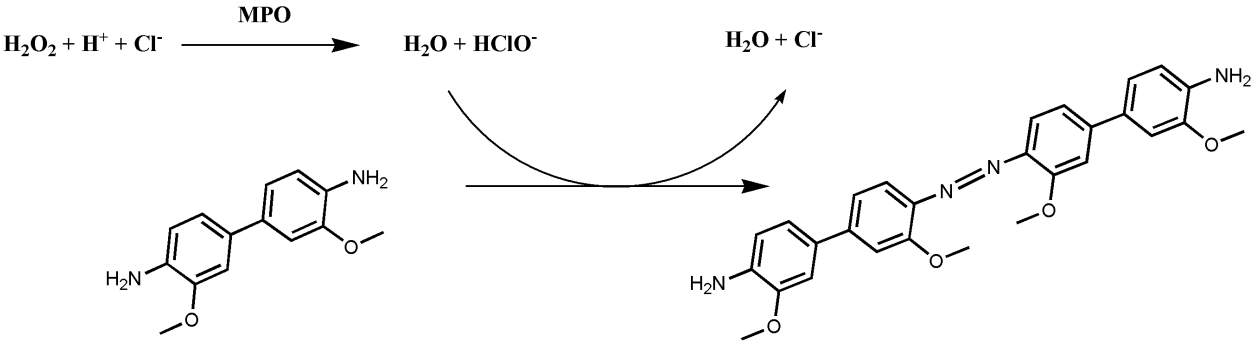

Schematic 20 – The chemical reaction that occurs in the designed myeloperoxidase assay. Hydrogen peroxide is oxidized enzymatically into hypochlorite which then acts upon the o-dianisidine.

6.4 Experimental Design Optimization in Studies

While the study procedure for IBD has been demonstrated by previous research groups using inbred mice, our group hoped to define a model with outbred mice that described the efficacy of compounds to reduce inflammation. While the genetic variance of the population was an advantage towards a compound's robust response to different genotypes, it led to complications in transferring the method which required further optimization of the study. This section outlines the series of modifications to the study that were conducted to allow for the implementation of the outbred CFW mice within our study.

6.4.1 Optimization Irritant Concentration

The first study that was conducted was set to determine the efficiency in inducing colon inflammation in the CFW mice. A literature dose of 200 mg/kg DNBS for BALB/c mice resulted in a poor response in the single installation of the DNBS prompting a second dose of 200 mg/kg during the second day of the study. Two groups of six mice underwent this procedure. One group

that was provided with dexamethasone and the second group given the vehicle, both provided through IP injection. The diluent for the drug was in 5:40:55 DMSO:polyethylene glycol 400: phosphate buffered saline. In this study mouse weights were monitored for the five days following the first dose of the DNBS.

The weight changes are shown if **Figure 33**. The red dashed line represents the expected weight loss of mice in the study that had a proper installation of the DNBS inducing colitis. The negative control group average percent weight loss was found to be -21.5% ± 2.1% while the dexamethasone treated mice had an average percent weight loss of -7.1% ± 3.8%. By the fourth day of the study, there was statistical significance $P < 0.001$ between the treated group and the non-treated group suggesting a reduction in inflammation. Colons were collected from the necropsy and photographed for visual signs inflammation. The images are shown in **Figure 34**. Widespread inflammation was observed with two of the mice having severe colon inflammation. Fecal consistency also varied widely among the group suggesting that the consistency of the dexamethasone treatment had high variance.

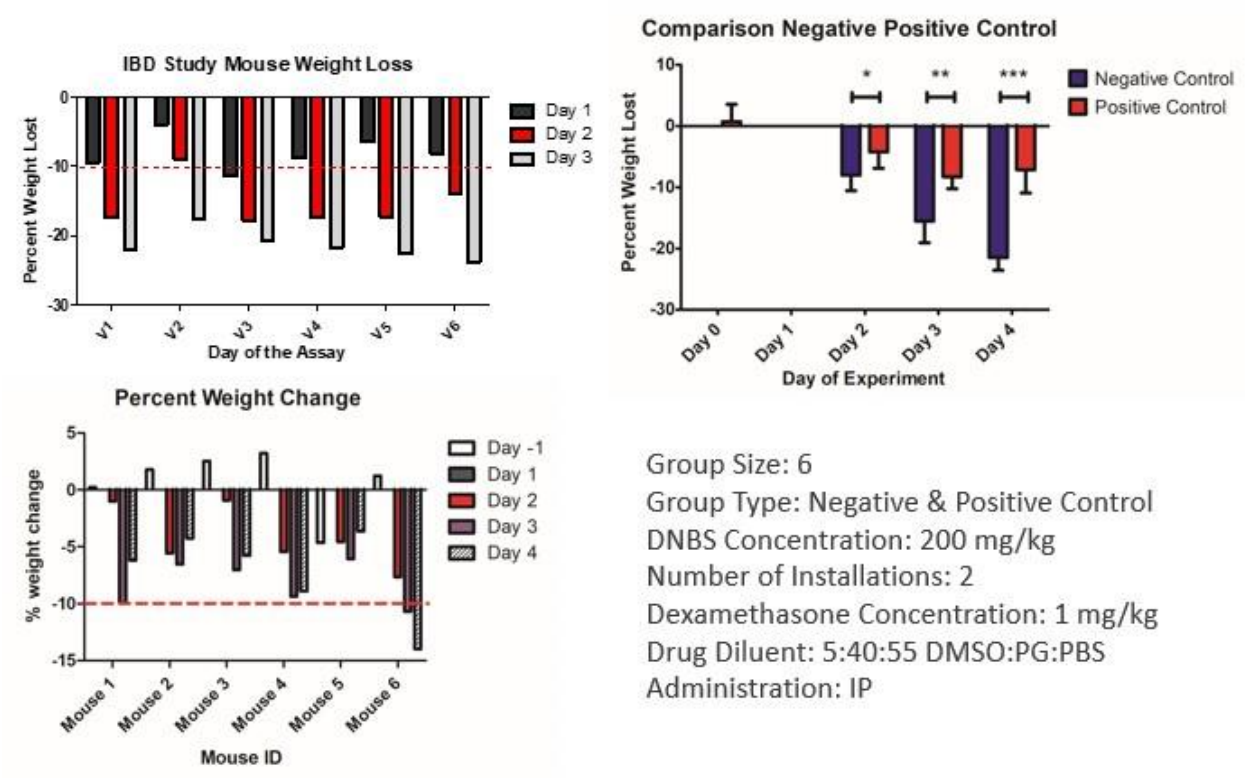

Figure 33 – Weight loss of the mice as a percentage of the initial body weight at the beginning of the study. The two graphs on the left represent the indiviual mice within the study and the graph on the left shows the groups combined for statistical analysis.

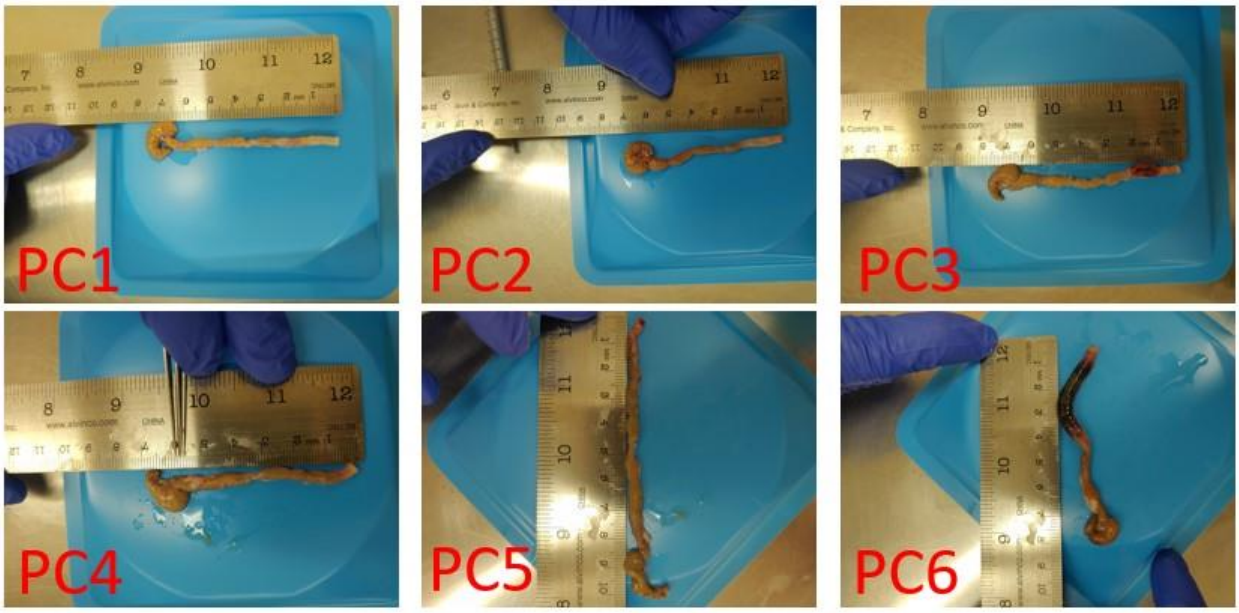

Figure 34 – Images of the colons in the positive control group of the intial IBD study. The explected length of an untreated colon would be near 9.5 cm while all members of this group fell below that meaure.

Finally, MPO assays were conducted following the procedure described above to determine the oxidative enzyme activity in the colon homogenates. A set of absorbance of samples run over 15 min is shown in **Figure 35**. The negative control represents mice that were provided with the vehicle and DNBS, the positive control group received dexamethasone and DNBS, the negative control received no DNBS. As was expected, the group that did not receive the DNBS installation have very low activity of oxidative enzymes in their colon homogenates. It was unexpected that the group that received dexamethasone did not have a significant reduction in inflammation when compared to the group that were untreated. It was of interest that the two mice that had strong visual inflammation scores were seen to have higher levels of inflammation than the negative control group. It was speculated that the vehicle group may have not had a strong enough inflammation response for the dexamethasone to be able to reduce the inflammation. The study was repeated with two groups during the same week to see if the deviation of the visual inflammation and MPO activity was truly an outlier or the expected response of the assay.

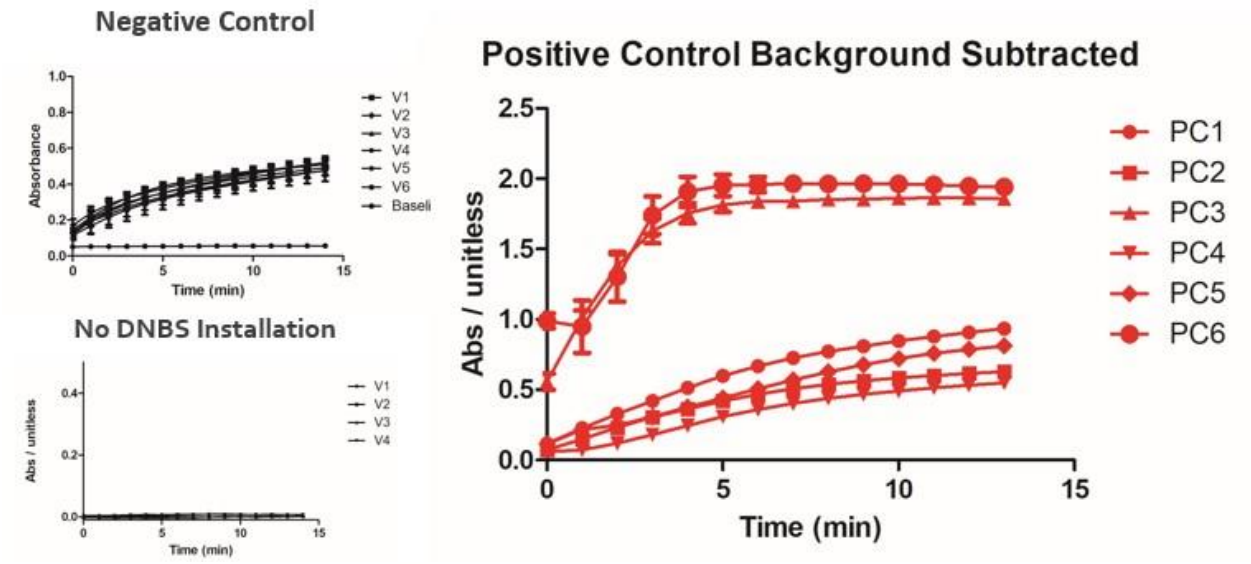

Figure 35 – Collection of MPO assays conducted on the three different groups of the intial study. The left side of the graph contains both the mice given vehicle and the chemical irritant, DNBS while the figure below it shows mice with no chemical irratant. The graph on the right is the MPO assay conducted upon mice that were given 1.0 mg/kg dexamethasone after installation of DNBS.

The comparison of the two groups by weight is shown in **Figure 36**. While not significate, it was observed that a trend between the two groups was observed two days after the installation. This did not carry through the remaining days of the study and the two groups converged on similar % weight loss. It was also noted that two mice that were in the vehicle group did not maintain a weight above the humane end point and were removed from the study before the final day. The summary of colon images can be seen in **Figure 37**. Of the mice that were alive during the final day of the study, one mouse in the vehicle group and one in the positive control had high visual inflammation scores. Minor inflammation was observed in one colon from the dexamethasone group. The MPO assay was conducted following the previously described procedure on colon homogenates shown in **Figure 38**. No significant difference in the activity was observed between the two groups. There were concerns about the concentration of the DNBS

but the requirement for an elevated oxidative response in the sample suggested that modification to the corticosteroid concentration may be better suited for separating these two groups.

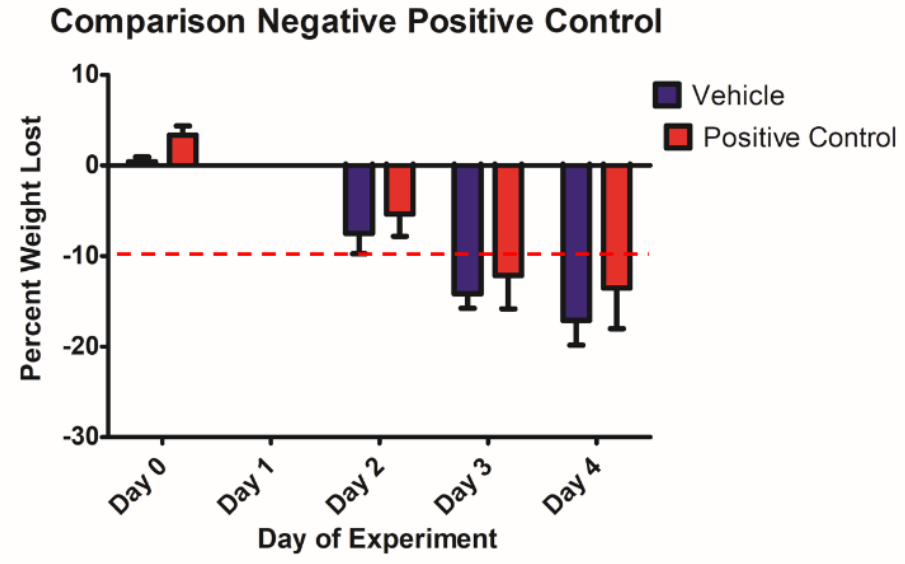

Figure 36 – A comparsion of the treated and vehicle groups of mice in the replicate of the intial study. No statistical signifcance was seen between the two groups.

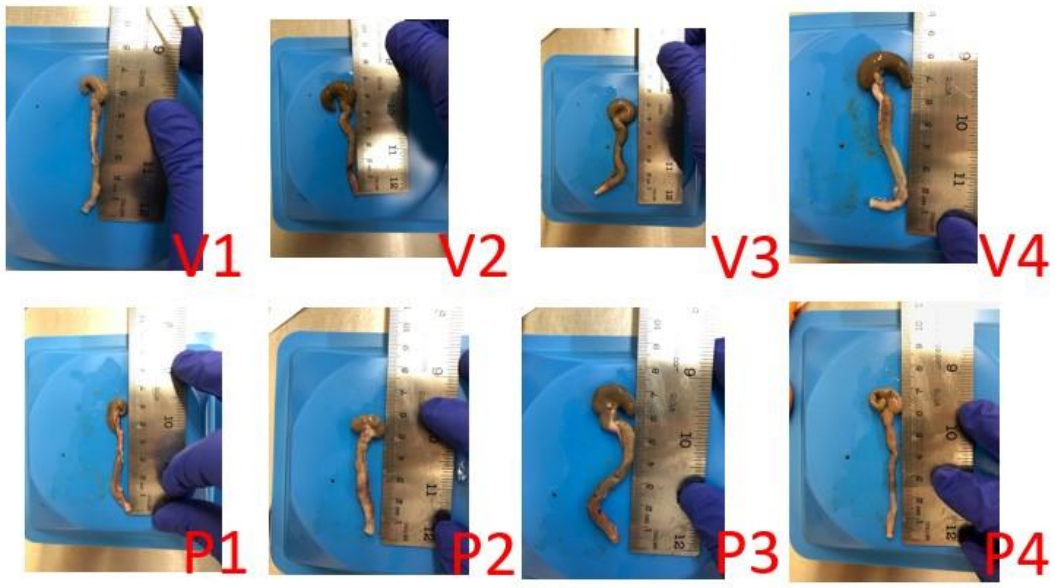

Figure 37 – Colon images of the replicate of the initial sample conditions. The severity of the inflamation seen in these groups was greater than what was measured in the first study.

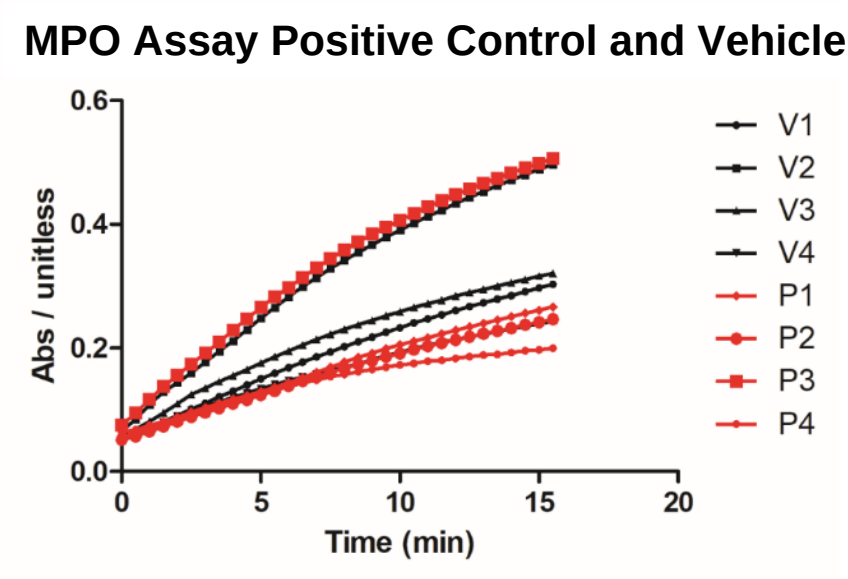

Figure 38 – Overlay of the MPO assay indiviual colon homogenates for the vehicle group (black) and the positive control group (red).

To explore whether the concentration of the dexamethasone could be increased to reduce colon inflammation within the positive control group, mice were treated with 5 mg/kg of dexamethasone. The resulting comparison with a vehicle group is presented in **Figure 39**. The standard deviation of each of these groups was very large. Each of the individual weights throughout the study is shown in **Figure 39** as well. DNBS installation did not appear to be effective in two mice, showing low weight loss over the study. It was unexpected that the visual determination of inflammation did not correspond well to the weight loss data collected over the study. The images are shown in **Figure 40**. Fecal consistency varied between the two groups, adding to the concerns of correlation between weight loss and colon inflammation. The MPO assay results conducted with colon homogenates are shown in **Figure 41**. The inconsistency of the two groups suggested the design of the MPO assay not sensitive enough to determine the oxidative enzyme activity.

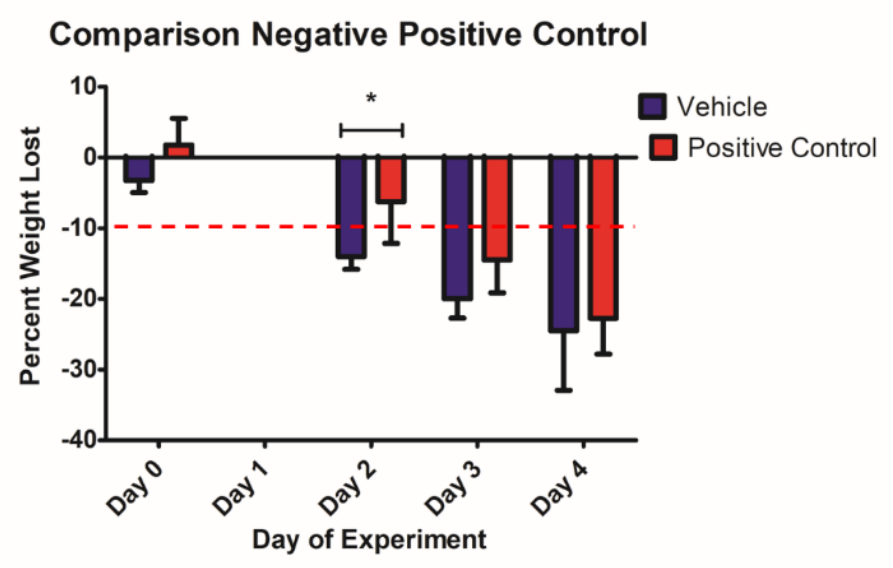

Figure 39 – Comparison of the vehicle (blue) and positive control group (red) now provided a higher concentration of 5 mg/kg dexamethasone.

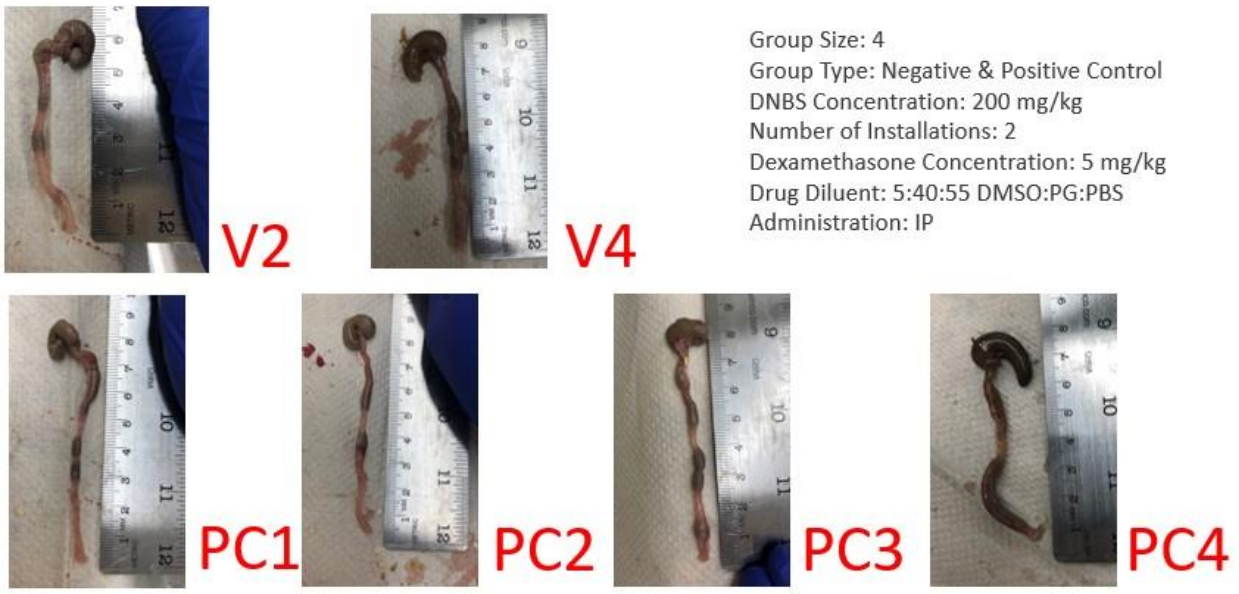

Figure 40 – Collected colon images of mice during the study (V for vehicle and PC for the postive control). The postive control received the higher concentration of 5 mg/kg dexamethasone.

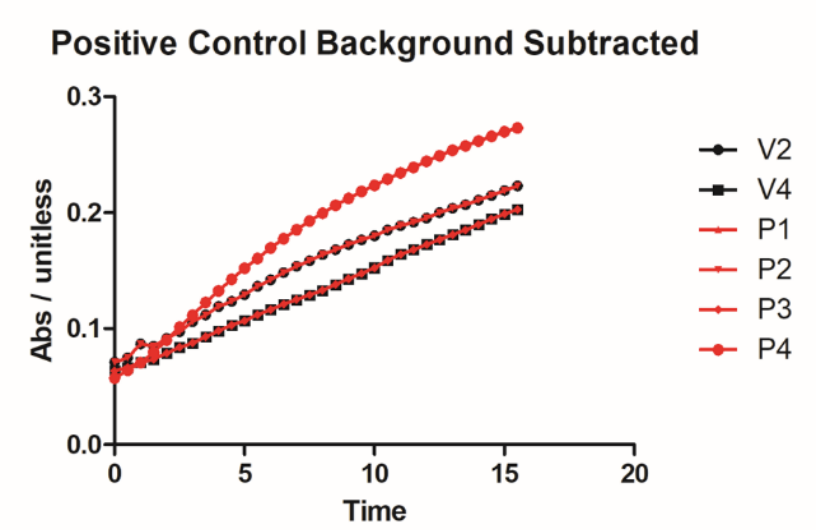

Figure 41 – MPO assay overlay of the higher dose 5 mg/kg dexamethasone group (red) compared to the vehicle (black).

6.4.2 Removing Nonchemical Inflammation

The high level of variance of inflammation within both groups rose concerns that the method of delivering the compound might be inducing a physical irritation near the site of interest. The 100 µL IP injection was considered a large quantity for the administration of a propylene glycol solution that may not have proper clearance over the time before the next dose.

Alternative formulation was performed with a 1:15 (2-Hydroxypropyl)-ß-cyclodextrin:PBS solution containing 5% DMSO for improved solubility of the dexamethasone. The dose was held constant from the previous study of both the dexamethasone and DNBS. The weights were collected following the same procedure as described above. The percent weight loss is shown in **Figure 42**. Similar to what was observed between the past studies, no significant difference between the two groups was observed. The standard deviation of the two groups both seemed lower as all mice in the study underwent a colitis-like response from the DNBS. All mice within

the model had a visual inflammation response that would be expected from the induction of colitis as shown in **Figure 43**. The MPO assay data collected with colon homogenates are shown in **Figure 44**. The response between the two groups was not found to be significant. This was expected based on the weight percent weight loss, as well as the visual inflammation and fecal consistency measures. One colon, V3, in the assay still had a significant higher oxidative enzyme activity. This mouse was considered an outlier of the assay. It was concluded that the formulation was not the reason for the data inconsistency. At this point in the study development there were two issues that needed to be addressed before this study could be used to investigate new compounds. The MPO assay had to be adjusted so that the variance between measurement would allow for comparison between the two groups. Beyond that problem, the inflammation severity within the vehicle group needed consistency to allow for the efficacy of the positive control to be shown.

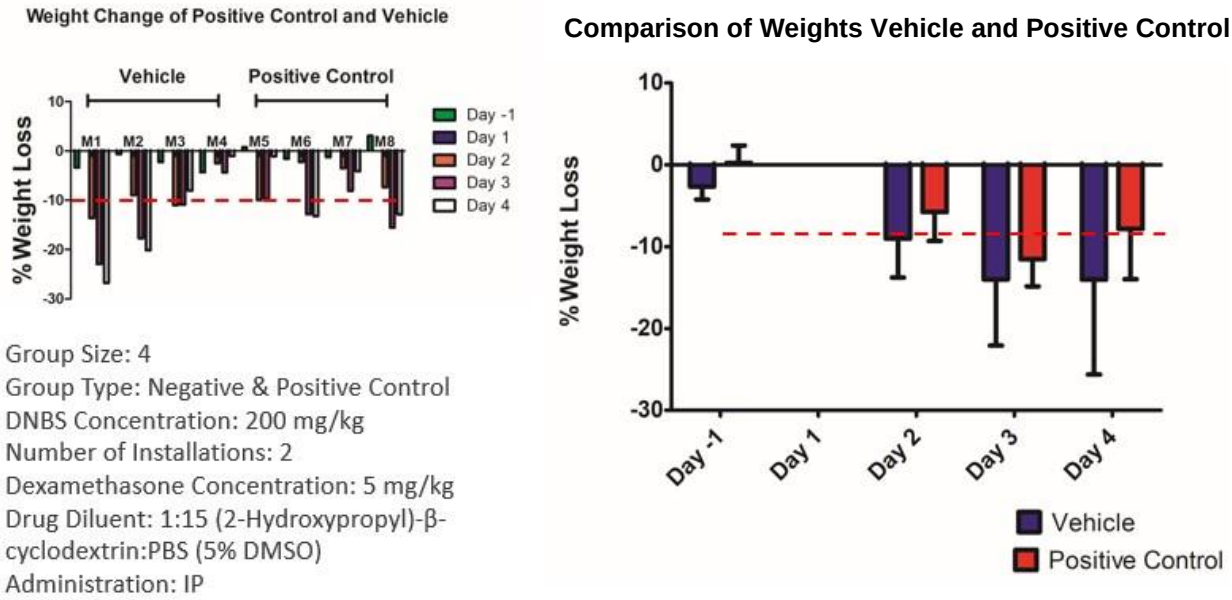

Figure 42 – A comparision of mouse weights indivual (left) and grouped (right) for mice treated with a new vehicle.

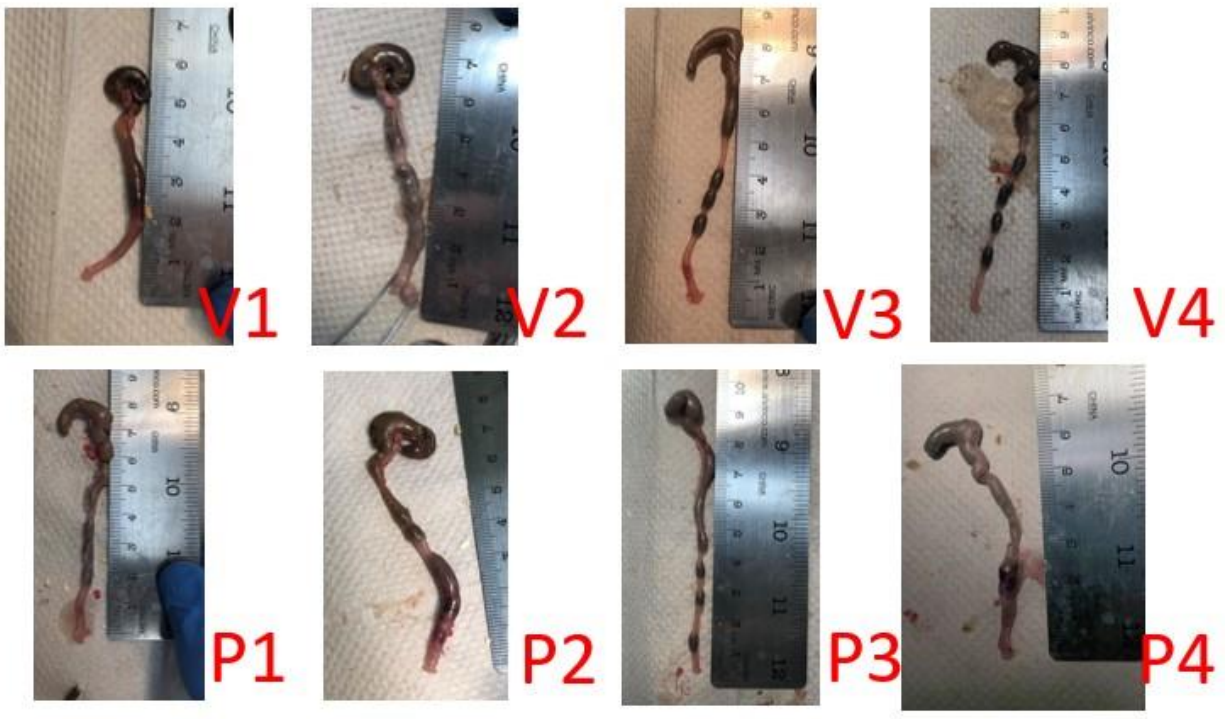

Figure 43 – Colons collected from the two groups of mice vehicle (top) and dexamethsone (bottom). The varience in length as well as localized inflamation was observed in this study similar to previous studies.

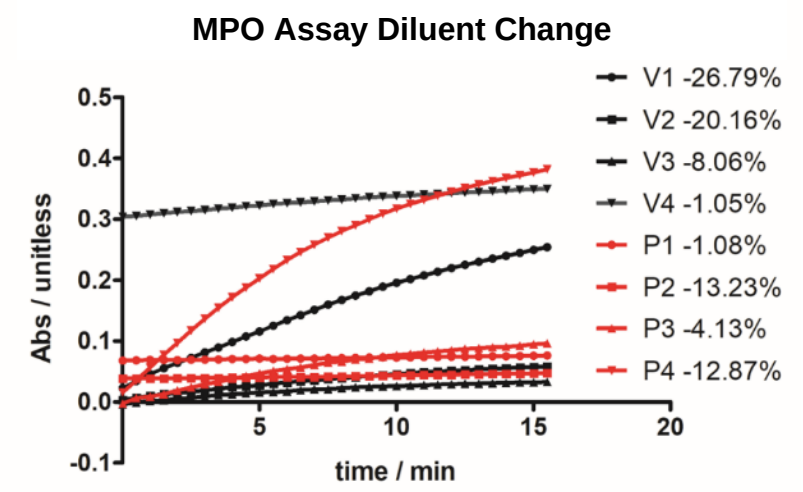

Figure 44 – The MPO Assay overlay of the postive control (red) and vehicle (black) groups. Several colon homogenates had higher than expected activity based on the visual and weight loss observed during the study.

6.4.3 Colon Homogenate Preparation

Adjustments upon the sample preparation procedure were posed to see if less colon washes could prevent the loss of oxidative enzyme activity. It was speculated that the rinse of the colons with PBS could have removed most granulocytes that would be present within the colon and caused greater variance in the MPO assay measurements. The new study that was conducted hoped to explore the activity of colon homogenates that used mechanical removal of feces alternative to solvent rinses.

Two groups of n = 4 mice were separated and treated with vehicle and dexamethasone prepared at 5 mg/kg daily over the study. The percent weight loss is shown in **Figure 45**. The percent weight loss between the two groups was not significant. The corresponding colons are shown in **Figure 46**. Large sites of discoloration and enlargement were seen in all colons of both groups of the study. Fecal consistency was soft for all the mice that underwent necropsy. The oxidative activity of colon homogenates is shown in **Figure 47**. These data correlate well with the visual inflammation that was observed but not with what was expected based on the percent weight change. The variance between individuals within each group was very low excluding the outlier P3. Due to this improvement of the MPO assay, all future studies incorporated the non-solvent based fecal separation.

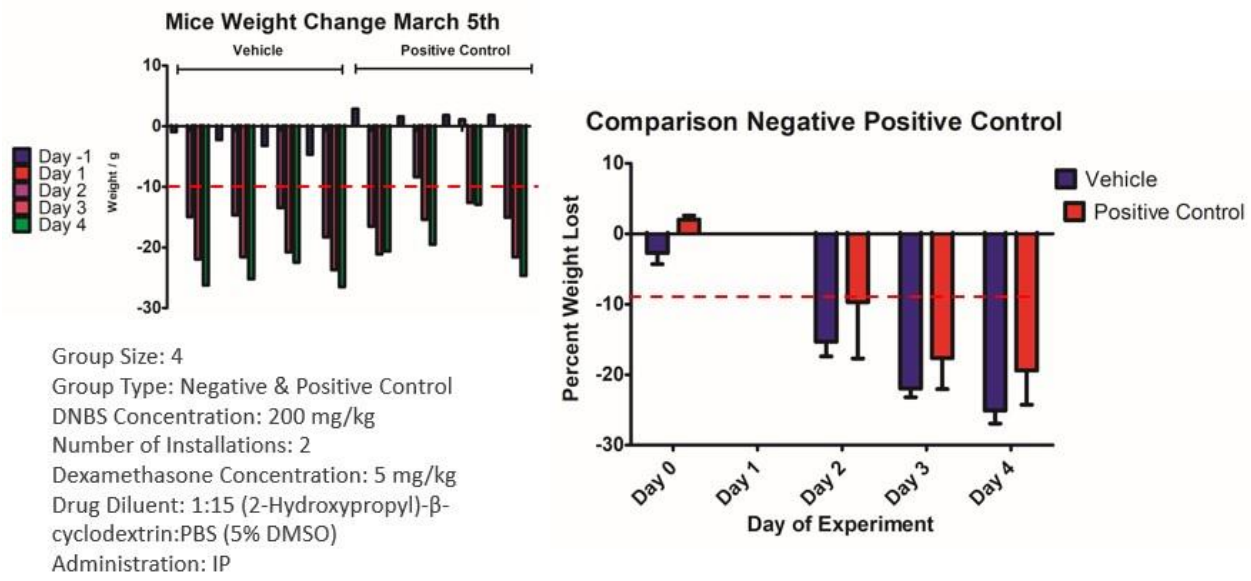

Figure 45 – Weight lose of inividual mice (left) and grouped (right) as a percentage of the initial weight at the beginning of the study. No statistical difference was observed between the two groups.

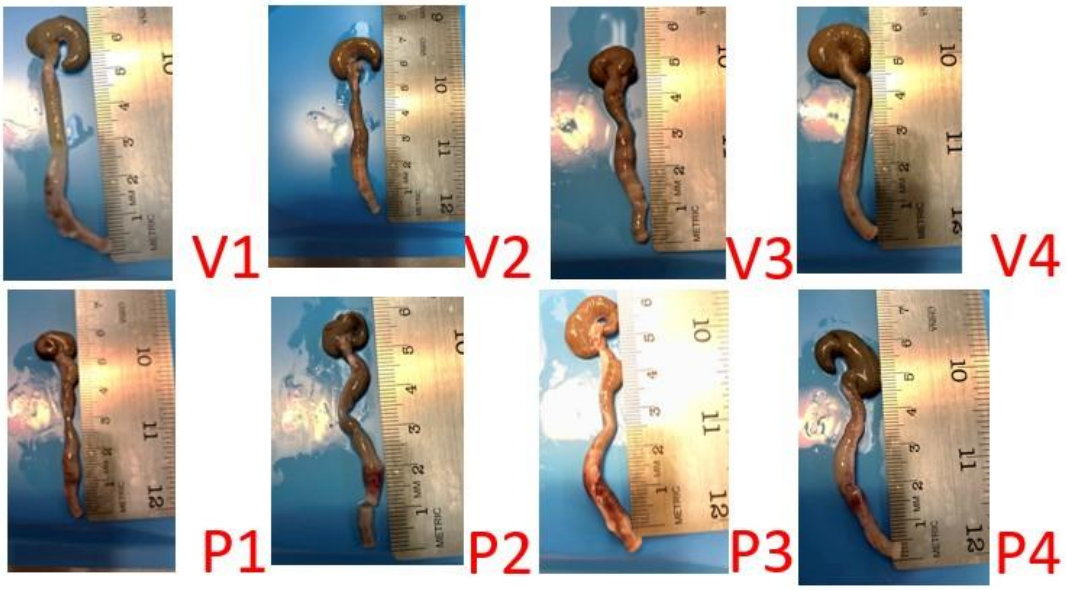

Figure 46 – Colon images of mice in the vehicle group (top) and the positive control (bottom). High levels of inflamation were present in both groups.

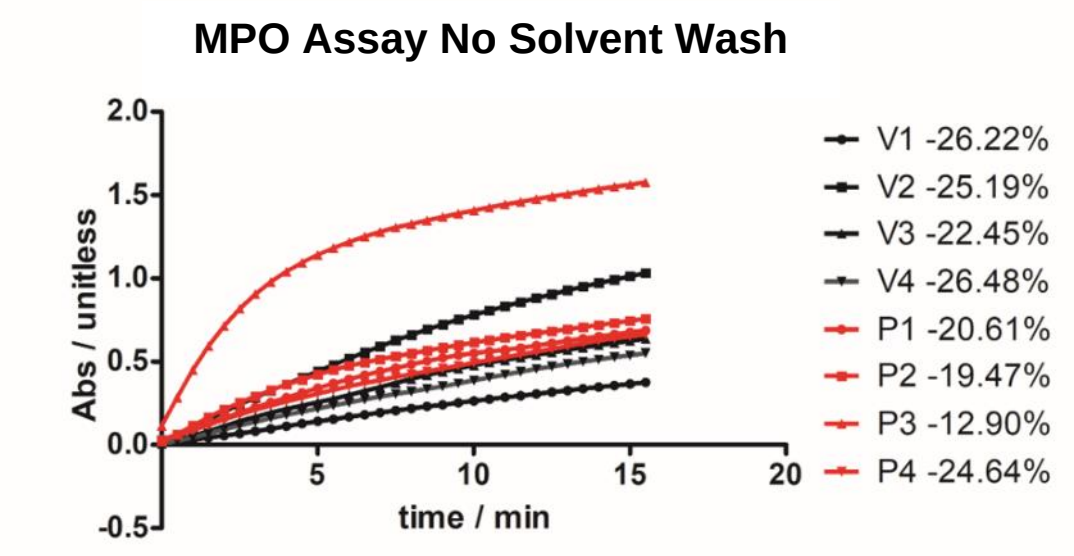

Figure 47 – MPO assay overlay of indiviual mice from the vehicle and positive control groups. The colons underwent manual fecal remove to try and preserve oxidative activity.

6.4.4 Corticosteroid Administration

Intraperitoneal injection (IP) of compounds was used for all previously described studies. Due to the variance of data within the studies it was posed that the site of injection may be too close to the intestinal tract and may interfere with the installation of DNBS. To address this issue, IP injections were changed to an oral administration of dexamethasone. An oral dose 5.0 mg/kg of dexamethasone was prepared in 5:95 ration of polyethylene glycol 400: 2.5 % aqueous solution of hydroxypropylmethylcellulose (HPMC). Mice were treated on the same schedule as described above.

The dose of the dexamethasone was maintained in hopes of inducing a significant reduction of inflammation in the treated group. Under these changed conditions groups of six mice were used. During the study, two mice were removed due died before the final day of the study. The weights of the mice are shown in **Figure 48**. It was found that the weights did not significantly vary between the two groups. The visual inflammation can be observed in **Figure 49**.

V2 and V6 were the only mice to show little visual signs of colonic inflammation and firm fecal consistency. The results of the MPO assay conducted with the colon homogenates are shown in **Figure 50**. It was observed that each group had a response consistent with high oxidative activity. The colon V3 was an outlier within the study and the activity was much higher than the other samples. Correlating the visual identification of inflammation, the response of the V6 colon was low suggesting accuracy of the assay. No conclusions of the effectiveness of dexamethasone were able to be drawn from the data of this study, suggesting that there remained a fundamental issue with the assay that needed to be addressed before compounds could be screened for their efficacy of reducing the induced colitis.

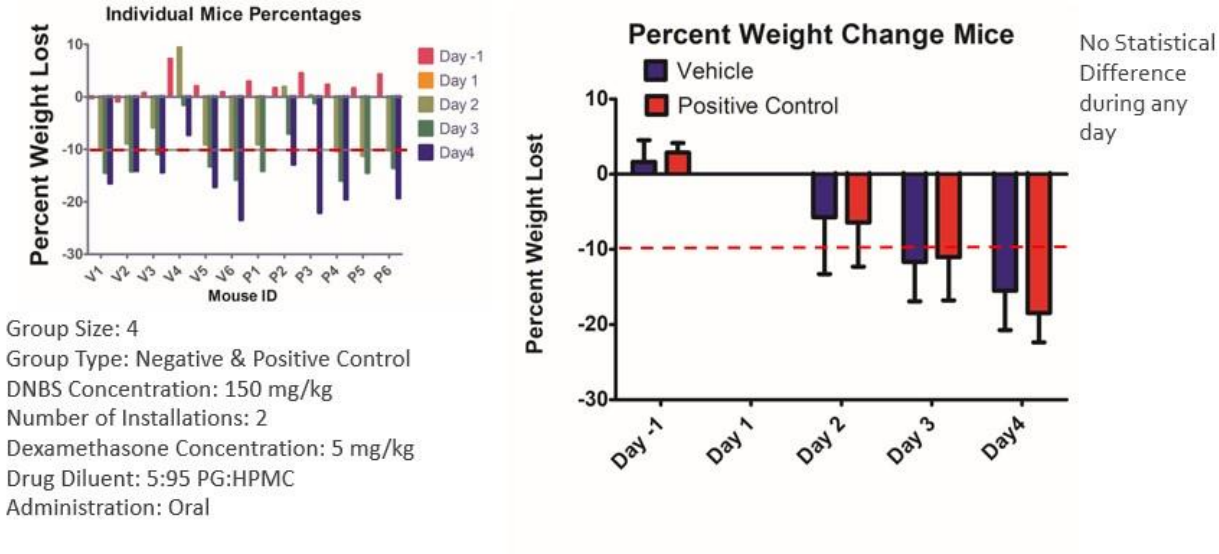

Figure 48 – Comparison weights of individual mice (left) and grouped (right) given vehicle and 5.0 mg/kg dexamethasone through oral gavage.

Figure 49 – Images of colons of mice give vehicle (top) and the mice provided with 5.0 mg/kg dexamethasone (bottom) through oral gavage.

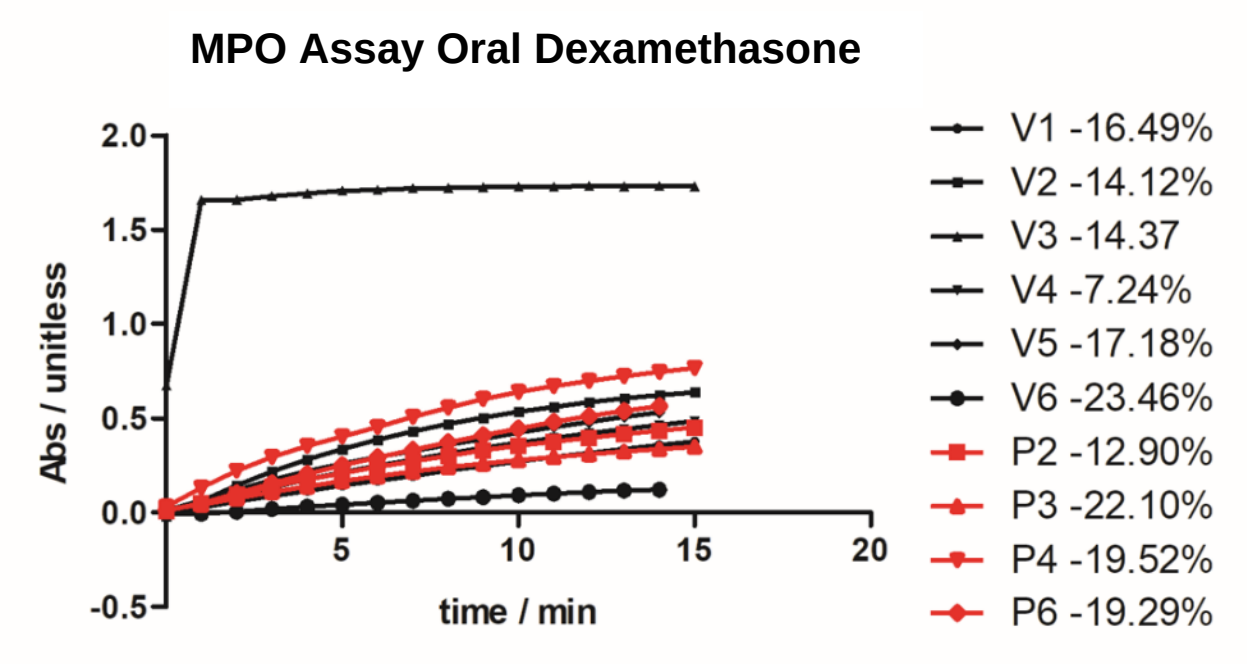

Figure 50 – Overlay of the MPO assay of the positive control (red) and negative control (black). The "soft" sample preparation method was used for this study.

6.4.5 Corticosteroids as Positive Controls

Other corticosteroids were explored to compare to their efficacy with dexamethasone. Prednisone was explored as an alternative corticosteroid for the reduction of colitis. Prednisone, shown in **Schematic 21** along with DNBS, has previously been explored by other groups and is an FDA approved treatment for inflammation. The procedure that was used for these studies followed the same modification of oral administration, lower installation volume for DNBS, and soft wash for sample preparation to maintain any advantages that were observed in the previous studies.

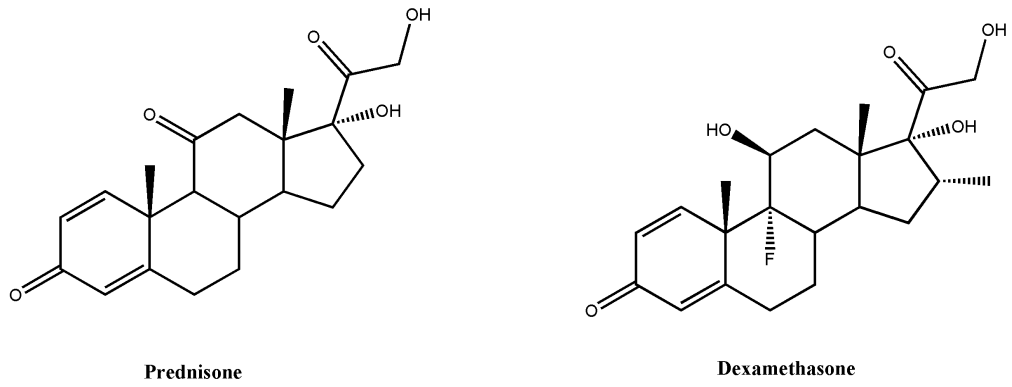

Schematic 21 – Structure of the corticosteroids used within the studies.

Two groups of four mice were separated and housed during the study while treated with prednisone. Prednisone was administered at 5 mg/kg daily by oral gavage. The formulation for the preparation was 5:95 PG:HPMC. Mouse weights were monitored daily and summarized in **Figure 51**. High variance of weight loss was observed within both groups. During necropsy, the colons were photographed and shown in **Figure 52**. The percent weight loss correlated with the degree of visual inflammation, suggesting inconsistency of the installation process with DNBS and subsequent colon inflammation. The MPO assay was conducted using colons that underwent the mechanical removal of feces before analysis. The results are shown **Figure 53**. Three distinct groups were observed that included mice with no inflammation, mild inflammation, and severe inflammation.

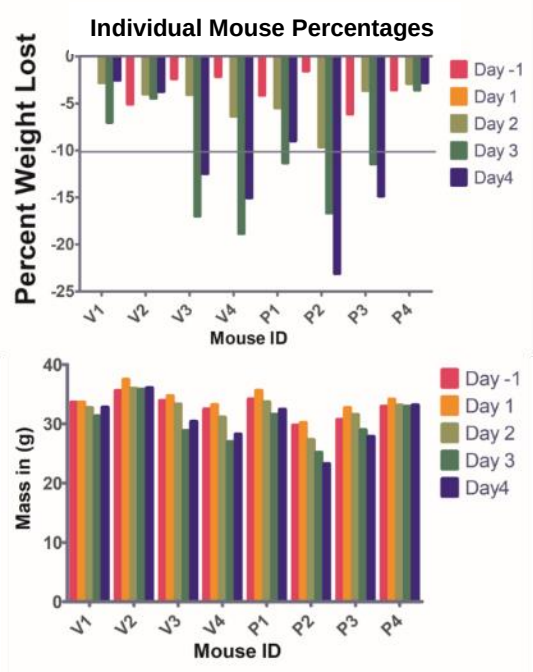

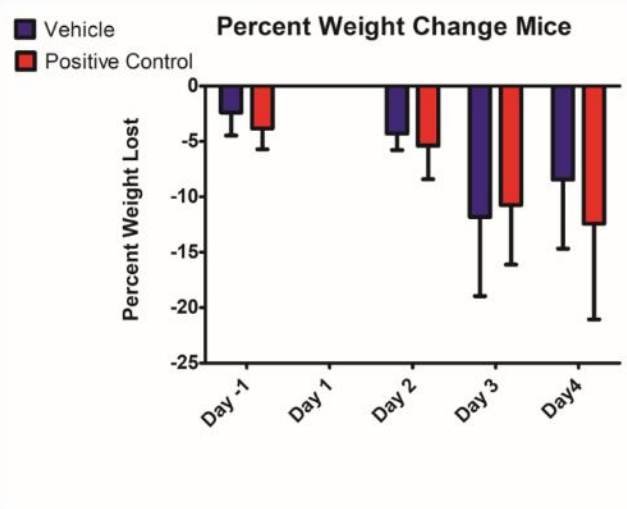

Figure 51 – Weight comparison of indidual mice (right) and the grouped weight change (left). Positive control mice were given a 5 mg/kg prednisone through oral gavage.

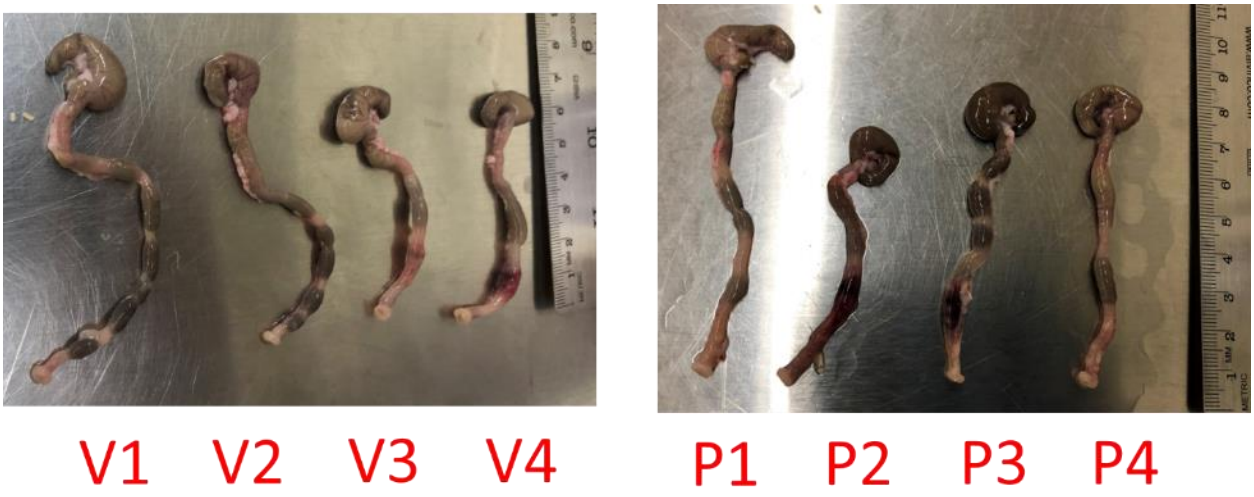

Figure 52 – Colons of vehicle mice (left) compared to mice treated with 5.0 mg/kg prednisone (right).

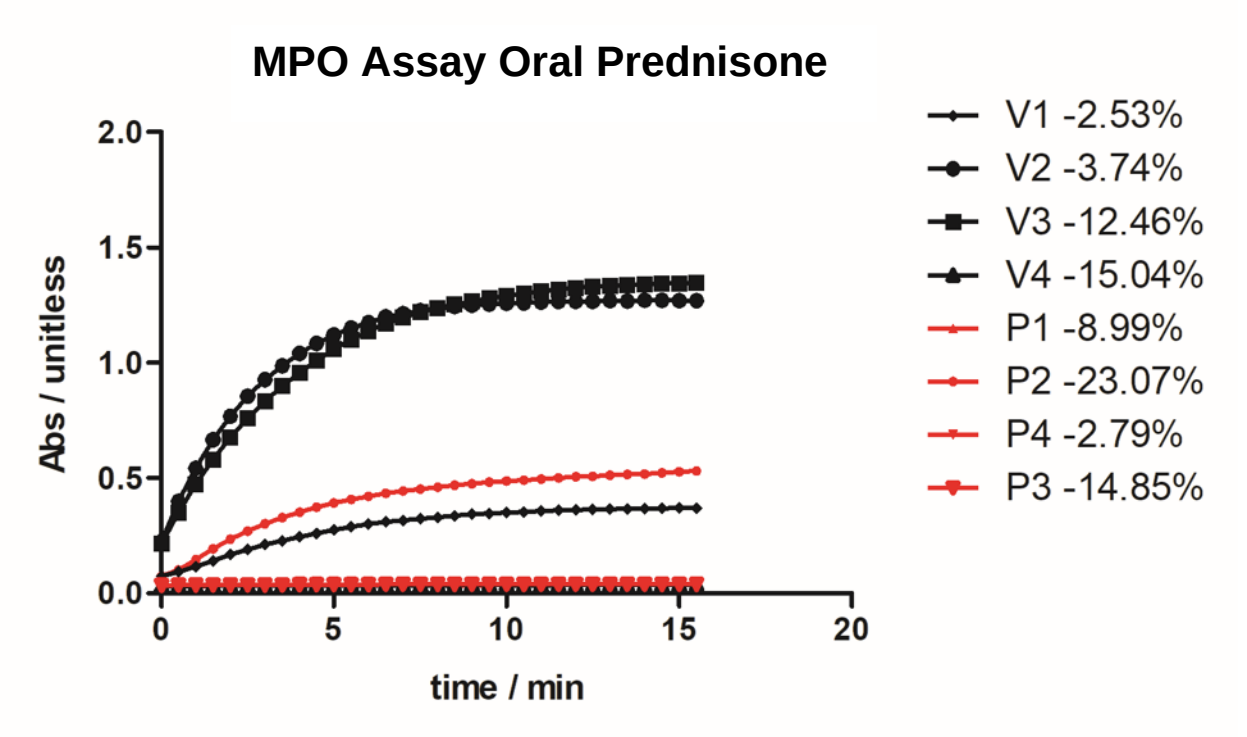

Figure 53 – MPO Assay overlay of the mice treated with prednisone (red) and vehicle (black). Multiple colon homogenatates did not show any absorbance and were excluded from the measurement.

It was speculated that the DNBS model may be producing inconsistent forms of inflammation within the CFW mice that may prevent the use of the small group size that was used during these pilot studies. Alternatively, to the DNBS model, other colitis models have been widely established for colitis such as the dextran sodium sulfate (DSS) model[80]. The general structure of DSS is shown in **Schematic 22**. The molecule is a polymer that contains the sulfate functionalities leading to a range of sizes in the initial reaction that generates the material. Dextran sodium sulfate operates by disturbing the intercellular permeability causing for permeation of intestinal bacteria into the intestinal lining and blood stream and recruitment of neutrophils to the affected area. The size of the polymer is closely linked to the ability to

permeate through membranes and produce the desired inflammatory effect. It has previously been reported that the size range of 40-50 kDa is ideal for the modeling of IBD[81].

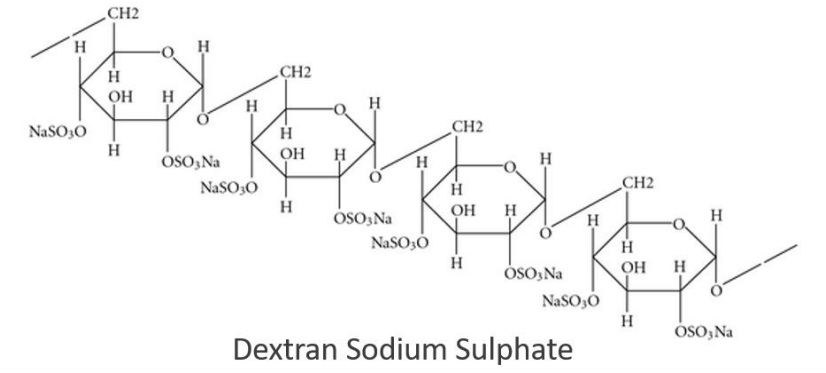

Schematic 22 – Structure of the polymer of DSS size can range from 5 kDa to 60 kDa.

Unlike the DNBS model, the most common form of administration is the incorporation of the compound into the water supply of the animal within the study for their consumption *ad libitum*. This change to the procedure can cause a relationship between the behavior of the mice to efficacy of the compound in longer studies. Due to its administration, DSS was expected to induce a less localized form of inflammation in the large intestine. While this method has been used by previous researchers, the use of CFW outbred mice had previously not been demonstrated[11, 82, 83]. For this reason, the concentration of DSS that was used during the study was initially based on the BALB/c model than adjusted to the observations within the CFW mice.

A group of two mice were provided with a water supply with 2.0% w/v DSS after the 7-day accumulation period in the research facility. Both mice were given the vehicle through oral gavage daily over the course of the study. The weights of the mice were collected and are summarized in **Figure 54**. Both mice in the study saw a trend of weight loss each day during the study on the same magnitude suggesting a similar effect. The MPO assay was conducted using

the procedure described above and the results are shown in **Figure 55**. The small group size of this study did not allow for strong conclusions to be drawn from the study, but it was found that both mice developed colitis. A different degree of inflammation was observed for the MPO assay results. However, the DSS model was able to induce a response and the group size could be increased to further understand the oxidative activity in larger group sizes.

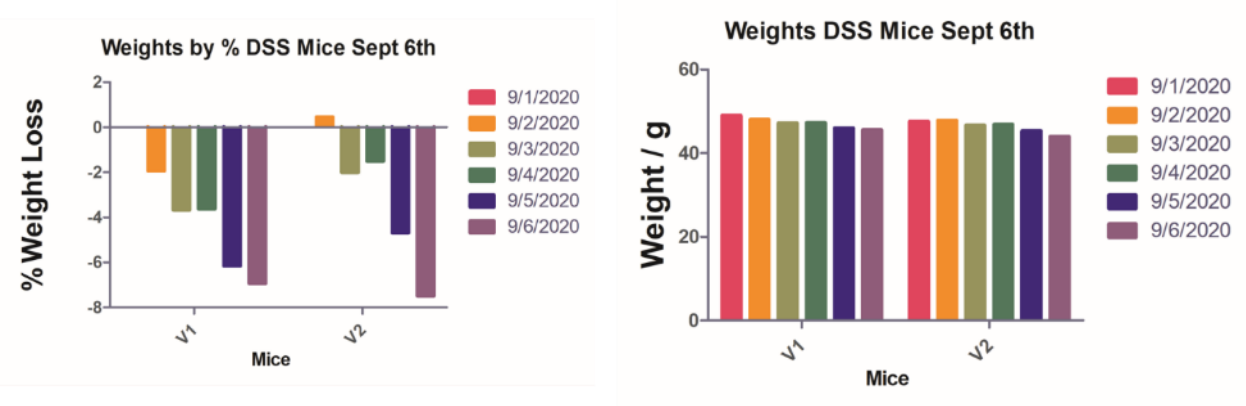

Figure 54 – Comparision of the wieghts of inidivual mice by weight lose (left) and weight over the study (left).

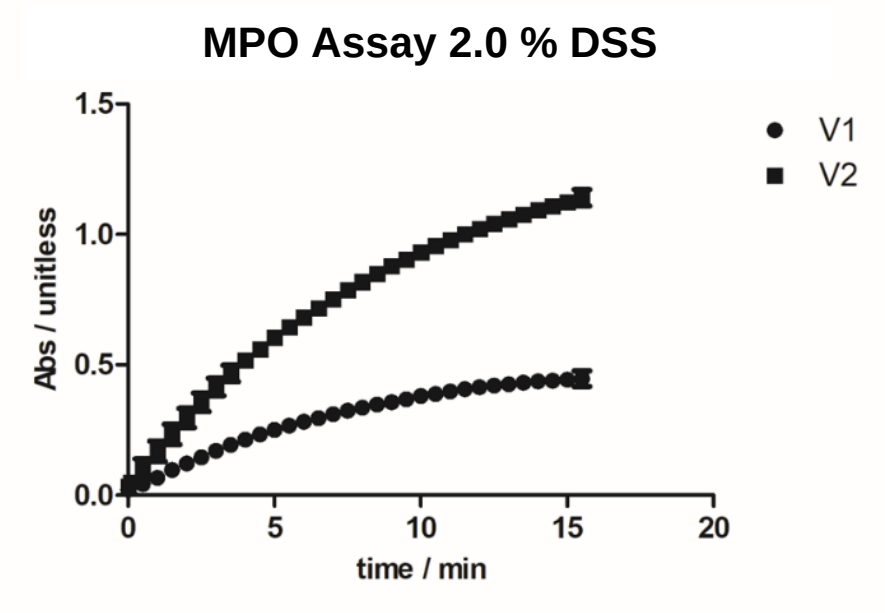

Figure 55 – MPO assay of the two mice treated with dextran sodium sulfate.

A second group of mice, n = 4, were then treated with DSS for 10 days to determine if the oxidative activity in the large intestine homogenates would unify towards the later days of the study. The MPO assay results are shown in **Figure 56**. Similar to what was observed in previous studies it was found that the weight loss over the study did not correlate well to the oxidative activity in the MPO assay. Additionally, three of the mice were observed to have an elevated level of oxidative activity while V4 had an extreme oxidative response. The conclusion of the study was that the mice may be in different phases of the colitis model. Some of the mice were entering a chronic response phase while others were still undergoing the acute response to the chemical irritant. To address this issue the length of the study was returned to the 7-day period.

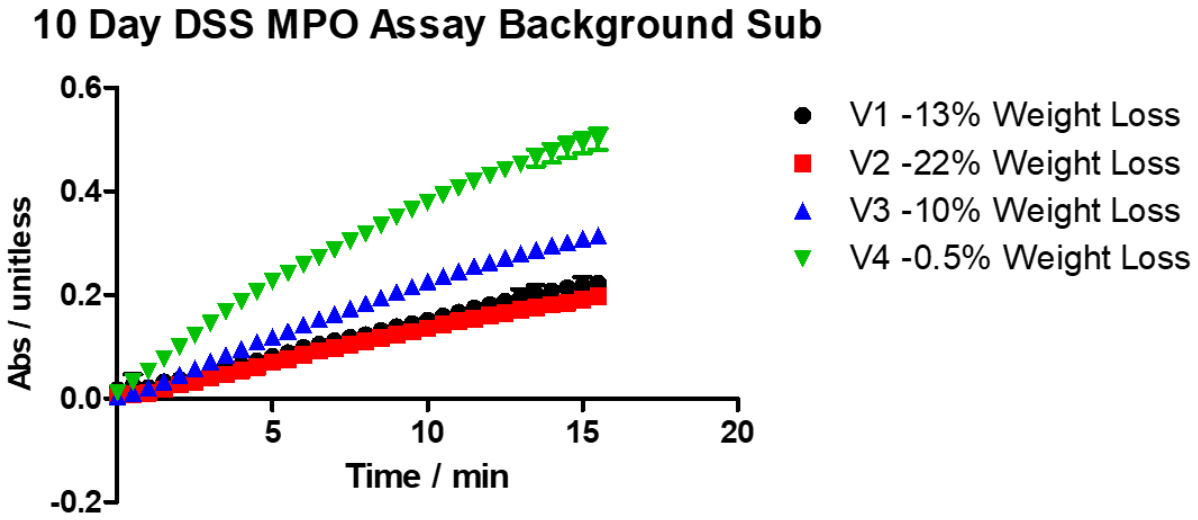

Figure 56 – Replicate of the DSS model10-day study n=4.

Furthermore, the concentration of DSS was increased from 2.0% w/v of the previous studies to 3.0% w/v. The increase in the concentration was postulated to increase the colitis within the mouse while remaining in the timeframe considered acute inflammation. The weight loss of the group of mice in this study are shown in **Figure 57**. All mice during this study saw

weight loss, although no mice crossed the previously determined threshold of 10% weight loss. The MPO assay was then conducted on the colon homogenates collected and prepared at the end of the 7-day study. The results of the MPO assay are shown in **Figure 58**. It was found that the grouping of the oxidative response of all four colons within the study were closely grouped. This would allow for a clear elevation of oxidative activity that could be reduced by the compound provided in future studies.

The current procedure that can be used for the measurement of inflammatory response are as follows. Mice colons are transferred to a biological hood for homogenization in PBS solution on ice. Samples are transferred to test tubes and their masses are measured. Colons are then homogenized after the addition of 1 mL of 50 mM phosphate buffer at pH 6.0 with a detergent of 50 mM hexadecyltrimethylammonium bromide. The homogenates are then transferred to centrifuge tubes and centrifuged at 10,000 RPM for 10 min. The BCA assay as described above is then conducted along with a calibration curve to determine the protein concentration of the homogenates. The protein concentration of an aliquot of each colon homogenate is then diluted to 2000 µg/mL. 62 µL of 50 mM phosphate buffer at pH 6.0 is then added to a series of wells in a clear 384 well plate. 8 µL of each sample is then transferred into a corresponding will for a total of n = 4 replicates. A replicate series of wells is created on the plate. 10 µL of water is added to the new row creating a set of references for the background of each sample. The active set has 10 µL 0.0024 % v/v hydrogen peroxide solution added to initiate the assay. The plate is monitored in 30 s intervals for 15 min to create the traces of the oxidative activity.

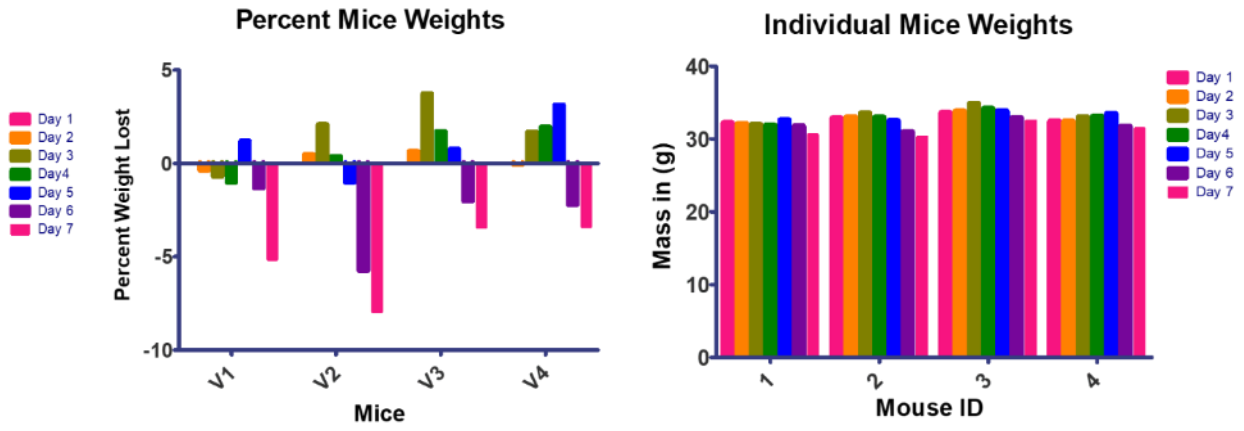

Figure 57 – Weight lose of individual mice shown as a percentage of total starting mass (right) and indiviual mass (left).

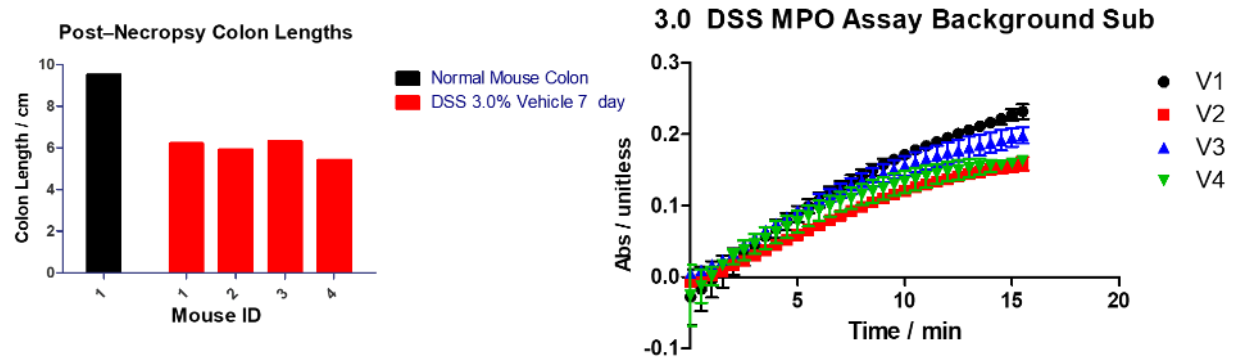

Figure 58 – A compareson to the expected length of a mouse colon to the measure length of the mice within the study (left). The MPO assay of the mice treated with 3.0% DSS and provided vehicle (right).

6.4.6 Other Measurements of Colitis Intensity

Initial measurement of the mice during these sets of studies hope to include measures of coat quality, cage fecal consistency, and inflammation of the anus. Due to the incongruencies in the initial weight loss and oxidative activity many of these measurements were excluded from the initial study development to simplify the procedure to allow for the fast, and least resource intensive development of this study using CFW mice. It was found that mice treated with 3.0% w/v DSS *ad libitum had* a consistent response with the weight loss and oxidative activity of their colons. The coat quality of the mice during the study seemed to poorly reflect upon the amount

of inflammation observed in necropsy in all but the most severe cases of colitis. External rectal inflammation was monitored in all the collected studies but found to have little significance to the internal inflammation that would be attributed to colitis. For this reason, both the coat quality and the external inflammation were used only to suggest a humane end point of the study but not as a quantitative measure. Fecal consistency was a poor predicting factor towards colitis. Mice in these studies were housed in groups of four, prevented the distinction of individuals feces. It is suggested to maintain groups of four in housing to prevent the changes in social behavior affecting dietary habits of the mice during the study. With this constraint, cage fecal consistency would not be recommended for future studies.

The hematological and morphological analysis were removed from the analysis to allow for the efficient optimization of the MPO assay during these studies, however, it would bolster conclusions drawn on the colitis intensity and inflammatory response. Based on the initial hematological data, it would be expected that mice that were experiencing colitis would have elevated levels of granulocytes. The procedure of the hematological analysis is time sensitive similar to the analysis done for the MPO Assay. A second researcher will need to perform this analysis which is done off site to make sure that both measurements are collected within the appropriate time frame. Morphological analysis will be interesting to measure the closer of crypts within the intestinal lining. This measure is dependent upon the area that is sampled within the colon but can add to the conclusion of severity of inflammation and mechanism of prevention.

6.5 Future Studies on Inflammation

Future studies that will be conducted with the developed procedure for the measurement of the colitis in mice will implement the developed method to screen compounds for efficacy on the colitis model. Our goal is to gain an understanding about calcitroic acid and its efficacy in preventing the inflammatory response. A study conducted with the positive control group of dexamethasone will establish the new method showing the expected reduction of colitis. Once a positive control compound has been found to reduce the level of inflammation within CFW mice, this study will be used to screen both calcitroic acid and other compounds of interest of our group for their efficacy. Compounds modeled after the structure of calcitroic acid that our group has synthesized can in the future be screened using this method if a significant reduction in inflammation is observed.

6.6 Conclusion

Inflammatory bowel disease affects a significant portion of the world population. Treatments currently for this disease come with a wide range of side effects and some treatments may not be optimal for every patient. Preliminary studies conducted by our group showed that calcitroic acid was a part bile duct hepatic circulation possibly as a protecting agent against inflammation induced by lithocholic acid. Our group set out to develop a method that would show if calcitroic acid played a role as an anti-inflammatory agent within the intestinal tract. Our study sought to use an outbred strand of mice that would model the human population more accurately. The initial chemical irritant methods that were designed for DNBS were found to induce too strong of an inflammatory response within the mice with a high degree of variance between the mice. Some parameters such as the method of administration were changed from

the initial procedure such as the use of IP administration to prevent injuries of the intestine. The final method that was developed was a 7-day study in which mice are provided *ad libitum* 3.0% DSS w/v in their water supply. It was observed based on the visual inflammation, weight loss as well as the oxidative activity of colon homogenate that the DSS treated mice had symptoms of inflammation. While the efficacy of calcitroic acid still needs to be determined, the assay that has been designed has a close variance between the vehicle mice allowing for the reduction of inflammation to accurately be determined in future studies.

References

1. Molodecky, N. A.; Soon, I. S.; Rabi, D. M.; Ghali, W. A.; Ferris, M.; Chernoff, G.; Benchimol, E. I.; Panaccione, R.; Ghosh, S.; Barkema, H. W.; Kaplan, G. G., Increasing incidence and prevalence of the inflammatory bowel diseases with time, based on systematic review. *Gastroenterology* **2012,** *142* (1), 46-54.e42; quiz e30.

2. Kong, J.; Zhang, Z.; Musch, M. W.; Ning, G.; Sun, J.; Hart, J.; Bissonnette, M.; Li, Y. C., Novel role of the vitamin D receptor in maintaining the integrity of the intestinal mucosal barrier. *Am J Physiol Gastrointest Liver Physiol* **2008,** *294* (1), G208-16.

3. Dubois-Camacho, K.; Ottum, P. A.; Franco-Muñoz, D.; De La Fuente, M.; Torres-Riquelme, A.; Díaz-Jiménez, D.; Olivares-Morales, M.; Astudillo, G.; Quera, R.; Hermoso, M. A., Glucocorticosteroid therapy in inflammatory bowel diseases: From clinical practice to molecular biology. *World Journal of Gastroenterology* **2017,** *23* (36), 6628-6638.

4. Morampudi, V.; Bhinder, G.; Wu, X.; Dai, C.; Sham, H. P.; Vallance, B. A.; Jacobson, K., DNBS/TNBS colitis models: providing insights into inflammatory bowel disease and effects of dietary fat. *J Vis Exp* **2014,** (84), e51297.

5. Melgar, S.; Karlsson, A.; Michaelsson, E., Acute colitis induced by dextran sulfate sodium progresses to chronicity in C57BL/6 but not in BALB/c mice: correlation between symptoms and inflammation. *Am J Physiol Gastrointest Liver Physiol* **2005,** *288* (6), G1328-38.

6. Sann, H.; Erichsen, J.; Hessmann, M.; Pahl, A.; Hoffmeyer, A., Efficacy of drugs used in the treatment of IBD and combinations thereof in acute DSS-induced colitis in mice. *Life Sci* **2013,** *92* (12), 708-18.

7. Araujo, D. F. S.; Guerra, G. C. B.; Pintado, M. M. E.; Sousa, Y. R. F.; Algieri, F.; Rodriguez-Nogales, A.; Araujo, R. F., Jr.; Galvez, J.; Queiroga, R.; Rodriguez-Cabezas, M. E., Intestinal anti-inflammatory effects of goat whey on DNBS-induced colitis in mice. *PLoS One* **2017,** *12* (9), e0185382.

8. Ho, Y.-J.; Lee, A.-S.; Chen, W.-P.; Chang, W.-L.; Tsai, Y.-K.; Chiu, H.-L.; Kuo, Y.-H.; Su, M.-J., Caffeic acid phenethyl amide ameliorates ischemia/reperfusion injury and cardiac dysfunction in streptozotocin-induced diabetic rats. *Cardiovascular Diabetology* **2014,** *13* (1), 98.

9. Smith, P. K.; Krohn, R. I.; Hermanson, G. T.; Mallia, A. K.; Gartner, F. H.; Provenzano, M. D.; Fujimoto, E. K.; Goeke, N. M.; Olson, B. J.; Klenk, D. C., Measurement of protein using bicinchoninic acid. *Analytical Biochemistry* **1985,** *150* (1), 76-85.

10. Perse, M.; Cerar, A., Dextran sodium sulphate colitis mouse model: traps and tricks. *J Biomed Biotechnol* **2012,** *2012*, 718617.

11. Eichele, D. D.; Kharbanda, K. K., Dextran sodium sulfate colitis murine model: An indispensable tool for advancing our understanding of inflammatory bowel diseases pathogenesis. *World J Gastroenterol* **2017,** *23* (33), 6016-6029.

12. Chassaing, B.; Aitken, J. D.; Malleshappa, M.; Vijay-Kumar, M., Dextran Sulfate Sodium (DSS)-Induced Colitis in Mice. *Current Protocols in Immunology* **2014,** *104* (1).

13. Froicu, M.; Cantorna, M. T., Vitamin D and the vitamin D receptor are critical for control of the innate immune response to colonic injury. *BMC Immunol* **2007,** *8*, 5.

14. Kishimoto, S.; Haruma, K.; Tari, A.; Sakurai, K.; Nakano, M.; Nakagawa, Y., Rebamipide, an antiulcer drug, prevents DSS-induced colitis formation in rats. *Dig Dis Sci* **2000,** *45* (8), 1608-16.

REFERENCES

1. Deluca, H. F., History of the discovery of vitamin D and its active metabolites. *BoneKEy Reports* **2014,** *3*.

2. Funk, C., On the chemical nature of the substance which cures polyneuritis in birds induced by a diet of polished rice. *J Physiol* **1911,** *43* (5), 395-400.

3. McCollum, E. V.; Davis, M., The Necessity of Certain Lipins in the Diet during Growth. *J. Biol. Chem* **1913,** *15*, 167-175.

4. Hart, E. B.; McCollum, E. V.; Steenbock, H.; Humphrey, G. C., Physiological Effect on Growth and Reproduction of Rations Balanced from Restricted Sources. *Proceedings of the National Academy of Sciences* **1917,** *3* (5), 374-382.

5. Velluz, L.; Amiard, G., Pre-calciferol. *C R Hebd Seances Acad Sci* **1949,** *228* (8), 692-4.

6. Bikle, D. D., Vitamin D metabolism, mechanism of action, and clinical applications. *Chemistry & biology* **2014,** *21* (3), 319-329.

7. Blunt, J. W.; DeLuca, H. F.; Schnoes, H. K., 25-Hydroxycholecalciferol. A biologically active metabolite of vitamin D3. *Biochemistry* **1968,** *7* (10), 3317-3322.
8. Esvelt, R. P.; De Luca, H. F., Calcitroic acid: Biological activity and tissue distribution studies. *Archives of Biochemistry and Biophysics* **1981,** *206* (2), 403-413.
9. Onisko, B. L.; Esvelt, R. P.; Schnoes, H. K.; DeLuca, H. F., Metabolites of 1 alpha, 25-dihydroxyvitamin D3 in rat bile. *Biochemistry* **1980,** *19* (17), 4124-30.
10. Reddy, G. S.; Tserng, K. Y., Calcitroic acid, end product of renal metabolism of 1,25-dihydroxyvitamin D3 through the C-24 oxidation pathway. *Biochemistry* **1989,** *28* (4), 1763-1769.
11. Froicu, M.; Cantorna, M. T., Vitamin D and the vitamin D receptor are critical for control of the innate immune response to colonic injury. *BMC Immunol* **2007,** *8*, 5.
12. Mellanby, E., An Experimental Investigation on Rickets. *Nutrition Reviews* **1976,** *34* (11), 338-340.
13. Chick, H.; Dalyell, E.; Hume, M.; Smith, H. H.; Mackay, H. M., The Ætiology of Rickets in Infants : Prophylactic and Curative Observations at the Vieanna University Kinderklinik. *The Lancet* **1922,** *200* (5157), 7-11.
14. Huldschinsky, K., Heilung von Rachitis durch künstliche Höhensonne. *DMW - Deutsche Medizinische Wochenschrift* **1919,** *45* (26), 712-713.
15. Steenbock, H., THE INDUCTION OF GROWTH PROMOTING AND CALCIFYING PROPERTIES IN A RATION BY EXPOSURE TO LIGHT. *Science* **1924,** *60* (1549), 224-5.
16. Esvelt, R. P.; Schnoes, H. K.; DeLuca, H. F., Vitamin D3 from rat skins irradiated in vitro with ultraviolet light. *Archives of Biochemistry and Biophysics* **1978,** *188* (2), 282-286.
17. Havinga, E., Vitamin D, example and challenge. *Experientia* **1973,** *29* (10), 1181-93.
18. Askew, F. A.; Bourdillon, R. B.; Bruce, H. M.; Jenkins, R. G. C.; Webster, T. A., The Distillation of Vitamin D. *Proceedings of the Royal Society. Series B.* **1930,** *107*, 76-90.
19. Drummond, J. C., The Nomenclature of the so-called Accessory Food Factors (Vitamins). *Biochemical Journal* **1920,** *14* (5), 660-660.
20. Bauer, G. C.; Carlsson, A., Metabolism of bone salt investigated by simultaneous administration of 45Ca and 32P to rats. *J Bone Joint Surg Br* **1955,** *37-B* (4), 658-62.
21. Carlsson, A., Tracer experiments on the effect of vitamin D on the skeletal metabolism of calcium and phosphorus. *Acta Physiol Scand* **1952,** *26* (2-3), 212-20.
22. DeLuca, H. F.; Holick, M. F.; Schnoes, H. K.; Suda, T.; Cousins, R. J., Isolation and identification of 1,25-dihydroxycholecalciferol. A metabolite of vitamin D active in intestine. *Biochemistry* **1971,** *10* (14), 2799-2804.
23. Sakaki, T.; Sawada, N.; Komai, K.; Shiozawa, S.; Yamada, S.; Yamamoto, K.; Ohyama, Y.; Inouye, K., Dual metabolic pathway of 25-hydroxyvitamin D3 catalyzed by human CYP24. *European journal of biochemistry* **2000,** *267* (20), 6158-65.
24. Reddy, G. S.; Tserng, K. Y., Calcitroic Acid, End Product of Renal Metabolism of 1,25-Dihydroxyvitamin D3 through C-24 Oxidation Pathway. *Biochem J* **1989,** *28*, 1763-1769.
25. Jones, G.; Prosser, D. E.; Kaufmann, M., 25-Hydroxyvitamin D-24-hydroxylase (CYP24A1): its important role in the degradation of vitamin D. *Arch Biochem Biophys* **2012,** *523* (1), 9-18.
26. Jones, G.; Kung, M.; Kano, K., The isolation and identification of two new metabolites of 25-hydroxyvitamin D3 produced in the kidney. *J Biol Chem* **1983,** *258* (21), 12920-8.

27. Reddy, G. S.; Tserng, K. Y.; Thomas, B. R.; Dayal, R.; Norman, A. W., Isolation and identification of 1,23-dihydroxy-24,25,26,27-tetranorvitamin D3, a new metabolite of 1,25-dihydroxyvitamin D3 produced in rat kidney. *Biochemistry* **1987,** *26* (1), 324-31.
28. Reddy, G. S.; Omdahl, J. L.; Robinson, M.; Wang, G.; Palmore, G. T.; Vicchio, D.; Yergey, A. L.; Tserng, K. Y.; Uskokovic, M. R., 23-carboxy-24,25,26,27-tetranorvitamin D3 (calcioic acid) and 24-carboxy-25,26,27-trinorvitamin D3 (cholacalcioic acid): end products of 25-hydroxyvitamin D3 metabolism in rat kidney through C-24 oxidation pathway. *Arch Biochem Biophys* **2006,** *455* (1), 18-30.
29. Shipley, P. G.; Kramer, B.; Howland, J., Calcification of Rachitic Bone In Vitro. *American Journal of Diseases of Children* **1925,** *30* (1), 37-39.
30. Brumbaugh, P. F.; Haussler, M. R., lα,25-dihydroxyvitamin D3 receptor: competitive binding of vitamin D analogs. *Life Sciences* **1973,** *13* (12), 1737-1746.
31. Pike, W. M., M; Lee, S.M., The Vitamin D Receptor: Biochemical, Molecular, Biological, and Genomic Era Investigations. In *Vitamin D*, Pike, W. S., N. K., Ed. 2011; Vol. 3rd Ed, pp 97-135.
32. Reschly, E. J.; Krasowski, M. D., Evolution and function of the NR1I nuclear hormone receptor subfamily (VDR, PXR, and CAR) with respect to metabolism of xenobiotics and endogenous compounds. *Curr Drug Metab* **2006,** *7* (4), 349-65.
33. Brumbaugh, P. F.; Haussler, D. H.; Bursac, K. M.; Haussler, M. R., Filter assay for 1alpha, 25-dihydroxyvitamin D3. Utilization of the hormone's target tissue chromatin receptor. *Biochemistry* **1974,** *13* (20), 4091-7.
34. Galior, K.; Ketha, H.; Grebe, S.; Singh, R. J., 10 years of 25-hydroxyvitamin-D testing by LC-MS/MS-trends in vitamin-D deficiency and sufficiency. *Bone Rep* **2018,** *8*, 268-273.
35. Skoog, D. A.; West, D. M.; Holler, F. J., *Fundamentals of Analytical Chemistry*. 9th ed.; Saunders College: New York, 1988.
36. Eliuk, S.; Makarov, A., Evolution of Orbitrap Mass Spectrometry Instrumentation. *Annu Rev Anal Chem (Palo Alto Calif)* **2015,** *8*, 61-80.
37. Griffiths, J., A brief history of mass spectrometry. *Anal Chem* **2008,** *80* (15), 5678-83.
38. Skoog, D. A.; Holler, F. J.; Crouch, S. R., *Principles of Instrumental Analysis*. 7th ed.; Saunders College Pub.: Philadelphia, 1997.
39. Loos, G.; Van Schepdael, A.; Cabooter, D., Quantitative mass spectrometry methods for pharmaceutical analysis. *Philos Trans A Math Phys Eng Sci* **2016,** *374* (2079).
40. Tswett, M., Physical-chemical studies of chlorophyll. Adsorption. *German Botanical Society* **1906,** *3-10*, 384-393.
41. Martin, A. J.; Synge, R. L., Separation of the higher monoamino-acids by counter-current liquid-liquid extraction: the amino-acid composition of wool. *Biochem J* **1941,** *35* (1-2), 91-121.
42. van Deemter, J. J.; Zuiderweg, F. J.; Klinkenberg, A., Longitudinal diffusion and sesistance to mass transfer as causes of nonideality in chromatography. *Chemical Engineering Science* **1956,** *5* (6), 271-289.
43. Paolini, M.; Bauer, C.; Corsi, C.; Del Carratore, R.; Nieri, R.; Bronzetti, G., Stability of microsomal mono-oxygenase during incubations for the liver microsomal assay with S9 fractions of mouse liver under various inductions. *Mutat Res* **1983,** *110* (2), 221-30.
44. Nelson, D. L.; Cox, M. M., *Principles of Biochemistry*. Fifth ed.; Sara Tenney 2008; p 1158.

45. Zimmerman, D. R.; Reinhardt, T. A.; Kremer, R.; Beitz, D. C.; Reddy, G. S.; Horst, R. L., Calcitroic acid is a major catabolic metabolite in the metabolism of 1 alpha-dihydroxyvitamin D(2). *Arch Biochem Biophys* **2001,** *392* (1), 14-22.
46. Onisko, B. L.; Esvelt, R. P.; Schnoes, H. K.; Deluca, H. F., Excretion of metabolites of 1 alpha, 25-dihydroxyvitamin D3 in rat bile. *Arch Biochem Biophys* **1980,** *205* (1), 175-9.
47. Meech, R.; Hu, D. G.; McKinnon, R. A.; Mubarokah, S. N.; Haines, A. Z.; Nair, P. C.; Rowland, A.; Mackenzie, P. I., The UDP-Glycosyltransferase (UGT) Superfamily: New Members, New Functions, and Novel Paradigms. *Physiol Rev* **2019,** *99* (2), 1153-1222.
48. Gamage, N.; Barnett, A.; Hempel, N.; Duggleby, R. G.; Windmill, K. F.; Martin, J. L.; McManus, M. E., Human sulfotransferases and their role in chemical metabolism. *Toxicol Sci* **2006,** *90* (1), 5-22.
49. Hofmann, A. F.; Hagey, L. R., Key discoveries in bile acid chemistry and biology and

their clinical applications: history of the last

eight decades. *Journal of Lipid Research* **2014,** *55* (8), 1553-1595.
50. Epstein, E. H., Jr.; Han, A.; Shackleton, C. H., Failure of steroid sulfatase to desulfate vitamin D3 sulfate. *J Invest Dermatol* **1983,** *80* (6), 514-6.
51. Shimada, K.; Mitamura, K.; Nakatani, I., Characterization of monoglucuronides of vitamin D2 and 25-hydroxyvitamin D2 in rat bile using high-performance liquid chromatography-atmospheric pressure chemical ionization mass spectrometry. *Chromatography B* **1997,** *690*, 348-354.
52. Vollmer, M.; Klingebiel, M.; Rohn, S.; Maul, R., Alamethicin for using in bioavailability studies? - Re-evaluation of its effect. *Toxicol In Vitro* **2017,** *39*, 111-118.
53. Oleson, L.; Court, M. H., Effect of the beta-glucuronidase inhibitor saccharolactone on glucuronidation by human tissue microsomes and recombinant UDP-glucuronosyltransferases. *J Pharm Pharmacol* **2008,** *60* (9), 1175-82.
54. Kuehl, G. E.; Bigler, J.; Potter, J. D.; Lampe, J. W., Glucuronidation of the aspirin metabolite salicylic acid by expressed UDP-glucuronosyltransferases and human liver microsomes. *Drug Metab Dispos* **2006,** *34* (2), 199-202.
55. Axelson, M., 25-Hydroxyvitamin D3 3-sulphate is a major circulating form of vitamin D in man. *FEBS Lett* **1985,** *191* (2), 171-5.
56. Shimada, K.; Mitamura, K.; Saito, K.; Ohtake, Y.; Nakatani, I., Enzymatic hydrolysis of the conjugate of vitamin D and related compounds. *J Pharm Biomed Anal* **1997,** *15* (9-10), 1207-14.
57. Falany, C. N.; Johnson, M. R.; Barnes, S.; Diasio, R. B., Glycine and taurine conjugation of bile acids by a single enzyme. Molecular cloning and expression of human liver bile acid CoA:amino acid N-acyltransferase. *J Biol Chem* **1994,** *269* (30), 19375-9.
58. Makin, G.; Lohnes, D.; Byford, V.; Ray, R.; Jones, G., Target cell metabolism of 1,25-dihydroxyvitamin D3 to calcitroic acid. Evidence for a pathway in kidney and bone involving 24-oxidation. *Biochem J* **1989,** *262* (1), 173-80.
59. Inc, P. Sample Preparation. (accessed March 29th).
60. Norman, A. W.; Lund, J.; Deluca, H. F., Biologically active forms of vitamin D3 in kidney and intestine. *Archives of Biochemistry and Biophysics* **1964,** *108* (1), 12-21.

61. Mawer, E. B.; Lumb, G. A.; Schaefer, K.; Stanbury, S. W., The Metabolism of Isotopically Labelled Vitamin D3 in Man: The Influence of the State of Vitamin D Nutrition. *Clinical Science* **1971,** *40* (1), 39-53.
62. Aronov, P. A.; Hall, L. M.; Dettmer, K.; Stephensen, C. B.; Hammock, B. D., Metabolic profiling of major vitamin D metabolites using Diels–Alder derivatization and ultra-performance liquid chromatography–tandem mass spectrometry. *Analytical and Bioanalytical Chemistry* **2008,** *391* (5), 1917-1930.
63. Giera, M., Bioanalytical derivatization: is there still room for development? *Bioanalysis* **2015,** *7*, 2439-2441.
64. Shimada, K.; Oe, T.; Mizuguchi, T., Cookson-type reagents: highly sensitive derivatization reagents for conjugated dienes in high-performance liquid chromatography. *Analyst* **1991,** *116* (12), 1393-1397.
65. Kaufmann, M.; Gallagher, J. C.; Peacock, M.; Schlingmann, K. P.; Konrad, M.; DeLuca, H. F.; Sigueiro, R.; Lopez, B.; Mourino, A.; Maestro, M.; St-Arnaud, R.; Finkelstein, J. S.; Cooper, D. P.; Jones, G., Clinical utility of simultaneous quantitation of 25-hydroxyvitamin D and 24,25-dihydroxyvitamin D by LC-MS/MS involving derivatization with DMEQ-TAD. *J Clin Endocrinol Metab* **2014,** *99* (7), 2567-74.
66. Cookson, R. C.; Gilani, S. S. H.; Stevens, I. D. R., Diels–Alder reactions of 4-phenyl-1,2,4-triazoline-3,5-dione. *Journal of the Chemical Society C: Organic* **1967,** (0), 1905-1909.
67. Higashi, T.; Shimada, K., Application of Cookson-type reagents for biomedical HPLC and LC/MS analyses: a brief overview. *Biomedical Chromatography* **2017,** *31* (1), e3808.
68. Higashi, T.; Awada, D.; Shimada, K., Simultaneous determination of 25-hydroxyvitamin D2 and 25-hydroxyvitamin D3 in human plasma by liquid chromatography-tandem mass spectrometry employing derivatization with a Cookson-type reagent. *Biol Pharm Bull* **2001,** *24* (7), 738-43.
69. Jones, G.; Kaufmann, M., Vitamin D metabolite profiling using liquid chromatography-tandem mass spectrometry (LC-MS/MS). *J Steroid Biochem Mol Biol* **2016,** *164*, 110-114.
70. Yu, O. B.; Arnold, L. A., Calcitroic Acid-A Review. *ACS Chem Biol* **2016,** *11* (10), 2665-2672.
71. Molodecky, N. A.; Soon, I. S.; Rabi, D. M.; Ghali, W. A.; Ferris, M.; Chernoff, G.; Benchimol, E. I.; Panaccione, R.; Ghosh, S.; Barkema, H. W.; Kaplan, G. G., Increasing incidence and prevalence of the inflammatory bowel diseases with time, based on systematic review. *Gastroenterology* **2012,** *142* (1), 46-54.e42; quiz e30.
72. Kong, J.; Zhang, Z.; Musch, M. W.; Ning, G.; Sun, J.; Hart, J.; Bissonnette, M.; Li, Y. C., Novel role of the vitamin D receptor in maintaining the integrity of the intestinal mucosal barrier. *Am J Physiol Gastrointest Liver Physiol* **2008,** *294* (1), G208-16.
73. Dubois-Camacho, K.; Ottum, P. A.; Franco-Muñoz, D.; De La Fuente, M.; Torres-Riquelme, A.; Díaz-Jiménez, D.; Olivares-Morales, M.; Astudillo, G.; Quera, R.; Hermoso, M. A., Glucocorticosteroid therapy in inflammatory bowel diseases: From clinical practice to molecular biology. *World Journal of Gastroenterology* **2017,** *23* (36), 6628-6638.
74. Morampudi, V.; Bhinder, G.; Wu, X.; Dai, C.; Sham, H. P.; Vallance, B. A.; Jacobson, K., DNBS/TNBS colitis models: providing insights into inflammatory bowel disease and effects of dietary fat. *J Vis Exp* **2014,** (84), e51297.

75. Melgar, S.; Karlsson, A.; Michaelsson, E., Acute colitis induced by dextran sulfate sodium progresses to chronicity in C57BL/6 but not in BALB/c mice: correlation between symptoms and inflammation. *Am J Physiol Gastrointest Liver Physiol* **2005,** *288* (6), G1328-38.
76. Sann, H.; Erichsen, J.; Hessmann, M.; Pahl, A.; Hoffmeyer, A., Efficacy of drugs used in the treatment of IBD and combinations thereof in acute DSS-induced colitis in mice. *Life Sci* **2013,** *92* (12), 708-18.
77. Araujo, D. F. S.; Guerra, G. C. B.; Pintado, M. M. E.; Sousa, Y. R. F.; Algieri, F.; Rodriguez-Nogales, A.; Araujo, R. F., Jr.; Galvez, J.; Queiroga, R.; Rodriguez-Cabezas, M. E., Intestinal anti-inflammatory effects of goat whey on DNBS-induced colitis in mice. *PLoS One* **2017,** *12* (9), e0185382.
78. Ho, Y.-J.; Lee, A.-S.; Chen, W.-P.; Chang, W.-L.; Tsai, Y.-K.; Chiu, H.-L.; Kuo, Y.-H.; Su, M.-J., Caffeic acid phenethyl amide ameliorates ischemia/reperfusion injury and cardiac dysfunction in streptozotocin-induced diabetic rats. *Cardiovascular Diabetology* **2014,** *13* (1), 98.
79. Smith, P. K.; Krohn, R. I.; Hermanson, G. T.; Mallia, A. K.; Gartner, F. H.; Provenzano, M. D.; Fujimoto, E. K.; Goeke, N. M.; Olson, B. J.; Klenk, D. C., Measurement of protein using bicinchoninic acid. *Analytical Biochemistry* **1985,** *150* (1), 76-85.
80. Perse, M.; Cerar, A., Dextran sodium sulphate colitis mouse model: traps and tricks. *J Biomed Biotechnol* **2012,** *2012*, 718617.
81. Eichele, D. D.; Kharbanda, K. K., Dextran sodium sulfate colitis murine model: An indispensable tool for advancing our understanding of inflammatory bowel diseases pathogenesis. *World J Gastroenterol* **2017,** *23* (33), 6016-6029.
82. Chassaing, B.; Aitken, J. D.; Malleshappa, M.; Vijay-Kumar, M., Dextran Sulfate Sodium (DSS)-Induced Colitis in Mice. *Current Protocols in Immunology* **2014,** *104* (1).
83. Kishimoto, S.; Haruma, K.; Tari, A.; Sakurai, K.; Nakano, M.; Nakagawa, Y., Rebamipide, an antiulcer drug, prevents DSS-induced colitis formation in rats. *Dig Dis Sci* **2000,** *45* (8), 1608-16.

CURRICULUM VITAE

Elliot Di Milo

Introduction

A graduate student from the University of Wisconsin Milwaukee working under the supervision of Prof. Arnold. My Research focuses on the quantification and distribution of vitamin D metabolites. In our project I have been able to explore multiple facets of the analytical field including but not limited to off and on–line solid–liquid phase extraction (SPE), high–performance and ultra–high–performance liquid chromatography (HPLC and UHPLC), and mass spectrometry. In addition, my project explores pharmacokinetics and metabolism through microsomal stability assays and inflammation in animal models. I have had the opportunity to work with Eurofins scientific and Millipore–Sigma on quantitative sample analysis and quality control development to gain insight into industrial practices.

Professional Experience

Sept 2020 – Dec 2020 Research Assistant (RA) in Prof. Arnold's Research Group at University of Wisconsin Milwaukee

- UHLC–MS/MS Analysis
- Analytical Separation Method Development
- Microsomal Stability Assays
- Metabolic Research
- Pharmacokinetics

June 2020 – Aug 2020 Internship with Millipore–Sigma Synthesis Quality Control Development

- Quality Control Development for Industrial Synthesis
- Identification of Synthesis Byproducts
- Preparatory LC
- NMR Spectroscopy
- UHPLC-MS/MS
- Presentation and Written Final Report of Findings

Sept 2018 – May 2019 Internship at Eurofins Scientific as Mass Spectrometric Specialist

- Consumer Sample Impurity Analysis
- HPLC UV/VIS Measurement
- UHPLC-MS/MS Analysis
- Weekly Presentations for Eurofins Scientific Clients
- Wrote Final Industrial Reports

Sept 2015 – Present Teaching Assistant (TA) for Introduction to General Chemistry at University of Wisconsin Milwaukee

- Worked with Classrooms of up to 18 students.
- Managed student grades
- Graded Material for courses
- Designed

Sept 2014 – Sept 2015 Research Assistant (RA) in Prof. Aldstadt's analytical chemistry lab through Student Undergraduate Research Funding (SURF)

- Sequential Injection Analysis with Low Field NMR Spectroscopy
- Parallel Plate Dialysis (PPD)
- Cyclic Voltammetry and Amperometry
- Real-time Reaction Monitoring
- Nonenzymatic Browning Reactions

Sept 2011 – May 2014 Framing Consultant and Material Overseer at The Great Frame Up

Education

Fall 2016 – Present A Chemistry Doctorate in Philosophy from the University of Wisconsin Milwaukee Doctoral Program in Chemistry Analytical and Instrumental Division

Graduated with a 3.929 GPA from the chemistry department working with in the analytical chemistry division. Course background on topics of molecular kinetics, pharmacology, physical organic chemistry, mass spectrometry, nuclear magnetic resonance spectroscopy, and analytical separation.

Fall 2012 – Fall 2015 A Chemistry with a Biochemical Option Bachelor's in Science from the University of Wisconsin Milwaukee Undergraduate Program

Graduated with a 3.715 GPA in chemistry with a biochemical option. Degree consisted of introduction into all divisions of chemistry as well as many courses in mathematics, biology, and physics. Historian for the Student Association with the American Chemical Society.

Fall 2008 – Spring 2012 Highschool Diploma from Whitefish Bay Highschool in Whitefish Bay, Wisconsin

Skills and Techniques

Scientific Skills and Techniques

- Quantitative Analytical Sample Preparation
- Solid-Liquid Phase (SPE) Extraction
- Liquid Chromatographic (LC) Separation
- Gas Chromatographic (GC) Separation
- Mass Spectrometric (MS) and Tandem Mass Spectrometric Analysis (MS/MS and MS^n)
- Mouse handling, Anesthetization, and Necropsy
- Nuclear Magnetic Resonance (NMR) Spectra collection and Interpretation
- Parallel Plate Dialysis (PPD)
- Sequential Injection Analysis (SIA)

Professional Skills and Techniques

- Experience with presentations of scientific findings to colleagues, members of other division of science, and laypeople
- Proficiency in Scientific Literature Research
- Experience in writing for scientific reports of internal and external industrial purposes
- Minor background in coding including, Java, C++, C#, HTML5, and Python
- Proficiency Microsoft Office software
- Proficiency in remote conferencing and Virtual Private Network (VPN) Access

Certification

2020 – Present	Annual Continued Education for Research Animal Users
2019	UWM Animal Facility Training
2016 – Present	Annual Title IX, Information Security, and Mandatory Reporting of Child Abuse and Neglect Training
2015 - Present	Annual Chemical Hygiene Plan (CHP) and Safety Training
2015	Fire Safety and Fire Extinguisher Training

Publications

Mutchie, T. R., Yu, O. B., **Di Milo, E. S**., & Arnold, L. A. (2019). Alternative binding sites at the vitamin D receptor and their ligands. Molecular and Cellular Endocrinology, 485(January), 1–8.

Gandhi, D. M., ..., **Di Milo, E. S**. …, Dockendorff, C. (2019). The Parmodulin NRD-21 is an Allosteric Inhibitor of PAR1 Gq Signaling with Improved Anti-Inflammatory Activity and Stability. Bioorganic & Medicinal Chemistry, 27(17), 3788–3796.

Yu, O. B., Mutchie, T. R., **Di Milo, E. S.**, & Arnold, L. A. (2019). Synthesis and biological evaluation of calcioic acid. Steroids 2020, 154, 108536.

Porter, J. D., …, **DiMilo, E.S.,** …, & Dockendorff, C. (2019). An anthrone-based Kv7.2/7.3 channel blocker with improved properties for the investigation of psychiatric and neurodegenerative disorders. Bioorganic and Medicinal Chemistry Letters, 29(23), 126681. https://doi.org/10.1016/j.bmcl.2019.126681

Pending Submission

Mutchie, T.R., Webb, D.A., **Di Milo, E.S.**, Arnold, L.A. Ligand Design for the Vitamin D Receptor. Nuclear Receptors, Badr M.Z. Ed. 2020 in press.

DiMilo E.S., Mutchie T.R., Yu O.B., Webb, D.A., and Chen, T., Li, W. Rochel, N. and coworkers, Arnold, L. A. Biological Evaluation of calcitroic acid. (2021 Pending).

Presentations

June 2021	Great Lakes Regional Meeting (GLRM) hosted by the American Chemical Society (ACS)
Apr 2019	*Metabolic Stability and Optimization of Extraction of Calcitroic Acid to Enable its Quantification by Liquid Chromatography Tandem Mass Spectrometry* at University of Wisconsin Milwaukee Chemistry Research Symposium
Jan 2019	*Metabolic Stability and Optimization of Extraction of Calcitroic Acid to Enable its Quantification by Liquid Chromatography Tandem Mass Spectrometry* at Milwaukee Analytical Chemistry Conference
Apr 2018	*Liquid Chromatography Tandem Mass Spectrometry for Quantification of Calcitroic Acid in Tissue and Microsomal Stability Assays* at University of Wisconsin Milwaukee Chemistry Research Symposium

Jan 2018	*Single Cell Mass Spectrometry* at University of Wisconsin Milwaukee Seminar Symposium
Apr 2017	*Quantification of Calcitroic Acid using Liquid Chromatography Tandem Mass Spectrometry* at University of Wisconsin Milwaukee Chemistry Research Symposium

Grants and Scholarships

June 2020	Research fellowship awarded for the collaboration with Millipore-Sigma.
Sept 2018	Research fellowship awarded for the collaboration with Eurofins Scientific.

Achievements

Spring 2018	University of Wisconsin Chemistry Department Symposium Research Award
Spring 2015	Awarded Junior of the Year by University of Wisconsin Milwaukee Chemistry Department
Fall 2012- Spring 2014	Dean's Honor List

Volunteering

Summer 2014	Research Assistant (RA) in Prof. Aldstadt's analytical chemistry lab